

Effect of prostate cancer-related plexin-B1 mutations on cell signalling and function

by

Chun ZHOU

Prostate Cancer Research Center
Division of Surgery and Interventional Science
University College London

A thesis submitted
for the Degree of Doctor of Philosophy
at University College London

November 2009

DECLARATION

I declare that this thesis represents my own work. Where information has been derived from other sources, I confirm that this has been indicated in the thesis.

Chun ZHOU

ACKNOWLEDGEMENT

I would like to thank University College London and the committee of Dorothy Hodgkin Postgraduate Award for funding me during my PhD study. I would also like to give my sincere thanks to my supervisor Professor John W. Masters for funding and supervising me throughout my research work. I am extremely thankful to Dr. Magali Williamson for her enduring guidance, invaluable advice and cheerful encouragement during the whole process of my PhD study and thesis writing. Without her supervision and support, this thesis would not have been completed.

I am thankful to Dr. Sharon Cole, Dr. Oscar Wong, Dr. Hide Yamamoto, and every member in prostate cancer research center for their help in the past four years.

I would like to give my thanks to my parents and Mr. Haiming Ma for their unconditional support.

Publication

Wong OG, Nitkunan T, Oinuma I, **Zhou C**, Blanc V, Brown RS, Bott SR, Nariculam J, Box G, Munson P, Constantinou J, Feneley MR, Klocker H, Eccles SA, Negishi M, Freeman A, Masters JR, Williamson M. Plexin-B1 mutations in prostate cancer. Proc Natl Acad Sci USA. 2007 Nov 27; 104(48): 19040-5.

Conference Abstract

Oral presentation

Zhou C, Masters J, Williamson M. Prostate cancer related mutations in Plexin-B1 effect RhoD signalling and cell function. Minisymposium in Cellular and Molecular Biology Session, AACR 100th Annual Meeting, Denver, USA, April 17-22, 2009.

Abstract

Prostate cancer is one of the most common cancers in the Western world. The metastasis of prostate cancer cells is the major cause of prostate cancer-related death. Understanding which genes are altered in prostate cancer and their implications for cell signaling and function is crucial for designing therapy strategies. Our group has identified a high frequency of somatic missense mutations in the plexin-B1 gene in localized and metastatic prostate cancer. The mutations are correlated with elevated metastatic features such as increased cell invasion, adhesion and decreased cell collapse relative to wildtype. Given the fact that Sema4D/plexin-B1 regulates cell signaling through coupling with tyrosine kinases and small GTPases, I hypothesized that plexin-B1 mutations may contribute to prostate cancer cell progression through affecting these pathways. The aims of this study were to characterize the molecular features of the three mutated forms of plexin-B1, A5359G, A5653G, and T5714C and to determine how the mutations affect cell signaling. It was found, using co-immunoprecipitation assays, that none of the three mutations affected the binding of either ErbB-2 or Met to plexin-B1. Sema4D/plexin-B1 mediated cell motility depending on the stoichiometry of plexin-B1, ErbB-2 and Met in prostate cancer cells. In addition, positive evidence was found for the impact of wildtype and mutant plexin-B1 on PI3K/Akt and MAPK pathways. All the three mutants exhibited an increased binding ability to RhoD GTPase relative to wildtype in GST-pulldown assays. This increased binding to RhoD is also associated with increased cell motility as shown in transwell migration assays. My study suggests that the three mutants confer a gain of metastatic phenotype to the cells through inactivating inhibitory pathways and has lead to the construction of a new model describing the mechanism by which plexin-B1 mutations contribute to cancer progression.

CONTENTS

TITLE	1
DECLARATION	2
ACKNOWLEDGEMENT	3
PUBLICATION.....	4
ABSTRACT	5
CONTENTS	6
LIST OF FIGURES	11
LIST OF TABLES	12
LIST OF ABBREVIATIONS.....	13
CHAPTER 1 INTRODUCTION	15
1.1 Prostate cancer	16
1.1.1 The prostate	16
<i>1.1.1.1 General features of the prostate</i>	16
<i>1.1.1.2 Role of androgens during prostate development</i>	19
1.1.2 Prostate cancer.....	20
<i>1.1.2.1 Overview of prostate cancer</i>	20
<i>1.1.2.2 Prostate cancer development</i>	21
<i>1.1.2.3 Genetic alterations associated with prostate cancer</i>	24
<i>1.1.2.4 Risk factors</i>	25
<i>1.1.2.5 Treatment of prostate cancer</i>	25
1.2 Semaphorins and plexins	28
1.2.1 Overview of semaphorins and plexins	28
1.2.2 Structural organization of semaphorins and plexins	30

1.2.3 The interactions of semaphorins and plexins	31
1.2.4 Signalling of semaphorins and plexins	32
1.2.5 Biological functions of semaphorins	34
1.2.5.1 <i>Semaphorins and neural development</i>	34
1.2.5.2 <i>Semaphorins and immune system</i>	36
1.2.5.3 <i>Semaphorins and vascular morphogenesis</i>	38
1.2.5.4 <i>Semaphorins and cancer</i>	39
1.3 Signalling pathways of Sema4D/plexin-B1	42
1.3.1 Rac1	45
1.3.2 Rnd1	47
1.3.3 R-Ras	48
1.3.4 M-Ras	51
1.3.5 RhoD	52
1.3.6 PDZ-RhoGEF/LARG	53
1.3.7 p190-RhoGAP	56
1.3.8 Met and Ron	57
1.3.9 ErbB-2	59
1.3.10 PI3K/Akt, PYK2, Src, MEK, and MAPK	61
1.4 Plexin-B1 mutations in prostate cancer	63
Hypothesis	65
CHPATER 2 MATERIALS AND METHODS	67
2.1 Cell culture	68
2.2 RNA extraction	69
2.3 RT-PCR	69
2.4 Agarose electrophoresis for DNA	71
2.5 Plasmid constructs	71

2.6 Transformation of E. Coli	72
2.7 DNA purification	72
2.8 Lipofectamine transfection	74
2.9 Protein extraction	75
2.10 Protein concentration measurement	75
2.11 SDS-PAGE and protein blotting	77
2.12 Western-blotting	79
2.13 Immunoprecipitation	81
2.14 Coomassie blue staining of SDS-polyacrylamide gel	82
2.15 Inducing competence and transforming of BL21	82
2.16 GST-cyto plexin-B1 purification	84
2.17 GST-pull down assay	85
2.18 Generation and purification of Sema4D	85
2.19 Dialysis of Sema4D concentrates	87
2.20 Migration assay	87
2.21 Statistical analysis	88
CHAPTER 3 Plexin-B1 expression in cancer cells	89
3.1 Introduction	90
3.2 Results	90
3.2.1 Expression of plexin-B1 and Sema4D at the mRNA level	90
3.2.2 Expression of plexin-B1 and Sema4D at the protein level	93
3.3 Discussion	96
CHAPTER 4 PLEXIN-B1 MUTATION AND TYROSINE KINASES	99
4.1 Introduction	100
4.2 Results	105

4.2.1 Interaction between plexin-B1 and ErbB-2	105
4.2.2 Interaction between ErbB-2 and mutated forms of plexin-B1	109
4.2.3 Interaction between plexin-B1 and Met	111
4.2.4 Interaction between Met and mutated forms of plexin-B1	114
4.2.5 Effect of ErbB-2 and Met expressions on cell migration in prostate cancer cells	116
4.2.6 Plexin-B1 and Akt/MAPK pathways in epithelial cells	120
4.2.7 Plexin-B1 mutations and MAPK pathways	127
4.3 Discussion	129
4.3.1 Plexin-B1 mutations and receptor tyrosine kinases	129
4.3.2 Plexin-B1 mutations and the Akt/MAPK pathways	131
CHAPTER 5 MUTATION OF PLEXIN-B1 AND CELL MIGRATION	133
5.1 Introduction	134
5.2 Results	134
5.3 Discussion	137
CHAPTER 6 PLEXIN-B1 MUTATION AND RhoD GTPase	139
6.1 Introduction	140
6.2 Results	141
6.2.1 Interaction between RhoD and full length plexin-B1	141
6.2.2 Interaction between RhoD and cyto-plexin-B1 wildtype/mutants	144
6.3 Discussion	148
CHAPTER 7 DISCUSSION	152
7.1 Significance of this study	153
7.2 Contribution of plexin-B1 mutations to the progression of prostate cancer ...	158

7.3 Future work	162
APPENDIX 1 (vector maps).....	164
APPENDIX 2 (chemicals and reagents).....	169
APPENDIX 3 (raw data of migration assays).....	170
REFERENCE LIST	172

LIST OF FIGURES

Figure 1.1 The prostate and surrounding organs	17
Figure 1.2 Zones of the prostate	18
Figure 1.3 Schematic diagram representing the Gleason grading system	23
Figure 1.4 Structural organization of semaphorins and plexins	29
Figure 1.5 Sema4D/plexin-B1 transduction pathways	44
Figure 3.1 mRNA expression levels of plexin-B1 and Sema 4D in cell lines	92
Figure 3.2 Plexin-B1 and Sema4D protein expressions in different cell lines	95
Figure 4.1 Reciprocal roles of ErbB-2 and Met on plexin-B1 signaling.....	102
Figure 4.2 Interaction between plexin-B1 and ErbB-2	108
Figure 4.3 Effect of plexin-B1 mutations on ErbB-2 and plexin-B1 interaction	110
Figure 4.4 Interaction between plexin-B1 and Met	113
Figure 4.5 Effect of plexin-B1 mutations on Met and plexin-B1 interaction	115
Figure 4.6 Effect of Sema4D on PC3 cell motility	118
Figure 4.6S Sema4D increases the motility of LNCaP cells	119
Figure 4.7 Akt and MAPK pathways under the effect of Sema4D	122
Figure 4.8 Effect of Sema4D in different solvents on MAPK activation	125
Figure 4.9 MAPK activation in cells expressing plexin-B1 wildtype/mutants	128
Figure 5.1 The motility of cells expressing plexin-B1 wildtype/mutants	136
Figure 6.1 Interaction between RhoD and full length plexin-B1	143
Figure 6.2 Coomassie blue staining of GST-fused products	146
Figure 6.3 Interaction between RhoD and cyto plexin-B1 wildtype/mutants	147
Figure 7.1 Proposed model of how plexin-B1 mutations affect cell signalling.....	161

LIST OF TABLES

Table 1.1 Protein function changes of the plexin-B1 mutations relative to wildtype.....	64
Table 2.1 Cell line information.....	68
Table 2.2 Scaling up or down transfections	74
Table 2.3 BSA standards preparation	76
Table 2.4 Recipe of SDS-polyacrylamide gel	77
Table 2.5 Antibody list	80
Table 7.1 Protein functions changes of the plexin-B1 mutations relative to wildtype...153	

LIST OF ABBREVIATIONS

AR	androgen receptor
BSA	bovine serum albumin
CDK5	cyclin-dependent kinase-5
CRAM	CRMP-associated molecule
CRD	cysteine-rich domain
CRIB	Cdc42/Rac-interactive binding
CRMP	collapsing response mediator protein
DC	dendritic cell
DH	Dbl homology
DRG	dorsal root ganglia
DTT	dithiothreitol
ECL	enhance chemiluminescent
ECM	extracellular matrix
EDTA	ethylenediaminetetraacetic acid
EGFR	epidermal growth factor receptor
ERK	extracellular signal-regulated kinase
GAP	GTPase activating protein
GEF	GTPase-exchanger factor
GST	glutathione S-transferase
HGF	hepatocyte growth factor
HRP	horseradish peroxidase
LARG	leukemia-associated RhoGEF
LOH	loss of heterozogosity
LPA	lysophosphatidic acid

MAPK	mitogen-activated protein kinase
MEK	MAPK/ERK kinase
OTK	receptor tyrosine kinase Off-track
PAK	p21-activated kinase
PCR	polymerase chain reaction
PDZ	PSD-95/Dlg/ZO-1
PH	pleckstrin homology
PI3K	phosphatidylinositol 3-kinase
PIN	prostatic intraepithelial neoplasia
PMSF	phenylmethylsulfonyl fluoride
PSA	prostate specific antigen
PSI	plexin-semaphorin-integrin
PTEN	phosphatase and tensin homolog
RIPA	radioimmunoprecipitation
RGS	regulator of G protein signaling
SDS	sodium dodecyl sulphate
SSCP	single strand conformation polymorphism
VSV	vesicular stomatitis virus

Chapter 1

Introduction

1.1 Prostate cancer

1.1.1 The prostate

1.1.1.1 General features of the prostate

The prostate gland is part of the male reproductive system that helps make and store seminal fluid. It functions to store and secrete a lightly alkaline fluid that helps neutralize the acidity of the vaginal tract, prolonging the lifespan of sperm. The prostate is a ductal-acinar exocrine gland that develops from the urogenital sinus. The development of the gland begins in fetal life and is completed at sexual maturity. It is located under the urinary bladder and in front of the rectum in the pelvis (Figure 1.1). The prostate surrounds part of the urethra that carries urine from the bladder during urination and semen during ejaculation. The mature human prostate is typically around 3 centimeters long and weighs about twenty grams. Human prostate is divided anatomically into the non-glandular fibromuscular stroma which permeates and surrounds the organ and three glandular regions termed central, peripheral, and transitional zones (Figure 1.2) (McNeal, 1983a; McNeal, 1983b). The peripheral zone is the largest region and is the principal site of prostatitis and carcinoma of the prostate (McNeal, 1969). The transitional zone consists of two small lobes surrounding the prostatic urethra, with ducts opening to the prostatic urethra. Prostate cancer rarely develops within the transitional zone. However, the transitional zone is the site of development of benign prostate hyperplasia (BPH) (McNeal, 1983a). The central zone surrounding the ejaculatory ducts is conical shaped; its ducts empty into the urethra proximal to the verumontanum. The central zone is virtually disease-free.

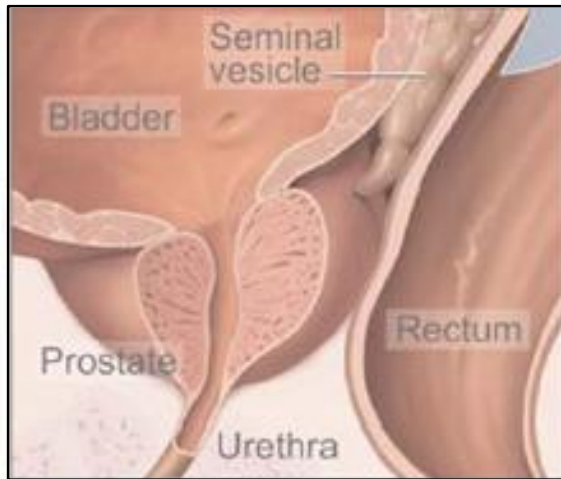


Figure 1.1 The prostate and surrounding organs. This figure illustrates the inside anatomy of the male pelvis. The prostate is below the bladder and surrounding urethra. The picture is adapted from the National Cancer Institute under the topic of prostate cancer (<http://www.cancer.gov>).

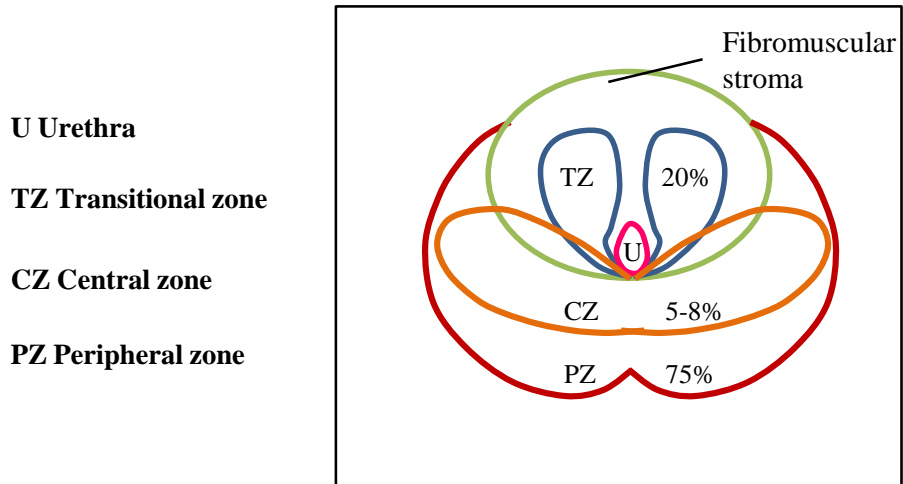


Figure 1.2 Zones of the prostate. This figure shows the four distinct glandular regions. The peripheral zone is the largest region, from which region more than 60% of prostatic cancer originates. The central zone surrounds the ejaculatory ducts and cancer from the central zone tends to be more aggressive. The transitional zone consists of two small lobes surrounding the prostatic urethra. The anterior zone is mainly composed of fibroblast and muscle tissues. This picture is adapted from the National Cancer Institute under the topic of prostate anatomy (<http://training.seer.cancer.gov/prostate>).

1.1.1.2 Role of androgens during prostate development

Development of the prostate is dependent on reciprocal interactions between mesenchyme and epithelium, as well as on androgens. During the embryonic stage of prostate gland development, androgen receptors (ARs) are detected in the urogenital sinus mesenchyme while the epithelium is initially AR-negative (Cooke et al., 1991; Takeda and Chang, 1991). Androgen receptors are detectable in developing prostatic epithelium shortly after birth in both mouse and rats (Moeller et al., 1987; Prins and Birch, 1995). Cunha and his colleagues performed tissue combination studies using wildtype and AR-negative testicular feminization mice (tfm) to elucidate the role of androgen receptors in both mesenchyme and epithelium during prostate development (Cunha and Young, 1991a) . Wildtype mesenchyme is able to induce normal prostatic morphogenesis when combined with either wildtype epithelium or tfm epithelium from urogenital sinus (Cunha et al., 1992a; Cunha et al., 1992b). However, tfm mesenchyme fails to stimulate the prostate gland development when in combination with either wildtype or tfm epithelium. These findings indicate that the presence of androgen receptors in the mesenchyme is crucial in the morphogenesis and development of the epithelium of the prostate. Cunha et al. further revealed the role of ARs on epithelial cells. The combination of wildtype mesenchyme and wildtype epithelium from urogenital sinus gives rise to a functional prostatic gland that produces secretory proteins. The combination of wildtype mesenchyme with tfm epithelium though could stimulate development of the prostatic phenotype, but failed to express prostatic secretory proteins (Cunha and Young, 1991b; Donjacour and Cunha, 1993). These findings indicate that

epithelial ARs are necessary for the production of prostatic secretory proteins, but are not essential for prostatic morphogenesis.

1.1.2 Prostate cancer

1.1.2.1 Overview of prostate cancer

Prostate cancer is the malignancy of the prostate gland. It is a common male disease across the world, with more than 670,000 men diagnosed with prostate cancer each year worldwide. The highest rates of detection are in Europe and the United States whilst lower frequencies are in South and East Asia. In the UK, prostate cancer is the most common cancer in men and accounts for nearly 24% of all new male cancer diagnoses. In 2006, there were 35,515 new cases of prostate cancer diagnosed in UK (data from Cancer Research UK). In the past 30 years the incidence of prostate cancer has tripled, however, much of the increase is largely due to the widespread use of prostate-specific antigen (PSA) testing since 1986 (Welch and Albertsen, 2009). Prostate cancer is the second most common cause of cancer death in UK men. It is estimated that each year around 10, 200 men in the UK die from this disease.

Majority of prostate cancer cases are adenocarcinoma consisting of epithelial cells and 70% of all prostatic adenocarcinoma arises from peripheral zone of the prostate (McNeal et al., 1988). Compared to normal prostate, prostate cancer is characterised by irregular glands and clumps of cells. Prostate cancer progresses from an early, androgen-dependent, localized disease to advanced, androgen-independent, metastatic disease. The

localized or early metastatic disease can be effectively treated with radical prostatectomy or androgen-deprivation therapy (Westin et al., 1995). However, approximately 18-24 months after the start of therapy, the tumor may eventually recur and becomes hormone-refractory and more aggressive (Santen, 1992). At this stage of the disease, chemotherapy is one of the options for controlling tumor progression. There are currently no effective cytotoxic chemotherapeutic agents available for effective control and improving the survival of patients with hormone-refractory disease.

1.1.2.2 Prostate cancer development

Prostate cancer is the main type of prostatic disease in adult males. Prostate cancer tends to develop in men above the age of 50. With increasing age, the incidence of prostate cancer increases. Approximately 75% of the clinically diagnosed prostate cancers are in men between the ages of 50-70 years old (Brawley et al., 1998). In fact, most men display signs of prostate malignancy at some time point during their lifetime. Although prostate cancer is one of the most prevalent types of cancer in men, many never exhibit symptoms or may eventually die with prostate cancer but not from this disease. This is because cancer of prostate is a slow growing cancer in most cases. Early prostate cancer usually causes no symptoms. However, prostate cancer does cause symptoms at a later stage. It is associated with urinary dysfunction as the prostate gland surrounds the prostatic urethra, causing frequent urination and painful urination. Once prostate cancer develops from the organ-confined disease to the metastatic disease, tumor cells become highly invasive and spread to distant organs. The main sites of metastasis of prostate

cancer are the regional lymph nodes and the bone system. Approximately 70% of the prostate cancer patients die of this disease with metastatic disease in their bone (Zetter, 1990). The most common symptom is bone pain.

Prostate cancer is graded by using Gleason's grading system based on the histological tumor patterns clinically. Together with other parameters, Gleason's grading system predicts prognosis and helps guide therapy. Figure 1.3 illustrates the patterns of Gleason's grading system. High-grade prostatic intraepithelial neoplasia (PIN) is considered as the most likely precursor of adenocarcinoma (McNeal and Bostwick, 1986). It arises by proliferation of the luminal epithelium in the peripheral and transition zone of the prostate (De Marzo et al., 1998). After a period of time, prostate cancer becomes very heterogeneous. Gleason's grading system is used to assess the complexity of prostate cancer (Gleason, 1977). The pathologist assigns the most common tumor pattern and the next most common tumor pattern each a grade. The score is the sum of the two dominant grades by area, e.g. $4 + 5 = 9$. Generally more advanced prostatic adenocarcinoma is correlated with a higher Gleason score (Gleason, 1992). Prostate cancer is the result of the accumulation of mutations and other genetic alterations occurring in prostate cells. Significant genetic changes within the prostate tumor cells have been observed to be associated with their pathological malignancy (Konishi et al., 1995; Ruijter et al., 1999; Sakr et al., 1994).

**PROSTATIC ADENOCARCINOMA
(Histologic Grades)**

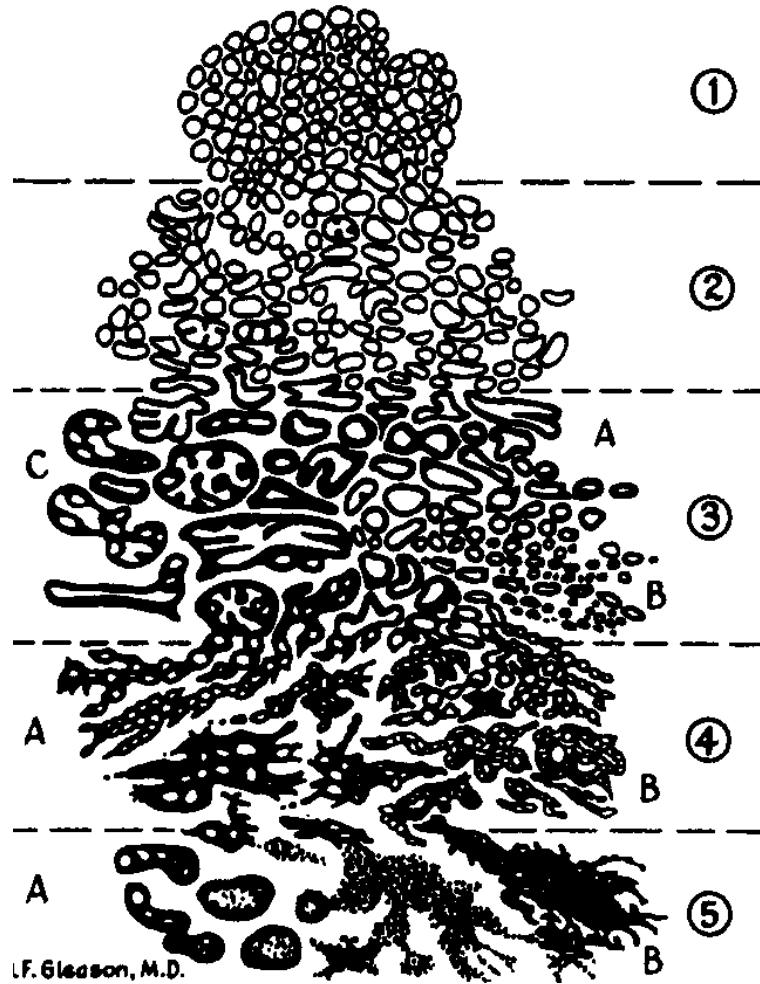


Figure 1.3. Schematic diagram representing the Gleason grading system. Gleason score is the sum of the two dominant grades by area. This picture is adapted from the book *Urologic Pathology: The Prostate* under the topic of Histologic grading and clinical staging of prostatic carcinoma (Gleason, 1977).

1.1.2.3 Genetic alterations associated with prostate cancer

Prostate carcinogenesis is a multi-step process that consists of initiation, proliferation, invasion and metastasis. This process is characterized by multiple aberrantly regulated pathways. At the molecular levels, the aberrant activities of these pathways result from the activation of oncogenes or inactivation of the tumor suppressor genes. Oncogenes are derived from proto-oncogenes that are oncogenic through genetic alterations such as mutation, partial deletion, rearrangement, over-expression and amplification of genes, leading to abnormal cell growth and proliferation. In haematological malignancies oncogene mutations predominate, however, like other epithelial tumourigenesis very few oncogenes have been defined in prostate tumor. Over-expressions of ErbB-2, myc, Bcl-2 have been reported to be correlated with advanced prostate cancer progression (Ross et al., 1993; Rosser et al., 2003; Sato et al., 1999). The exhibition of neoplastic phenotype in prostate cancer is a progressive and cumulative result of altered genotype. This process involves modifications in tumor suppressor genes such as deletion, mutations, rearrangement or methylation. Tumor suppressor gene inactivation is associated with tumor formation and progression of advanced prostate cancer. Several tumor suppressor genes have been identified and found to be mutated in advanced prostate cancer, but infrequently altered in early prostatic disease. For example, mutations of p53 gene in advanced stage of prostate cancer is higher in frequency than that in primary prostate tumors (Bookstein et al., 1993; Navone et al., 1999). Approximately 50% of advanced prostate tumors show PTEN mutations (Feilotter et al., 1998).

1.1.2.4 Risk factors

Although the specific causes of prostate cancer remain unclear, it is found that development of prostate cancer is associated with numerous factors such as age, race, dietary and environmental factors, steroid hormones, and family history. However, aging is the most important risk factor in prostate cancer development.

1.1.2.5 Treatment of prostate cancer

Up to now there is actually no best treatment for prostate cancer. Conventionally, treatment options depend on the stage of the disease at diagnosis, the Gleason score, and the PSA level. Other factors are the man's age and his general health. For patients with primary or organ-confined disease, radiotherapy or surgery is applicable, whereas hormone therapy is the standard treatment option for patients with metastatic disease. However, almost all patients with metastatic prostatic disease will finally become hormone unresponsive and refractory to hormone treatment. Chemotherapeutic agents have been developed recently; however, most of the chemotherapeutic options are palliative and cannot improve the survival of patients with advanced disease.

Watchful waiting or active surveillance is a concept in which the patient avoids active treatment but the disease is monitored by estimating the PSA at several time intervals. It is estimated that 50-80% of the prostate cancer patients will not become symptomatic even with no treatment (Yao and Lu-Yao, 2002). In some patients localized disease will not progress during their life time. The active surveillance is also applicable

for patients who have a life expectancy of less than 10 years. Due to the development of PSA screening, the majority of patients with prostate cancer are diagnosed at the stage of regional or localized disease. Radical prostatectomy is ideal for patients who present early, curable disease detected by the PSA test. It is also important that the patients should be under good healthy conditions to take the surgery. The life expectancy of patients should be at least 10 years after surgery so that patients can benefit from surgery. Radiotherapy is the most commonly used curative treatment for both early and locally advanced prostate cancer patients (Dearnaley, 1995). It is a treatment which kills cancer cells or inhibits cellular division of cancer cells using ionizing radiation (high-energy x-rays) without significant damage to the surrounding normal tissues. There are a number of irradiation methods for prostate cancer including brachytherapy, the most commonly used radiotherapy. Brachytherapy is the method in which the radiation source is placed close to or within the prostate cancer area. The overall survival rates were 96% and 86% for 5- and 10-year disease specific survival rate respectively from the Radiation Therapy Oncology Group (RTOG) 77-06 study (Hanks et al., 1991). The local recurrence rates of 5- and 10-year were 4 and 13%, respectively. Radiotherapy is one of the ideal treatments for patients with advanced local disease.

For patients undergoing radical prostatectomy or radiotherapy, the actuarial 10-year likelihood of biochemical disease recurrence is approximately 25% (Coen et al., 2002; Han et al., 2001). Among the prostate cancer 25-30% of the tumors behave aggressively (Parker et al., 1996). For patients who develop metastatic prostate cancer or those initially present advanced disease, ablation of androgen therapy is regarded as the optimal first-line treatment for advanced prostate cancer (Chodak et al., 2002). Initially

approximately 70-80% of the patients respond to androgen-depletion therapy with a remarkable reduction of androgen-responsive cancer cells (Gittes, 1991). However, after a median duration of 18-24 months, almost all tumors become hormone-refractory and more aggressive. Side-effects of androgen-depletion therapy include hot flushes and sexual problems. Over the last decade, much improvement has been made in the treatment of hormone-refractory prostate cancer. Chemotherapy is one of the options available. Historically, mitoxantrone is used as the most active chemotherapeutic agents that could ameliorate symptoms but do not show a provable effect on improving survival. The median duration of survival is 12.3 months on mitoxantrone (Tannock et al., 1996). More recently a new therapeutic alternative, docetaxel-based chemotherapy has demonstrated a survival advantage compared to mitoxantrone-based therapy when used in patients with metastatic hormone-refractory prostate cancer (Tannock et al., 2004). Patients with docetaxel-estramustine exhibit a high percentage of decreased PSA response than patients with mitoxantrone, and an increased of life expectancy by 15% (Petrylak et al., 2004). However, treatment of docetaxel-estramustine shows greater toxicity and side-effects. The potential of its therapeutic role in clinic needs well-designed trials before application.

1.2 Semaphorins and plexins

1.2.1 Overview of semaphorins and plexins

Semaphorins are a large family of secreted or membrane-bound proteins which were discovered as axon guidance cues in developing neuron system. In the neural system semaphorins regulate axon guidance, axonal fasciculation, dendritic guidance and neuronal migration (Kolodkin et al., 1993; Luo et al., 1993). It has subsequently been shown that semaphorins are involved in a wide range of biological processes including neural development, immune responses, morphogenesis, angiogenesis and tumor progression (Conrotto et al., 2005; Giordano et al., 2002; Ishida et al., 2003; Kanda et al., 2007). Plexin family members are single-pass transmembrane proteins and are the main receptors for semaphorins (Tamagnone et al., 1999). Both semaphorins and plexins are characterised by a sema domain, a ~500-amino acid conserved region, at their NH₂-terminal end. Up to date more than 30 semaphorins have been identified and classified into eight classes on the basis of sequence similarity and structural features (Semaphorin Nomenclature Committee, 1999) (Figure 1.4.A). Classes 1 and 2 are found in invertebrates, classes 3 to 7 are present in vertebrates, and class V are virus encoding semaphorins. Among them, classes 2, 3 and V are secreted proteins. Classes 1, 4, 5 and 6 are transmembrane molecules, and class 7 associates with the cell membrane through a glycosylphosphatidylinositol-anchor motif (Nakamura et al., 2000). Nine mammalian plexins have been identified and classified into four subfamilies: plexin-A1 to plexin-A4, plexin-B1 to plexin-B3, plexin-C1, plexin-D1 (Tamagnone et al., 1999) (Figure 1.4.B). There are two plexins found in invertebrate species.

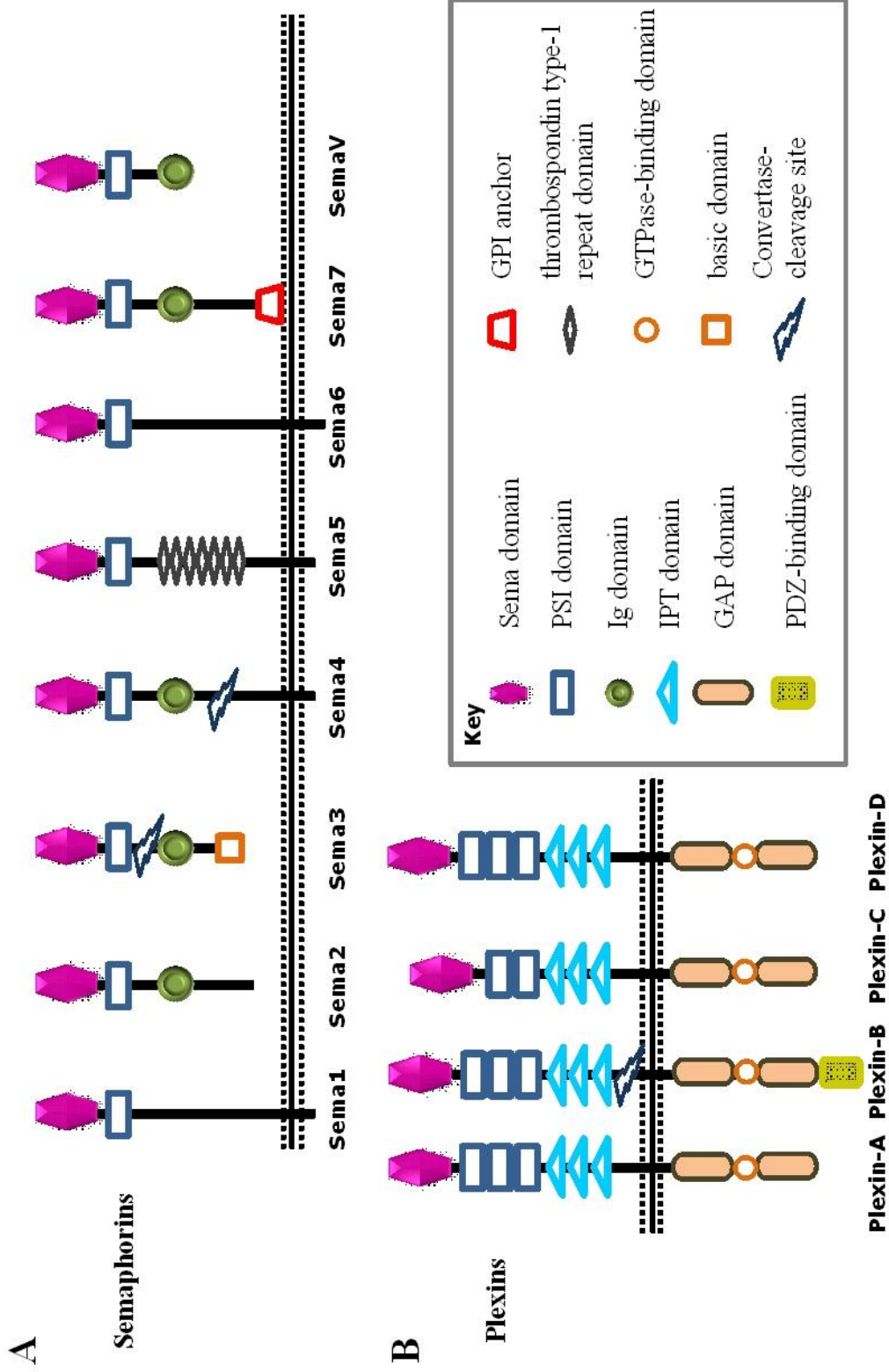


Figure 1.4 Structural organization of semaphorins and plexins. (A) Semaphorins are divided into eight classes on the basis of sequence similarity and structural features. (B) Plexins display conserved structural features across classes.

1.2.2 Structural organization of semaphorins and plexins

Semaphorins and plexins share an extracellular region of homology called the sema domain. This evolutionarily conserved domain is also found in the scatter factor receptors, MET and RON. The sema domain features a seven-blade β -propeller fold which is structurally similar to the β -propeller repeats of α integrins (Antipenko et al., 2003; Love et al., 2003). The sema domain is crucial for mediating protein-protein interaction and transducing signals in both semaphorins and plexins. Immediately C-terminal to the sema domain, all semaphorins with exception of some viral semaphorins contain a cysteine-rich domain (CRD). This motif is also referred as plexin-semaphorin-integrin (PSI) domain (Bork et al., 1999). At the sites C-terminal to PSI, semaphorins show great variation. Classes 2, 3, 4 and 7 semaphorins all contain a single copy of an immunoglobulin-like domain while class 5 semaphorins are unique in having seven thrombospondin repeats.

In contrast to semaphorins, plexins have a more uniform domain structure. Plexins have three copies of PSI domain following the sema domain at the carboxyl-end (Gherardi et al., 2004). Immediately C-terminal next to PSI domains, there are three IPT (Ig domain shared by plexins and transcription factors) (Bork et al., 1999). The plexin B family members are unique in having a convertase-cleavage site next to IPT domains (Artigiani et al., 2003). The cytoplasmic moiety of plexins (~600 amino acids) is highly conserved among all family members and is crucial for initiating intracellular signal pathways (Tamagnone et al., 1999). The cytoplasmic portion of plexins contains two domains, C1 and C2, which are highly conserved in all plexins. These domains show

sequence similarity to guanine triphosphatase activating protein (GAP) for small GTPase R-Ras (Oinuma et al., 2004a; Rohm et al., 2000). C1 and C2 contain primary and secondary Arg motifs which are the crucial structural features of various GAPs catalytic domains. The linker region between C1 and C2 is more divergent among plexin subfamilies. Within this linker region plexins bind to small GTPases such as Rnd1, Rac1 and RhoD (Tong et al., 2007; Vikis et al., 2000). There is a CRIB-like (Cdc42/Rac-interactive binding) motif in plexins A and B (Vastrik et al., 1999; Vikis et al., 2000). However, the CRIB-like motif is not involved in the interaction between these GTPases and plexin-B1 (Tong et al., 2007). Structural study shows that this region has a ubiquitin-like fold that is also found in Ras-binding proteins (Tong and Buck, 2005). The extreme C-terminal of plexins B also have a PDZ-domain-binding motif through which plexins interact with GTPase-exchanger factors (GEFs) such as PDZ-Rho GEF and Rac GEF FARP2 (Driessens et al., 2002; Toyofuku et al., 2005). In association with monomeric G-proteins plexins can trigger multiple signalling pathways in response to semaphorin stimulation.

1.2.3 The interactions of semaphorins and plexins

Semaphorins bind to their high-affinity receptors plexins to mediate cell migration, cytoskeletal remodelling, integrin-dependent adhesion, axon guidance, and other biological processes. It is believed that semaphorin binding releases the autoinhibition of plexin and induces clustering of plexins, resulting in plexin activation (Takahashi and Strittmatter, 2001). Membrane-bound semaphorins bind directly to plexins through their

sema domains. However, plexins alone are unable to interact with members of most class 3 secreted semaphorins. An exception to this rule is Sema3E which binds to plexin-D1 directly independent of neuropilins (Gu et al., 2005). Neuropilins are required to form a receptor complex with class A plexins to enable the binding to class 3 semaphorins and subsequent signal transduction (He and Tessier-Lavigne, 1997; Kolodkin et al., 1997). Neuropilins are transmembrane proteins of ~900 amino acids in length with very short cytoplasmic tails which do not show any intrinsic enzyme activity (Takagi et al., 1991). Neuropilins alone have low affinity to semaphorins and are incapable of transducing the signalling of class 3 semaphorins. Two neuropilins, neuropilin-1 and neuropilin-2, have been identified. Neuropilin-1 forms a complex with Plexin-A to form a co-receptor for Sema3A, mediating repulsion between neurons and axons (He and Tessier-Lavigne, 1997; Kolodkin et al., 1997). Neuropilin-2 has the same structure as neuropilin-1 with only a slight difference in protein sequence. Sema3F binds to neuropilin-2/Plexin-A complex with high affinity to induce hippocampal mossy fibers (Bagri et al., 2003; Chen et al., 1997). In contrast, Sema3C has similar binding affinities toward both neuropilin-1 and neuropilin-2 (Chen et al., 1997).

1.2.4 Signalling of semaphorins and plexins

Tyrosine phosphorylation is a pivotal mechanism in semaphorin signalling. Upon semaphorin stimulation, plexins become phosphorylated in their cytoplasmic domain. Plexins A and B have been extensively studied to determine the role of tyrosine phosphorylation in their signalling pathways and to determine which kinases are involved.

Intracellular tyrosine kinases Fes and Fyn associate with class A plexins in a ligand-independent manner (Mitsui et al., 2002; Sasaki et al., 2002). Sema3A enhances the binding of plexin-A1 and Fes. Fes phosphorylates plexin-A1 and the complex of CRAM (CRMP-associated molecule) and CRMP2 (collapsing response mediator protein), resulting in cell collapse in COS-7 cells and growth cones in dorsal root ganglion (DRG) neuron (Mitsui et al., 2002). Plexin-A2 associates with the tyrosine kinase Fyn. Active Fyn promotes the binding of plexin-A2 and CDK5 (cyclin-dependent kinase-5) (Sasaki et al., 2002). In response to Sema3A stimulation, CDK5 phosphorylation cascade is activated through the phosphorylation site of Fyn (Sasaki et al., 2002). The substrate of CDK5, Tau, is phosphorylated subsequently. Class B plexins associate with the receptor tyrosine kinases Met and ErbB2 (discussed in later sections).

In addition to tyrosine kinases, Rho GTPases have also been implicated in semaphorin signalling. The Rho GTPases are a group of small G proteins that control cell motility through actin reorganization. In association with Rho GTPases, plexins mediate cell migration through regulation on actin rearrangement. As described in section 1.2.2, the binding site for Rac, Rnd1 and RhoD is located in the cytoplasmic domain of plexin-A1. Rac functions upstream of plexin-A1 and Rac activity is necessary for Sema3A/plexin-A1-induced cell collapse in COS-7 cells (Turner et al., 2004). Rnd1 stimulates plexin-A1-induced cell collapse; however, RhoD exerts antagonistic effect of Rnd1 on plexin-A1 activation (Zanata et al., 2002). B-type plexins act as R-Ras and M-Ras GAPs. The features of plexins B will be discussed in later sections.

1.2.5 Biological functions of semaphorins

1.2.5.1 Semaphorins and neural development

During development of neuron network, individual axons are guided to their targets by sensing an array of environmental cues through the growth cones at the tip of axons (Song and Poo, 2001). Semaphorins are one of the categories of axon guidance cues, acting as repellents or attractants for navigating axons. Grasshopper Sema I (fasciclin I) is the first identified semaphorin and is expressed in the circumferential stripes of epithelial cells in developing limb buds, where the growth cones of pioneer sensory axons make a characteristic turn while extending toward the central nervous system (CNS) (Kolodkin et al., 1992). Blocking expression of Sema I in these stripes perturbs the trajectory of tibial pioneer growth cones. The *Drosophila* Sema1a shares homology in sequence to grasshopper Sema I and acts as an axonal repellent for motor axons, so that the motor neurons project to their target muscles precisely during embryo development (Yu et al., 1998).

Sema3A, the first identified vertebrate semaphorin, induces retraction and collapse of growth cones (Luo et al., 1993). Through exerting repulsive effects on developing axons, Sema3A repels axons of sympathetic, motor and sensory neurons away from the trigeminal, facial, vagal cranial ganglia, olfactory sensory, pontocerebellar mossy fiber and cortical neurons (Adams et al., 1997; Bagnard et al., 1998; Kobayashi et al., 1997; Rabacchi et al., 1999; Shepherd et al., 1996). Invertebrate axons are projected from neurons in the dorsal root ganglia (DRG) to different dorsoventral termini during the developmental process. At appropriate developmental stages high levels of Sema3A

expression in the ventral spinal cord prevents non-mature sensory afferent neurons from entering the dorsal cord (Messersmith et al., 1995). In Semaphorin 3A mutant mice, some sensory axons project into inappropriate regions of the spinal cord. In addition, these mutant mice exhibit an abnormal pattern of development in neuronal processes, embryonic bone and ventricle structure of heart (Behar et al., 1996). In the chicken embryo, *Sema3A* mediates the projection of olfactory sensory axons (Renzi et al., 2000). At the stage when axons first reach the telencephalon and undergo their waiting period before contacting olfactory bulb, *Sema3A* expression is strongest (embryonic day 5 to 7). The expression of *Sema3A* decreases at embryonic day 9 when axons invade into the bulb. The temporal pattern of *Sema3A* expression contributes to the precise control of axonal pathfinding. Multiple class 3 semaphorins are involved in fine-tuning the axonal growth during neuron projection. Their regulatory effects on axon guidance are bifunctional and dependent on the spatial expression pattern of semaphorins. During cortical development *Sema3E* is able to attract cortical axons, in contrast *Sema3D* inhibits axonal branching by inducing growth cone collapse (Bagnard et al., 1998). At the time when corticofugal projections are established, *Sema3D* and *Sema3E* are both expressed in the cortex. *Sema3D* is restricted in the ventricular zone of the neocortex whereas *Sema3E* is expressed in the subventricular zone. The synchronized expression of multiple semaphorins, both temporally and spatial, is responsible for the precise control of neural development.

The balance of attractive and repulsive semaphorins is responsible for mediating axonal fasciculation. Fasciculation is the process of segregating bundles of axons serving related functions at their appropriate targets. Peripheral axons of trigeminal, facial, vagal,

accessory and glossopharyngeal nerves are driven together into fascicles by the Sema3A protein secreted by their surrounding tissues (Kitsukawa et al., 1997; Taniguchi et al., 1997). Sema3A knockout mice demonstrate a highly defasciculated phenotype in these nerves. However, defasciculated axons are able to project near the surrounding area of their appropriate trajectories and targets, indicating that other molecules are involved in the process of axon guidance.

1.2.5.2 Semaphorins and immune system

Several viral and vertebrate semaphorins have been implicated in various phases of the immune response. Sema4D (also known as CD100) is the first semaphorin that has been well characterized in the immune system. Sema4D is constitutively expressed on T cells and expression levels are relatively low on B cells. In the immune system Sema4D recognizes CD72 rather than plexin-B1 as its receptor (Kumanogoh et al., 2000). Transfection of Sema4D into human B cells promotes their aggregation and survival in vitro (Hall et al., 1996). Sema4D-deficient mice exhibit severe abnormal B cell development and altered immune response (Shi et al., 2000). Sema4D ligation with CD72 turns off the inhibitory effect of CD72 on B cells, thus enhancing B cell activation. The interaction of Sema4D/CD72 also enhances CD40-dependent B cell activation (Kumanogoh et al., 2000). Given the fact that Sema4D and CD72 are expressed in T cells and B cells respectively, it is conceivable that Sema4D/CD72 signalling is involved in T cell-B cell interaction. Extensive study also reveals that Sema4D is crucially involved in initiating activation and differentiation of T cells. In mice deficient of Sema4D, CD4⁺ T

cells from the draining lymph nodes show impairment of proliferative responses and cytokine production after antigen re-stimulation (Shi et al., 2000). Soluble human Sema4D inhibits the spontaneous and MCP-3-induced migration of freshly isolated monocytes and monocytic cell lines, suggesting that Sema4D also plays a role in monocyte and macrophage migration (Delaire et al., 2001).

Sema4A is another member of class IV semaphorin subfamily and is implicated in regulation of T cell-mediated immune responses. Recombinant soluble Sema4A enhances T cell proliferation and IL-2 production after anti-CD3 antibody stimulation (Kumanogoh et al., 2002). Both in vitro and in vivo studies show that deficient expression of Sema4A results in impaired T cell priming (Kumanogoh et al., 2002; Kumanogoh et al., 2005). In addition, soluble Sema4A enhances the interaction between allogeneic T cells and dendritic cells (DCs) (Kumanogoh et al., 2002). Anti-Sema4A monoclonal antibodies block these mixed lymphocyte reactions, suggesting that Sema4A helps T cell activation through influencing the stimulatory interactions between T cells and DCs.

At the later stage of T cell-mediated immune response, inflammatory responses were triggered by antigen-specific effector T-cells through macrophage activation in peripheral tissues. Sema7A is highly involved in this phase. Sema7A expressed on activated T cells promotes macrophage recruitment to the site of inflammation. Through interaction with $\alpha_1\beta_1$ integrins, Sema7A initiates inflammatory cascades by stimulating cytokine production by macrophages (Suzuki et al., 2007).

Semaphorin receptors, plexins, have also been implicated in immune response. Plexin-A1 is expressed in DCs and is involved in interaction of T cells and DCs.

Expression of plexin-A1 in DCs is required for production of antigen-specific T cells in the presence of cognate antigens. Plexin-A1 deficient DCs fail to activate T cells both in vitro and in vivo (Takegahara et al., 2006).

1.2.5.3 Semaphorins and vascular morphogenesis

Vasculature is composed of large vessels that branch into small vessels and capillaries. The process of vasculature formation is mediated by endothelial cell movement. Semaphorins are highly involved in regulating guidance and remodelling of the vasculature. Sema6D and its receptor plexin-A1 are expressed in endothelial and myocardial cell populations during the early stages of embryonic development in chicken and mouse (Toyofuku et al., 2004a; Toyofuku et al., 2004b). Sema6D plays dual roles in coordinating the narrowing and bending of the developing ventricular chamber by enhancing and inhibiting cell migration of conotruncal segments and ventricle, respectively (Toyofuku et al., 2004a). Plexin-A1 and other co-receptors mediate the bifunctions of Sema6D. In association with plexin-A1 and the coreceptor OTK (receptor tyrosine kinase Off-track), Sema6D exerts its repulsive effect on ventricular expansion. When Sema6D forms a complex with plexin-A1 and receptor tyrosine kinase VEGFR2, Sema6D is acting as attractant for conotruncal segment cell migration. In addition to its role in regulating endothelial cell migration, Sema6D is also crucial in myocardial organization. Abl kinase is recruited to Sema6D and activated in the presence of plexin-A1, resulting in phosphorylation of Sema6D. This is an example of reverse plexin signalling that is common in many other plexin members. The activation of Sema6D

signalling pathway enhances the migration of myocardial cells into the trabeculae. Sema6D or plexin-A1 knockdown results in thin and small ventricular compact layer and defective trabeculation in chicken heart development (Toyofuku et al., 2004b).

Class 3 semaphorins are also involved in the development of cardiovascular system. Mice deficient of Sema3A exhibit cardiac defects, phenotyped with right ventricular hypertrophy and a grossly dilated right atrium (Behar et al., 1996). Sema 3C regulates crest cell migration into the proximal cardiac outflow tracts (Feiner et al., 2001). Sema3C knockout mice display strong dysfunctions of vasculature, characteristic of disruption of the aortic arch and inappropriate separation of the cardiac outflow tracts (Feiner et al., 2001). These severe cardiovascular system defects cause death within several hours after birth. In the mouse Sema3E secreted by developing somites controls the patterning of the growing vasculature through repelling plexin-D1-expressing endothelial cells growing. Deletion of Sema3E or plexin-D1 disrupts vascular patterning. These facts together show that class 3 semaphorins play important role during the development of cardiovascular system.

1.2.5.4 Semaphorins and cancer

Consistent with their regulatory role in fundamental cell behaviours including migration, semaphorins are also involved in cancer and tumorigenesis. Sema3B and Sema3F have been revealed as potential tumor suppressors, as they are located in chromosome 3p21 where homozygous deletion is frequent in lung and ovarian cancers

(Roche et al., 1996; Tse et al., 2002; Xiang et al., 1996). Hypermethylation of Sema3B promoter is observed in several human lung cancer cell lines and primary tumors (Kuroki et al., 2003). Both hypermethylation and loss of heterozygosity (LOH) are correlated with loss of expression of Sema3B mRNA. Sema3B inhibits lung cancer cell growth in tumor cells. In both lung and breast cancer, Sema3B induces apoptosis partly through blocking the VEGF autocrine activity (Castro-Rivera et al., 2004). Yet Sema3B can also be pro-metastatic. In vivo study shows that Sema3B inhibits tumor growth but induces metastasis (Rolny et al., 2008). Rolny et al. found that Sema3B induces the production of interleukin (IL) 8 by tumor cells through activating the p38-mitogen-activated protein kinase pathway. The released IL-8 then induces the recruitment of tumor-associated macrophages and metastatic dissemination to the lung. Sema3F expression is found to be down-regulated in lung tumors and cell lines (Lantuejoul et al., 2003). Transfection of Sema3F in A9 fibrosarcoma cells abolishes tumorigenicity in nude mice, suggesting its tumor suppressor role (Tse et al., 2002). In addition, Sema3F has inhibitory effects on cell attachment and spreading in breast cancer cell line MCF7, opposite to the effect of VEGF (Nasarre et al., 2003). Furthermore, Sema3F also acts as an inhibitor of tumor angiogenesis. Over-expression of Sema3F in tumorigenic cell line HEK293 inhibits its tumor-formation ability and suppresses tumor-associated blood vessels concentration (Kessler et al., 2004). In mice implanted with Sema3F-expressing metastatic human melanoma cells, tumor displays less invasive and vascular phenotype (Bielenberg et al., 2004). Other members in class 3 semaphorins, such as Sema3A, Sema3D, Sema3E and Sema3G have also been characterised as tumor suppressors and inhibitors of tumor angiogenesis (Kigel et al., 2008). All these four semaphorins possess anti-tumorigenic

properties. In addition Sema3A, Sema3D and Sema3G strongly reduce the density of blood vessels in tumors.

Besides their suppressive role in tumor development, semaphorins can also function as tumor promoters. Over-expression of Sema3E and Sema3C are both found to be correlated to the invasive and metastatic behaviours or drug resistance of tumor cells (Christensen et al., 1998; Martin-Satue and Blanco, 1999; Yamada et al., 1997). The report on Sema3E as a promoter of cancer is in contrast to the finding by Neufeld's group that Sema3E acts as a tumor suppressor. This might be explained by the difference of tumor types and whether the appropriate semaphorin receptors are expressed. Sema4D induces invasive growth and angiogenesis of endothelial cells through recruitment of Met to plexin-B1 (Conrotto et al., 2005; Giordano et al., 2002). Over-expression of Sema4D occurs in several carcinomas including breast, colon, lung and prostate cancers (Basile et al., 2006; Wong et al., 2007). Yet Sema4D also acts as a tumor suppressor in melanoma. The Sema4D receptor plexin-B1 blocks tumorigenesis in primary melanoma and suppresses migration in late-stage cells (Argast et al., 2009). The opposite effects of Sema4D on tumor may be due to co-receptors or binding partners of plexin-B1 that activates different signalling pathways. Signaling pathways transduced by Sema4D/plexin-B1 will be discussed in section 1.3.

1.3 Signalling pathways of Sema4D/plexin-B1

Plexin-B1 is the receptor for Sema4D. Like the other members of plexin family, plexin-B1 has the Sema domain at the extracellular region, through which plexin-B1 interacts with its ligand Sema4D and with tyrosine kinases. The cytoplasmic domain of plexin-B1 is characteristic of the general features of B plexins, with two segments homologous to R-Ras GAP linked by a region where several small Rho GTPases bind. Sema4D is the ligand for plexin-B1. The signalling pathways of Sema4D/plexin-B1 have been extensively studied recently. Since plexin-B1 lacks an intrinsic tyrosine kinases activity, plexin-B1 interacts with other partners to initiate signalling pathways. For example, small GTPases are importantly involved in Sema4D/plexin-B1 signal transduction. Tong and his colleagues have defined the small Rho GTPase binding site in the linker region of the two homologous segments (C1 and C2) in the cytoplasmic domain of plexin-B1. An ubiquitin-like fold consisting of β -strands 3 and 4 and a short α -helical segment located in the cytoplasmic domain of plexin-B1 is the site for interaction with Rac1, Rnd1 and RhoD (Tong et al., 2007). This binding motif is adjacent to the region where plexin-B1 protein is dimerized. Binding of these three GTPases induces a conformational change that destabilizes the dimer; this is necessary for activation of plexin-B1 signalling pathways involving Rho GTPases (Oinuma et al., 2004b; Oinuma et al., 2004a; Tong et al., 2007). Plexin-B1 also couples to receptor tyrosine kinases such as ErbB-2 and Met to initiate signalling pathways. Figure 1.5 illustrates the network of plexin-B1 signalling pathways. By binding to ErbB-2 or to Met, plexin-B1 mediates cell motility through regulating Rho activity in response to Sema4D. Small GTPases, Rac, Rnd and RhoD, bind to plexin-B1 at the same site. Active Rac is sequestered from

interacting with PAK by plexin-B1. Rnd1 constitutively binds to plexin-B1. Upon Sema4D stimulation, plexin-B1/Rnd1 hydrolyses R-Ras GTP through its R-Ras GAP activity. In the following sections I will review these proteins involved in Sema4D/plexin-B1 signalling and the cell functions regulated by these signalling pathways.

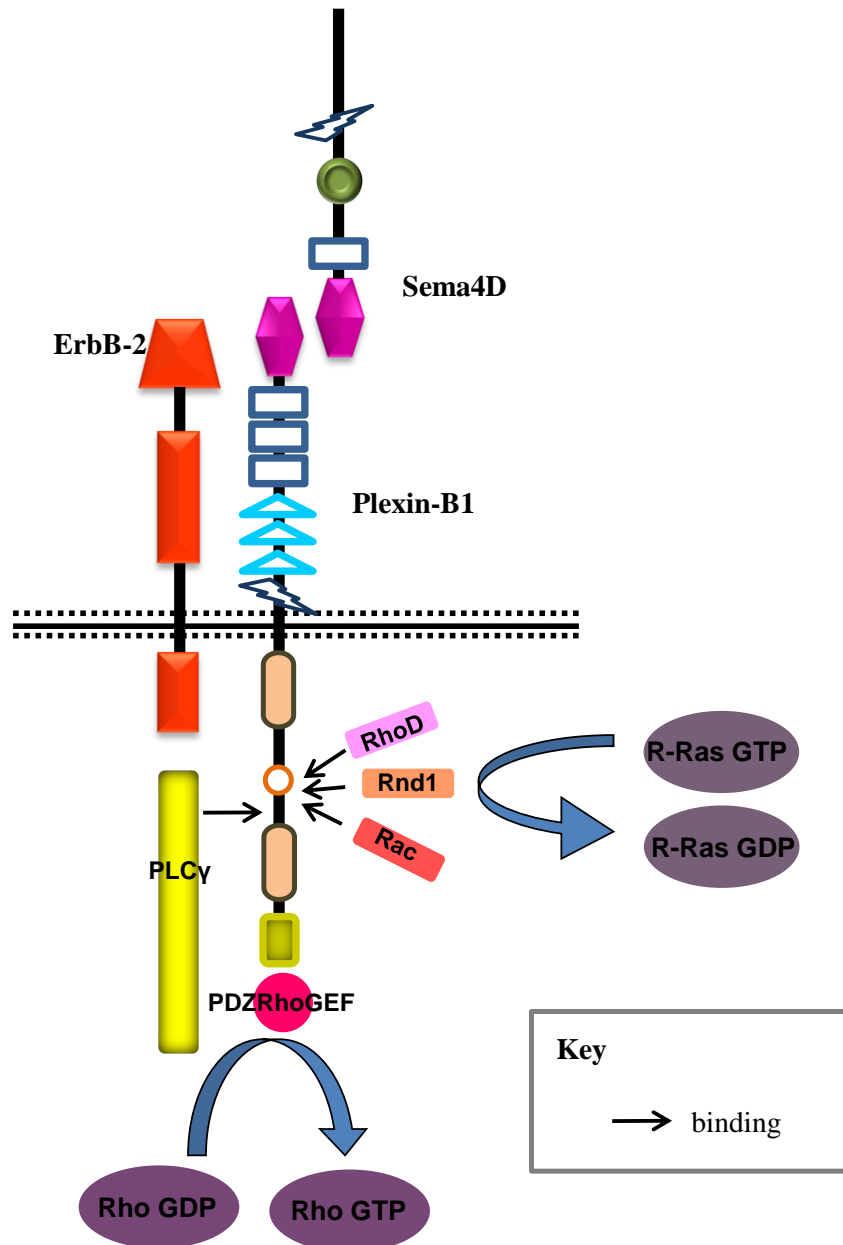


Figure 1.5 Sema4D/plexin-B1 transduction pathways. Sema4D/plexin-B1 transduces its signal through coupling with other proteins and forms a complex signaling network. Plexin-B1 binds to Rnd1, Rac, PDZ-RhoGEF and R-Ras. Upon Sema4D stimulation, the R-Ras GAP activity of plexin-B1 is activated, resulting in hydrolysis of R-Ras GTP. Plexin-B1 is thought to sequester Rac GTP from downstream effectors such as PAK. Tyrosine kinases ErbB-2 and Met (not shown in this figure) bind to plexin-B1 through the extracellular domains. Sema4D stimulation activates ErbB-2 which subsequently phosphorylates plexin-B1 on tyrosines 1708 and 1732. The phosphorylated plexin-B1 recruits PLC γ which activates PDZ-RhoGEF, resulting in Rho activation.

1.3.1 Rac1

Firstly, role of Rac1 and plexin-B1 interaction for plexin-B1 signal transduction will be discussed in this section.

Rac, Rho and Cdc42 comprise the Rho GTPase family proteins that are the key factors controlling cell motility through regulating the actin cytoskeleton and microtubule dynamics. Rho regulates stress fiber formation, whereas activation of Rac and Cdc42 controls formation of lamellipodia and filopodia, respectively. Neither Rho nor Cdc42 binds to plexin-B1. Rac1 in its active form, Rac1-GTP, interacts directly with cytoplasmic domain of plexin-B1 (Driessens et al., 2001; Vikis et al., 2000). The effector domain of Rac1 is required for its interaction with plexin-B1. Mutations at residues Y32, T34 and F37 completely abolish the ability of Rac to bind to plexin-B1 (Vikis et al., 2000). The ligand for plexin-B1, Sema4D, enhances the interaction between plexin-B1 and Rac.

PAK (p21-activated kinase) is a Rac downstream effector that is activated when Rac1 binds to its Rac-binding domain (RBD). Plexin-B1 and PAK compete for Rac binding. By sequestering active Rac from interacting with PAK, plexin-B1 inhibits Rac-induced PAK activation (Vikis et al., 2002). On the other side, Rac interaction with plexin-B1 enhances plexin-B1 expression at the cell membrane and slightly increases its receptor affinity, resulting in elevated interaction between plexin-B1 and its ligand Sema4D (Vikis et al., 2002). However, in cells co-expressing plexin-B1 and PDZ-RhoGEF Rac has no effect on surface expression of plexin-B1 (Swiercz et al., 2004). In these cells active Rac increases Sema4D-induced tyrosine phosphorylation of plexin-B1.

These observations suggest that active Rac promotes plexin-B1 phosphorylation either by increasing the affinity for Sema4D or by other mechanism that facilitates Sema4D-induced phosphorylation.

Given that semaphorins forms dimers and activate plexins through clustering, Sema4D activates plexin-B1 through clustering (Klostermann et al., 1998; Tamagnone et al., 1999). Driessens et al. constructed a chimeric protein in which cytoplasmic plexin-B1 is fused to the transmembrane and extracellular domains of CD2. They induced CD2/plexin-B1 clustering at cell surface in fibroblasts and found that crosslinking of plexin-B1 results in formation of stress fibers and some cell contraction, a phenotype characteristic of Rho activation (Driessens et al., 2001). No lamellipodial actin is detected suggesting Rac is not activated by crosslinking of plexin-B1. Dominant-negative Rac (N17) completely blocks the formation of actin stress fibers and cell contraction in fibroblasts, suggesting that RhoA is downstream of the Rac1 response to plexin-B1 activation through clustering. However, binding of Rac to plexin-B1 is not necessary for Rho activation, since cells expressing plexin-B1 lacking a Rac binding site still exhibit a Rho activation phenotype after plexin-B1 crosslinking. Another research group led by Oinuma shows that dominant negative Rac does not have an effect on cell contraction induced by Sema4D-mediated Rho activation in COS7 cells (Oinuma et al., 2003). These controversial findings of Rac1 on Sema4D/plexin-B1-mediated RhoA activation might be cell type-dependent. The crosstalk between Rac and Rho activation through plexin-B1 clustering is not clear, and remains to be addressed by further studies.

1.3.2 Rnd1

Rnd GTPases, including Rnd1, Rnd2, and Rnd3, comprise a subfamily of Rho family GTPases. Rnd1 is characterised by a low affinity for GDP and very low intrinsic GTPase activities, leading to its constitutively GTP-bound state (Foster et al., 1996; Nobes et al., 1998). Rnd1 is abundantly expressed in the nervous system and has been implicated in regulation of cell cytoskeleton and cell adhesion. Expression of Rnd1 in fibroblasts results in cell retraction and rounding, loss of stress fibers, and loss of integrin-based focal adhesion (Nobes et al., 1998). Recently, Rnd1 has been found to be involved in semaphorin signalling pathways. Before Tong revealed the structure for GTPase (Rac1, Rnd1, and RhoD) binding in the cytoplasmic domain of plexin-B1, Oinuma has shown that all Rnd subfamily GTPases interact with the cytoplasmic domain of plexin-B1 by immunoprecipitation (Oinuma et al., 2003; Tong et al., 2007). She has also narrowed down the binding site for Rnd1 between amino acids 1724 and 1915 of plexin-B1, overlapping with Rac binding site (aa1848-1890). Rnd1 constitutively interacts with plexin-B1 independent of Sema4D. Interaction of Rnd1 and plexin-B1 is required for Sema4D-induced cell contraction in COS7 cells, and the contraction is through activation of PDZ-RhoGEF/RhoA pathway. Either inhibition of plexin-B1/PDZ-RhoGEF interaction or suppression of RhoA by treatment with Rho-kinase inhibitor Y-27632 abolishes the Sema4D-induced cell rounding in COS7 cells. Rnd1 binding to plexin-B1 enhances the interaction between plexin-B1 and PDZ-RhoGEF and potentiates Sema4D/plexin-B1-mediated Rho activation in COS7 cells. The mechanism of how Rnd1 promotes the binding between plexin-B1 and PDZ-RhoGEF is not clear. It is hypothesized that interaction of Rnd1 and plexin-B1 may elicit a conformational change

in the cytoplasmic domain of plexin-B1, which facilitates the interaction of PDZ-RhoGEF and plexin-B1. Swiercz et al. also reported that Rnd1 increases surface expression of plexin-B1 in cells co-expressing plexin-B1 and PDZ-RhoGEF, which is consistent with the finding that Rnd1 promotes the interaction between plexin-B1 and PDZ-RhoGEF (Swiercz et al., 2004). This enhanced localization of plexin-B1 by Rnd1 may also explain the observation that Rnd1 increases Sema4D-induced tyrosine phosphorylation of plexin-B1 in cells co-expressing plexin-B1 and PDZ-RhoGEF.

Recently, plexin-B1 has been reported functioning as a GAP for R-Ras. Rnd1 is also critically involved in stimulating the R-Ras GAP activity of plexin-B1. The R-Ras GAP homology domains in cytoplasmic region of plexin-B1, C1 and C2, bind to each other in natural state (Oinuma et al., 2004b). Rnd1 binding to the linker region located between C1 and C2 disrupts this interaction. This Rnd1-induced conformation change is indispensable for R-Ras binding and Sema4D-mediated GAP activity toward R-Ras of plexin-B1. Detailed discussion regarding the GAP activity of plexin-B1 will be introduced in section 1.3.3. Rnd1 association with plexin-B1 is also required for initiation of Sema4D/plexin-B1-mediated M-Ras GAP activity that will be introduced in section 1.3.4.

1.3.3 R-Ras

R-Ras belongs to the Ras family which comprises a large group of small GTPases with similar structures and related functions (Kinbara et al., 2003). Like most of the small

GTPases, R-Ras cycles between an inactive GDP (guanine diphosphate)-bound state and an active GTP-bound state. The active form of R-Ras increases cell adhesion, cell migration, and neurite outgrowth by activating integrins (Keely et al., 1999; Zhang et al., 1996). The activation of R-Ras is down-regulated by GTPase-activating proteins (GAP) that stimulate the intrinsic GTPase activity of R-Ras, resulting in the hydrolysis of GTP-bound R-Ras into GDP-bound state. In addition to p98-R-RasGAP, activated plexin-B1 also acts as an R-Ras-specific GAP (Oinuma et al., 2004b; Oinuma et al., 2004a). Rnd1 binding to plexin-B1 opens the closed conformation of the cytoplasmic domain of plexin-B1, making plexin-B1 accessible for GTP-bound R-Ras binding. Activation of plexin-B1 by Sema4D results in clustering of plexin-B1, which stimulates the R-Ras GAP activity of Rnd1-associated plexin-B1. Therefore R-Ras activity is decreased through hydrolysis of GTP by R-Ras GAP activity and this phenomenon follows the same time course as plexin-B1 clustering. Clustering of Rnd-1-bound cytoplasmic domain of plexin-B1 by an antibody also initiates the R-Ras GAP activation, indicating that receptor clustering is a requisite step for expression of R-Ras GAP activity of plexin-B1. The Sema4D/plexin-B1 stimulated R-Ras GAP activity is responsible for cell collapse in COS7 cells, growth cone collapse and reduced neurite growth in rat hippocampal neurons (Oinuma et al., 2004b; Oinuma et al., 2004a). Thus plexin-B1 regulates Sema4D-induced repulsive axon guidance signalling through its R-Ras GAP activity.

Although Rnd1 is necessary for both PDZ-RhoGEF-mediated RhoA activation and R-Ras GAP activity of Sema4D/plexin-B1 signalling pathways, the plexin-B1-induced suppression of R-Ras activity is independent of plexin-B1-mediated RhoA activation. Inhibition of either activity does not affect the other. However inactivation of

either pathway results in inhibition of neurite retraction (Oinuma et al., 2004a; Perrot et al., 2002; Swiercz et al., 2002). Thus both R-Ras GAP activity and PDZ-RhoGEF mediated RhoA activation are required for Sema4D/plexin-B1-induced neurite retraction.

PI3K, an upstream kinase of Akt and GSK-3 β has been reported to be involved downstream of plexin-B1-mediated R-Ras GAP activity. Activated GSK-3 β phosphorylates CRMP2 (collapsing response mediator protein 2) to suppress its ability to promote microtubule polymerization and stabilization, leading to inhibition of axonal elongation. Phosphorylated PI3K is a negative regulator on GSK-3 β activity. Sema4D induces a decrease in Akt phosphorylation and GSK-3 β , resulting in activation of GSK-3 β and subsequent phosphorylation of CRMP2 in hippocampal neurons (Ito et al., 2006). This alteration follows the same time course as Sema4D-induced cell rounding in COS7 cells. Plexin-B1 lacking R-Ras GAP activity does not initiate Akt/GSK-3 β /CRMP2 phosphorylation in response to Sema4D, indicating that the R-Ras GAP activity is required for Sema4D/plexin-B1-induced inactivation of PI3K/Akt and activation of GSK-3 β . Thus plexin-B1 induces growth cone collapse by activating GSK-3 β through its R-Ras GAP activity in response to Sema4D.

Integrins are a family of cell surface receptors that bind to the ECM. Activation of integrins is essential for cell adhesion and migration (Hood and Cheresh, 2002). Integrins are regulated by activated R-Ras that induces integrin activation and increase cell adhesion and matrix assembly (Sethi et al., 1999; Zhang et al., 1996). Suppression of R-Ras results in decreased cell adhesion and neurite growth. Barberis and his colleagues have reported that Sema4D/plexin-B1 signalling inhibits integrin-mediated cell adhesion

and migration independent of Rho-kinase activity in a variety of cell lines (Barberis et al., 2004). The R-Ras GAP activity of plexin-B1 is found to be responsible for the inhibition of integrin-based adhesion and migration. Through its R-Ras GAP activity, activated plexin-B1 suppresses the ECM-dependent R-Ras activation and downstream PI3K kinase activity, subsequently resulting in inhibition of cell migration through inactivation of β_1 integrin (Oinuma et al., 2006).

1.3.4 M-Ras

M-Ras belongs to the Ras GTPase family and shares relatively similar homology with R-Ras. Distinct from the regulatory role of R-Ras in axonal growth, M-Ras is involved in the process of dendritic outgrowth and branching. M-Ras is predominantly expressed in the central nervous system of both human and mouse and it is particularly abundant in the cortex and hippocampus revealed by in situ hybridization (Kimmelman et al., 2002). In primary cultured cortical neurons from E18.5 rats, expression of M-Ras increases during the stage when dendrites begin to grow and it is required for normal dendrite development in cortical neurons (Saito et al., 2009). M-Ras knockdown impairs dendritic outgrowth and branching, while over-expression of constitutively active M-Ras promotes dendrite growth. In differentiated PC12 cells M-Ras stimulates the extracellular signal-regulated kinase (ERK) pathway through activating B-Raf, thereby promoting neurite outgrowth (Kimmelman et al., 2002; Sun et al., 2006). Plexin-B1 is associated with active M-Ras and the interaction between plexin-B1 and M-Ras requires Rnd1 binding to plexin-B1 (Saito et al., 2009). Upon stimulation by Sema4D, M-Ras activity is

suppressed by plexin-B1-mediated M-Ras GAP activity. The down-regulated M-Ras activity is correlated with Sema4D-induced dendrite remodelling in both cortical neurons and hippocampal neurons, indicating that Sema4D/plexin-B1 regulates remodelling of dendrite morphology through its GAP activity toward M-Ras. ERK signalling downstream of M-Ras is responsible for the Sema4D-induced decrease of dendrite growth. Sema4D decreases ERK phosphorylation and over-expression of constitutively active form of upstream kinase of ERK, MEK1, blocks the Sema4D-reduced dendritic outgrowth and branching (Saito et al., 2009). Therefore Sema4D/plexin-B1 regulates axonal growth and dendrite morphology through its R-Ras GAP and M-Ras GAP activity, respectively. This dual role of Sema4D/plexin-B1 signalling pathway is crucial for its fine-tuning in the complex formation of the neuronal network.

1.3.5 RhoD

RhoD GTPase is one of the members of the small GTPases and its functional properties in endosome dynamics have been well characterized. Protein RhoD localizes to the plasma membrane and early endosomes (Murphy et al., 2001). Over-expression of RhoD induces disassembly of stress fibres and focal adhesions, inhibits endosome fusion and decreases endosome motility (Murphy et al., 1996; Murphy et al., 2001). Therefore RhoD functions differently from other Rho family GTPase proteins and it functions to slow vesicle transport. Expression of constitutively active RhoD in the endothelial cells, BBCE, decreases cell motility. The role of RhoD in plexin signalling was firstly reported by Zanata's group. They have shown that RhoD binds to plexin-A1 in a GTP dependent

manner (Zanata et al., 2002). RhoD negatively regulates plexin-A1 signalling through inhibiting Rnd1-dependent cell collapse induced by Sema3A. Tong and his colleagues reported that plexin-B1 binds to RhoD through protein structure studies (Tong et al., 2007). Yet there is no in vivo evidence of interaction between plexin-B1 and RhoD. The biological function regulated by plexin-B1/RhoD signalling remains to be elucidated.

1.3.6 PDZ-RhoGEF/LARGE

PSD-95/Dlg/ZO-1 (PDZ)-RhoGEF (GEF, guanine nucleotide exchange factor) and leukemia-associated RhoGEF (LARG) are two Rho-specific guanine nucleotide exchange factors that stimulate the GDP-GTP exchange reaction of RhoA (Fukuhara et al., 1999; Fukuhara et al., 2000). PDZ-RhoGEF and LARG share high homology in sequence and both proteins contain multiple domains, including a RGS (regulator of G protein signalling) domain, a DH (Dbl homology) domain, a PH (pleckstrin-homology) domain and a PDZ domain. PDZ-RhoGEF/LARG interact through their RGS domains with activated G_{12}/G_{13} , which couples GPCRs (G protein-coupled receptors) to RhoA and regulates RhoA activation (Fukuhara et al., 1999; Fukuhara et al., 2001). Activation of RhoA results in actin/myosin contractility and subsequent process retraction or growth cone collapse. The DH and PH domains of PDZ-RhoGEF/LARG are critical for their ability to stimulate nucleotide exchange towards GTPase for RhoA. The PDZ domain of PDZ-RhoGEF/LARG binds to a consensus motif (S/TXV) in the carboxyl termini of partner proteins or other PDZ domains. The extreme C-terminal of plexin-B1 contains a sequence of VTDL that conforms to a typical PDZ-binding motif (Aurandt et al., 2002).

Several lines of evidence have shown that both PDZ-RhoGEF and LARG can specifically interact via their PDZ domains with the cytoplasmic PDZ-binding domain of plexin-B1 to regulate RhoA and cell cytoskeleton organization (Aurandt et al., 2002; Swiercz et al., 2002). Therefore PDZ-RhoGEF and LARG act as crucial signal transducers between plexin-B1 signalling and RhoA activation.

PDZ-RhoGEF/LARG and plexin-B1 in the nervous system show an overlapping expression pattern, providing supportive evidence for the interaction between plexin-B1 and PDZ-RhoGEF in neuronal compartments in vivo (Swiercz et al., 2002). PDZ-RhoGEF and plexin-B1 both distribute over neuropil of the hippocampus in adult mouse brain. In dissociated chick retinal ganglion neurons in culture, both PDZ-RhoGEF and plexin-B1 are enriched in axonal growth cones and exhibit a large overlap with each other. Both immunoprecipitation and yeast two-hybrid analysis reveal that PDZ-RhoGEF interacts with plexin-B1 (Swiercz et al., 2002). Either deletion of C-terminal amino acids in plexin-B1 or mutants of PDZ-RhoGEF lacking the PDZ domain results in abrogation of this interaction, indicating this interaction is mediated by the PDZ domain of PDZ-RhoGEF and the PDZ-binding motif in plexin-B1. In addition, PDZ-RhoGEF facilitates the enrichment of plexin-B1 at the plasma membrane. The PDZ domain is required for its binding to plexin-B1, whereas DH and PH domains are necessary for Sema4D/plexin-B1-induced Rho activation (Swiercz et al., 2002). Activation of plexin-B1 by Sema4D activates the activity of DH and PH domains of PDZ-RhoGEF, resulting in RhoA activation and subsequent growth cone collapse in primary hippocampal neurons, neurites retraction and cell rounding in differentiated rat pheochromocytoma (PC12) cells,

and cell contraction in COS-7 cells (Oinuma et al., 2003; Perrot et al., 2002; Swiercz et al., 2002).

LARG was identified as a mixed lineage leukemia fusion protein in patients with primary acute myeloid leukemia (Kourlas et al., 2000). The mechanism of LARG/plexin-B1 interaction is the same as that for PDZ-RhoGEF/plexin-B1. The PDZ domain of LARG contains a conserved structure which coordinates the protein's interaction with its corresponding binding proteins. Mutation of lysine 77 within this structure significantly weakens the binding of LARG to plexin-B1, indicating that PDZ domain is crucial in mediating the LARG/plexin-B1 interaction. In addition, the interaction between plexin-B1 and LARG is not dependent on Sema4D stimulation. LARG GEF activity is specific for the small GTPase RhoA (Reuther et al., 2001). Activation of plexin-B1 by Sema4D regulates coupled LARG, resulting in RhoA activation and further regulation of the cell cytoskeleton (Aurandt et al., 2002).

The PDZ-RhoGEF/LARG-mediated RhoA activation is an important step for migratory and pro-angiogenic response elicited by Sema4D in endothelial cells (Basile et al., 2004; Basile et al., 2007). In response to Sema4D, plexin-B1 activates PI3K/Akt and MAPK pathways through RhoA by regulating the integrin-dependent signalling network (Aurandt et al., 2006; Basile et al., 2007). This point will be fully discussed in section 1.3.10.

1.3.7 p190-RhoGAP

p190, also known as p190A, is a ubiquitously expressed GTPase activating protein (GAP). It is one of the main effectors of localized Rho down-regulation under the control of plasma membrane receptors and tyrosine kinases (Brouns et al., 2000). It has been shown that p190 plays a crucial role in regulating cytoskeletal dynamics through inhibiting focal adhesions and myosin-mediated F-actin contraction. Recently, it has been reported that p190 associates with plexins and is required for semaphorin signalling (Barberis et al., 2005). Plexin-B1 specifically associates with p190-RhoGAP and the interaction transiently increases upon stimulation with Sema4D. p190-RhoGAP down-regulates the RhoA activity and is required for semaphorin signalling functions in several different cell lines. Gene-deficient fibroblasts derived from p190^{-/-} mice do not exhibit disassembly of integrin-based focal adhesion or inhibition of cell-spreading on fibronectin upon plexin-B1 activation. Re-introduction of p190 expression in this p190-deficient fibroblast restores the phenotypes of disassembly of integrin-based focal adhesion and subsequent collapse. Barberis et al. also found that HUVEC cells defective in p190 expression by siRNA do not demonstrate the retraction in response to Sema4D compared with the wildtype. All together, their findings reveal the mechanism of RhoA inactivation in Sema4D/plexin-B1 signalling.

1.3.8 Met and Ron

The scatter factor receptors, Met, the tyrosine kinase receptor for hepatocyte growth factor (HGF), and RON, the receptor for the macrophage stimulating protein (MSP), are single-pass disulfide-linked α/β heterodimers with intrinsic tyrosine kinase activity (Gaudino et al., 1994; Naldini et al., 1991; Trusolino and Comoglio, 2002). In both proteins, the α -chains are completely extracellular, whereas the β -chains are transmembrane subunits containing the tyrosine kinase catalytic sites. Semaphorins, plexins, and scatter factor receptors are grouped into the semaphorin superfamily based on the structural homology of the extracellular sema domain. C-terminal next to the sema domain, both Met and RON have a copy of CRD that is termed as MRS (Met-related sequence), and four copies of an Ig domain, referred to as the transcription factor Ig domain (Gherardi et al., 2004). The cytoplasmic moieties of Met and RON are more divergent than their extracellular domain and are responsible for their kinase activity. Unlike wide expression of semaphorins and plexins across invertebrates and vertebrates, Met and RON proteins are only expressed in vertebrates. On ligand binding, Met and Ron become activated and trigger pleiotropic responses leading to invasive growth that is a complex biological programme instructing cell dissociation, migration, colonization, proliferation, and differentiation. Met activation is implicated in many biological processes such as epithelial morphogenesis, endothelial cell migration, and organization of new blood vessels during angiogenesis (Grant et al., 1993; Weidner et al., 1993).

Both Met and Ron interact with all the three members of plexin-B family irrespective of ligand binding (Conrotto et al., 2004). This interaction requires the

extracellular domains of both receptors and is specific to all the class B plexins (Giordano et al., 2002). Sema4D stimulation induces phosphorylation of plexin-B1 and indirectly activates Met and the substrate Gab-1 via plexin-B1. The mechanism underlying Sema4D-induced Met phosphorylation is not clear yet. However, it is hypothesized that Sema4D-induced plexin-B1 clustering drives oligomerization and activation of Met. Yet this needs to be further investigated and more evidence obtained. On Sema4D stimulation, Met and Ron are activated and promote invasive growth in several cell lines such as MLP29 and NIH 3T3. Suppression of Met activity results in impairment of Sema4D-induced invasive growth of cells, indicating that recruitment of Met through plexin-B1 is crucial for Sema4D-induced invasive growth. Interestingly over-expression of plexin-B1 is observed in several cancer cell lines derived from colon, liver, pancreas and gastric carcinomas, and the over-expressed plexin-B1 is constitutively tyrosine phosphorylated and associated with activated Met (Conrotto et al., 2004). Cells over-expressing plexin-B1 exhibit constitutive invasive phenotypes including spontaneously formed branched structures, constitutive motility and anchorage-independent growth (Conrotto et al., 2004; Giordano et al., 2002). On the other side, over-expression of Met is frequent in human tumors and Ron plays oncogenic role in several human carcinomas (Danilkovitch-Miagkova and Zbar, 2002; Maggiora et al., 1998; Zhou et al., 2003). The cross-talk between plexin-B1 and scatter factors in regulating cell invasion provides a new mechanism of finely tuning the invasive growth program both in physiological conditions and in tumor growth and metastasis.

In addition to its regulatory role in invasive growth of cells, the Sema4D/plexin-B1-induced Met activation is also involved in angiogenesis. In primary endothelial cells,

Sema4D stimulates EC migration, capillary-like tubes formation, and cytoskeletal reorganization through activating Met coupled by plexin-B1. During brain development, Sema4D-induced activation of plexin-B1-Met complex is also required for guiding GnRH-1 (Giacobini et al., 2008) cells to their appropriate destinations. Taken together scatter factors in conjunction with plexin-B1 play a broad spectrum of biological functions in migration, angiogenesis and embryonic development.

1.3.9 ErbB-2

ErbB-2 (also known as HER2) is a member of the ErbB (epidermal growth factor receptor) family that consists of four closely related type 1 transmembrane tyrosine kinase receptors, ErbB-1, ErbB-2, ErbB-3, and ErbB-4. They are potent mediators of normal cell growth and development and malfunctions of ErbB signalling network are correlated with cancer (Hynes and Lane, 2005; Yarden and Sliwkowski, 2001). ErbB-2 has the common structure shared by all the family members, an extracellular domain, an α -helical transmembrane segment and an intracellular tyrosine kinase domain (Olayioye et al., 2000). However, ErbB-2 is unique as it does not have a known ligand and can only be activated by dimerization with one of the other three ErbB proteins. In the normal state, ErbB-2 exists as inactive monomer folded to prevent dimerization. ErbB-2 has been strongly implicated in the development and progression of cancer. Over-expression of ErbB-2 has been reported in a number of human tumors including breast cancer, ovarian cancer, gastric carcinoma and salivary gland tumors (Jaehne et al., 1992; Slamon et al., 1987; Vermeij et al., 2008).

ErbB-2 associates with all the three plexins of class B through the extracellular domains of both receptors (Swiercz et al., 2004). Sema4D/plexin-B1 induces phosphorylation of ErbB-2 and subsequent plexin-B1 phosphorylation. The tyrosine residues 1139 and 1248 on ErbB-2 are phosphorylated in response to Sema4D, while tyrosines 1112, 1139, and 1248 are activated through ErbB-1/ErbB-2 heterodimer by EGF. The Sema4D-induced phosphorylation of ErbB-2 requires plexin-B1, whereas EGF-induced activation of ErbB-2 does not have the ability to activate plexin-B1. Therefore, Sema4D indirectly activates the tyrosine kinase of ErbB-2 and the subsequent autophosphorylation of ErbB-2 induces plexin-B1 activation. Grb 2 and Shc are two substrates of ErbB-2 and are activated through binding to phosphorylated tyrosine residues 1139 and 1248. Phosphorylated Shc then mediates ErbB-2-dependent Erk activation. Sema4D is found to activate Shc and Erk downstream of ErbB-2. ErbB-2 mutated of its cytoplasmic tyrosine kinase activity totally blocks Sema-4D-induced RhoA activation through plexin-B1/PDZ-RhoGEF, however Erk activation downstream of ErbB-2 is not required for RhoA activation. Interestingly, activated ErbB-2 by EGF does not initiate plexin-B1 phosphorylation and RhoA activation in response to Sema4D. ErbB-2 expression is found in axonal growth cones of primary hippocampal neurons cultured from rat embryos and staining with antibody against phosphorylated tyrosine 1248 reveals that Sema4D-induced activation of ErbB-2 occurs in the central region of the growth cones. ErbB-2 deleted of its tyrosine kinase completely abolishes plexin-B1/PDZ-RhoGEF-mediated growth cone collapse in hippocampal neurons. Thus ErbB-2 is critically involved in Sema4D-induced plexin-B1 activation and subsequent signalling process through RhoA activation.

Activation of RhoA via plexin-B1/PDZ-RhoGEF requires ErbB-2, while Met is required for RhoA inactivation. ErbB-2 and Met have pro-migratory and anti-migratory effects, respectively, based on the investigation on breast cancer cell lines MCF-7 and MDA-MB-468 (Swiercz et al., 2008). Exchange of ErbB-2 and Met is sufficient to convert the cellular response to Sema4D from pro- to anti-migratory and vice versa. These findings on regulatory role of Met on cell motility in context with plexin-B1 by Swiercz group are contradictory to the report of Giordano et al. (Giordano et al., 2002; Swiercz et al., 2008). The controversial role of Met might depend on cell types and other factors involved in plexin-B1 signalling. The discussion about this point will be provided in the introduction and discussion part in Chapter 4.

1.3.10 PI3K/Akt, PYK2, Src, MEK, and MAPK

It has been discussed in section 1.3.4 that the PI3K/Akt pathway is suppressed upon Sema4D activation via the R-RasGAP activity of plexin-B1 in hippocampal neurons. In contrast Swiercz and his colleagues have shown Akt is activated via plexin-B1/ErbB-2-mediated Rho activation (Swiercz et al., 2004). PI3K/Akt pathway has also been reported to be activated in response to Sema4D in endothelial cells and its activation is required for Sema4D/plexin-B1-mediated cell migration (Basile et al., 2005). Sema4D/plexin-B1-mediated activation of PI3K/Akt pathway is dependent on PYK2 and Src. PYK2 is a tyrosine kinase member of FAK family. Upon Sema4D stimulation, PYK2 is phosphorylated at its tyrosine residues 579, 580 and 881 leading to the relief of autoinhibition and consequent activation of PYK2. Src is often functionally associated

with FAK family members and in context with Sema4D/plexin-B1 signalling Src is phosphorylated on tyrosine 416. In consequence, PI3K becomes tyrosine phosphorylated on its p85 regulatory subunit and Akt is also activated. The activation of PI3K/Akt is Src-dependent and inhibition of Src enzymatic activity abolishes PI3K/Akt phosphorylation in response to Sema4D. On Sema4D binding, receptor plexin-B1 is also phosphorylated and activated. PYK2 has been reported to be required for plexin-B1 activation; however, Src is not necessary for plexin-B1 activation despite its indispensable role in Sema4D/plexin-B-mediated PI3K/Akt pathway signalling and subsequent endothelial cell migration. In fact PYK2 signals upstream of plexin-B1 activation. PYK2 associates with plexin-B1 after receptor stimulation and initiates plexin-B1 phosphorylation and Src-regulated cascade activation of PI3K/Akt. In addition, the p85 subunit of PI3K also associates with plexin-B1 soon after plexin-B1 stimulation and Src also associates with plexin-B1 in a complex. Therefore, Sema4D/plexin-B1 signalling pathway recruits PI3K and Src and activates PI3K/Akt pathway, resulting in endothelial cell migration.

The MAPK (mitogen-activated protein kinase) pathway is activated in response to Sema4D. In both endothelial cells and hippocampal cells expressing endogenous plexin-B1, MEK and its downstream kinase ERK both exhibit increased phosphorylation level in response to Sema4D stimulation (Aurandt et al., 2006; Basile et al., 2007; Swiercz et al., 2008). The activation of MAPK pathway requires Ras, which co-operates with Rho to activate Raf and downstream MAPK. The mechanism underlying the role of Ras and Raf in Sema4D/plexin-B1-mediated MAPK needs to be elucidated with more evidence.

The PDZ-RhoGEF/LARG-mediated RhoA activation is required for either PYK2-regulated activation of PI3K/Akt pathway or activation of MAPK pathway. In endothelial cells, Sema4D/plexin-B1 signalling initiates the actomyosin cytoskeleton reorganization through RhoA and ROK leading to promotion of integrin-dependent assembly of focal adhesion, which results in cell adhesion and facilitates cell migration. The focal adhesion complexes associate with PYK2 which in turn activate PI3K/Akt pathway in response to Sema4D. This observation of pro-migratory effect of Sema4D/plexin-B1 through activation of PI3K/Akt pathway in endothelial cells is opposite to the report that Sema4D/plexin-B1 inhibits migration and adhesion through suppression of PI3K by the Japanese group. The difference is possibly due to different cell types. On the other hand, MAPK pathway activation by Sema4D/plexin-B1 signalling is also abolished in cells in which PDZ-RhoGEF-mediated RhoA activity has been inhibited, indicating the requirement of RhoA activity in MAPK activation.

1.4 Plexin-B1 mutations in prostate cancer

Previously our group have reported plexin-B1 mutations in both prostate cancer cell lines and clinical samples of prostate cancer (Wong et al., 2007). Over-expression of plexin-B1 protein in primary prostate cancers was also observed. Using SSCP analysis, we screened exons 22-29 of the cytoplasmic domain of the plexin-B1 in DNA from tumor tissues. Mutations were detected in 89% (8 of 9) of prostate cancer bone metastases, in 41% (7 of 17) of lymph node metastases, and in 46% (41 of 89) of primary prostate tumors. Among all the mutations, some mutations are present in relatively higher

frequency. A5653G (Thr1795Ala) is present in 9 of 26 (35%) metastases and 38 of 89 (43%) primary cancers. T5714C (Leu1815Pro) is found in three metastases and in two primary tumors. A single nucleotide change (A5359G) in plexin-B1 in LNCaP changes threonine 1697 to an alanine. This mutation is present in two of the three copies of chromosome 3p in LNCaP cells. Previous studies on these three mutants revealed that the mutations altered the function of the plexin-B1 protein, increasing cell invasion, adhesion, and lamellipodia extension and decreasing collapse relative to wildtype plexin-B1 (Wong et al., 2007). The mutations inhibit or hinder Rac1 and R-Ras GTP binding and R-Ras GAP activity. Table 1.1 summaries the alterations of protein interaction of the three mutated forms relative to the wildtype plexin-B1.

Table 1.1 Protein function changes of the plexin-B1 mutations relative to wildtype

	Rac binding	Rnd binding	R-Ras binding	RhoD binding	ErbB-2 binding	Met binding	PDZ-RhoGEF binding
wt	binds	binds	binds	unknown	binds	binds	binds
A5359G	reduced	binds	lost	unknown	unknown	unknown	binds
A5653G	reduced	binds	lost	unknown	unknown	unknown	binds
T5714C	lost	lost	lost	unknown	unknown	unknown	binds

However, it is not yet known whether the mutations have any effect on the coupling of plexin-B1 to receptor tyrosine kinases such as ErbB-2 and Met. It is also not clear that if RhoD binding is altered by the mutations, given the fact that the mutated sites are located within the GTPase binding region. Therefore, my study aims to find answers to these

unknown questions and to further explore the effects of mutations on cell signalling and cell function.

Hypothesis

Based on the previous finding that plexin-B1 mutations are highly frequent in primary and metastatic prostate cancer and the mutations alter protein functions, I hypothesized that plexin-B1 mutations play an important role in prostate cancer progression through exerting effects on cell signalling and subsequently cell functions. The signalling pathways affected by plexin-B1 mutations may be (1) interaction with non-receptor/receptor tyrosine kinases such as Met, ErbB-2 and MAPK; (2) interaction with small GTPases such as RhoD. These pathways on top of other altered features by plexin-B1 mutations, e.g. R-Ras GAP activity, Rac1 binding ability, will contribute to the increased motility characteristic of plexin-B1 mutants.

Aim

The aim of this project was to characterize the effects of the three mutated forms of plexin-B1, A5359G, A5653G and T5714C, on cell signalling and cell functions.

Objectives

The objectives were to determine if mutation of plexin-B1 (1) alters interaction of plexin-B1 with Met; (2) alters interaction with ErbB-2; (3) alters interaction with RhoD; (4) affects motility of prostate cancer cells.

Chapter 2

Materials and Methods

2.1 Cell culture

All cell lines were maintained at 37°C, 5% CO₂ in T-25 flasks. Cell lines LNCaP, DU145, PC3, PC3-LN3, 22RV1, 1532NPT, 1542CPT and 1542NPT were maintained in RPMI1640 (Invitrogen) supplemented with 8% fetal bovine serum (FBS, Invitrogen). Cell lines HEK293, MCF7 and COS7 were cultured with DMEM (Invitrogen) supplemented with 8% FBS. PC12 cells were maintained in RPMI1640 medium supplemented with 10% horse serum.

Table 2.1 Cell line information

Name	Disease	Source	Species	Metastatic site
LNCaP	carcinoma	prostate	human	lymph node
DU145	carcinoma	prostate	human	brain
PC3	adenocarcinoma	prostate	human	bone
PC3-LN3	adenocarcinoma	prostate	human	lymph node
22RV1	carcinoma	prostate	human	N/A
1532NPT	benign	prostate	human	N/A
1542CPT	carcinoma	prostate	human	N/A
1542NPT	benign	prostate	human	N/A
HEK293	N/A	embryonic kidney	human	N/A
MCF7	adenocarcinoma	mammary gland	human	pleural effusion
COS7	N/A	kidney	monkey	N/A
PC12	pheochromocytoma	adrenal gland	rat	N/A

2.2 RNA extraction

RNA was extracted according to the manufacturer's instructions using the RNeasy Mini Kit (Qiagen). 80% confluent cells (no more than 1×10^7 cells) were washed with PBS (Invitrogen) and detached from culture flasks using trypsin (Invitrogen). Cells were centrifuged and collected as cell pellets in eppendorfs. Cells were loosened by flicking and then lysed in 350 μ l of Buffer RLT with β -ME (β -Mercaptoethanol) supplied by the Kit. The lysate was mixed by pipeting and loaded onto a QIAshredder spin column placed in a 2 ml collection tube, and centrifuged for 2 minutes at 13,000 rpm. An equal volume of 70% ethanol was then loaded onto an RNeasy mini column placed in a 2 ml collection tube and centrifuged for 15 seconds at 13,000 rpm. The flow-through was discarded. 700 μ l of Buffer RW1 (supplied by the Kit) was added to the RNeasy column and centrifuged for 15 seconds at 13,000 rpm. The flow-through was discarded after centrifuge. Columns were then washed twice with Buffer RPE (supplied by the Kit) by centrifuge for 15 seconds at 13,000 rpm. RNA in the RNeasy column was then eluted using 30-50 μ l of RNase-free water. RNA samples were stored at -70°C .

2.3 RT-PCR

All the procedures were performed using RNase free eppendorfs and tips. The first-strand cDNA was synthesized using SuperScript II RT (Invitrogen) at room temperature. RNA samples were mixed with Oligo (dT) and dNTP Mix, diluted to the appropriate volume in RNase free H_2O . The mixture was heated to 65°C for 5 minutes,

followed by quick chilling on ice. Appropriate quantities of 5 × First-strand buffer and 0.1M DTT were added to the mixture and mixed gently. The mixture was incubated at 42°C for 2 minutes. 1 µl of SuperScirp™ II Reverse Transcriptase was added to the mixture and incubated at 42°C for 50 minutes. The reaction was inactivated by heating at 70°C for 15 minutes. The synthesized cDNA was ready for PCR or stored at -20°C.

Primers

GAPDH	5'-CCACCCATGGCAAATTCCATGGCA-3'
GAPDH antisense	5'-TCTAGACGGCAGGTCAGGTCCAC-3'
Sema4D	5'-CGCCACAGCGACCTGCGTG-3'
Sema4D antisense	5'-GACATGAGGAGGCGGTTGTC-3'
Plexin-B1	5'-TGCCGCTCGCTGTGAAGTAC-3'
Plexin-B1 antisense	5'-CCACAGCAGCTGCAATCTGC-3'

PCR reactions

95°C 1 minute

95°C 50 seconds
60°C 50 seconds
68°C 1 minute

} 28 cycles

68°C 7 minutes

2.4 Agarose electrophoresis for DNA

DNA products were analyzed by agarose gel electrophoresis. 1% agarose gel was set by heat dissolving 1 g of agarose mixed with 100 0.5 × ml Tris-borate-EDTA (TBE, 90mM Tris-borate, 2mM EDTA, pH8.3) buffer. 2 µo of ethidium bromide (0.5 µg/ml) was added before the gel was set. DNA samples were mixed with 6 × DNA loading dye (0.25 bromophenol blue, 0.25% xylem cyanol FF, 30% glycerol) to make the final concentration of 1 × of loading dye. 0.5 µg of 1kb Plus DNA ladder (Invitrogen) was loaded as the marker for DNA sizes. Electrophoresis was carried out in TBE buffer in the electrophoresis unit Electro-4Gel Tank (Thermo Electron Corporation) at 150 V for around one hour. The DNA in complex with ethidium bromide was visualized using UV transilluminator (Gene Genius, Bio Imaging System).

2.5 Plasmid constructs

The vector maps are presented in Appendix 1. Constructs expressing Met and VSV-plexin-B1 wildtype were gifts from Dr. Luca Tamagnone (University of Torino School of Medicine, Italy). Plasmids encoding constitutively active RhoD pEF-BOS/Myc-RhoD (G26V) and dominant negative RhoD pEF-BOS/Myc-RhoD (T31K) were generously provided by Professor Takeshi Endo (Chiba University, Japan). Constructs expressing VSV-tagged plexin-B1mutants and GST-cyto-plexin-B1 WT/mutants were from previous group member Dr. Oscar Wong. Constructs encoding

Sema4D fused to human IgG₁ Fc fragment was provided by Dr. Hitoshi Kikutani (Osaka University, Japan).

2.6 Transformation of *E. Coli*

Subcloning EfficiencyTM DH5 α TM Competent cells (Invitrogen) were used for transformation. 0.25 μ g of plasmids was mixed with 50 μ l of competent cells gently and the mixture was then incubated on ice for 20 minutes. After the incubation the mixture was heat-shocked at 42°C for 1 minute and followed by 2 minutes incubation on ice. 300 μ l of S.O.C. medium (Invitrogen) was added to the cells and the mixture was incubated at 37 °C for one hour. After the incubation, 80 to 100 μ l of the mixture was spread on a LB agar plate supplemented with the appropriate selective antibiotic (ampicillin, 50 μ g/ml). The plate was then incubated at 37°C overnight and colonies were picked the next day.

2.7 DNA purification

Plasmid DNA was purified using the QIAGEN Plasmid Maxi Kit (Qiagen) at large scale. One single colony was picked from the overnight LB agar plate described in previous paragraph and inoculated into 2-5 ml of LB medium supplemented with the appropriate selective antibiotic. The starter culture was then incubated at 37 °C for 8 hours with vigorous shaking at 300 rpm. The starter culture was then diluted 1/500 to 1/1000 (100 ml or 500 ml) with selective LB medium. The culture was then incubated at

37 °C for 12-16 hours with vigorous shaking at 300 rpm. Bacterial cells were collected by centrifugation at 6,000 g for 15 minutes at 4 °C and then resuspended in 10 ml Buffer P1 (supplemented with RNase A which was supplied by the Kit). Until the cells were evenly suspended, 10 ml of Buffer P2 (supplied by the Kit) was added and mixed by inverting 4-6 times. The mixture was incubated at room temperature for 5 minutes. After that 10 ml of chilled Buffer P3 (supplied by the Kit) was added immediately and mixed gently by inverting 4-6 times. The mixture was incubated on ice for 20 minutes. At the end of incubation, the mixture was centrifuged at 20,000 g at 4°C for 30 minutes and the supernatant was collected. The supernatant was further cleared by another centrifugation at 20,000 g for 15 minutes at 4 °C. The DNA containing supernatant was then applied to a QIAGEN-tip 500 that was equilibrated with 10 ml of Buffer QBT (supplied by the Kit). The supernatant was allowed to enter the resin by gravity flow. The QIAGEN-tip was then washed with two portions of 30 ml of Buffer QC (supplied by the Kit) by gravity flow. DNA was eluted with 15 ml of Buffer QF (supplied by the Kit) and then precipitated by mixing with 10.5 ml of room temperature isopropanol. Immediately the mixture was centrifuged at 15,000 g for 30 minutes at 4°C. After the centrifuge the supernatant was removed. The DNA pellet was washed with 5 ml of room temperature 70% ethanol and centrifuged at 15,000 g for 10 minutes. The supernatant was removed and the pellet was left for air-dry for 5-10 minutes. The DNA was then dissolved in a suitable volume of TE buffer, pH 8.0 and DNA concentration was measured by spectrophotometry at a wavelength of 260nm/280nm using UV/Visible Spectrophotometer Ultrospec 3100 Pro.

2.8 Lipofectamine transfection

The ratio of DNA (μg) to LipofectamineTM 2000 (μl , Invitrogen) was dependent on the size of the culture flasks used. The details of different scales of transfection were listed in Table 2.2. The following protocol describes the transfection procedure in 6-well plates. One day before transfection, cells were plated in 2 ml of growth medium so that cells would be 95% confluent at the time of transfection. For each well, 4 μg of plasmid constructs was diluted in 250 μl of Opti-MEM[®]I medium (Invitrogen). 10 μl of LipofectamineTM 2000 was diluted in 250 μl of Opti-MEM[®]I medium and was incubated for 5 minutes at room temperature. After the incubation, the diluted DNA was mixed gently with diluted LipofectamineTM 2000 to give a total volume of 500 μl . The mixture was then incubated for 20 minutes at room temperature and added to the well containing cells and medium. Cells were incubated with the Lipofectamine-DNA complex for 4 hours and fresh medium was added. Cells were incubated for 24-48 hours before further study.

Table 2.2 Scaling up or down transfections

Culture vessel	Surface area per well	Volume of dilution medium	DNA	Lipofectamine TM 2000
6-well	10 cm ²	2 × 250 μl	4.0 μg	10 μl
60-mm	20 cm ²	2 × 250 μl	8.0 μg	20 μl
10-cm	60 cm ²	2 × 250 μl	24 μg	60 μl

2.9 Protein extraction

Cells ready for protein extraction were washed with cold 1 × PBS quickly and lysed in appropriate volume of modified radioimmunoprecipitation (RIPA) buffer [50 mM Tris-HCl, pH 7.4, 1% TritonX-100, 150 mM NaCl, 1 mM EDTA, 1 mM NaF, 1 mM Na₃VO₄, 1 protease inhibitor cocktails tablet per 10 ml of RIPA buffer (Roche)]. Cells were then scraped off using cell scraper (BD) and the cell lysate was transferred into a 1.5 ml eppendorf tube. The lysates were left on ice for 15 minutes and then centrifuged at 13,000 rpm for 15 minutes at 4°C. After the centrifuge the supernatant was collected in a pre-chilled eppendorf tube and ready for subsequent study or could be stored at -80°C.

2.10 Protein concentration measurement

The total protein concentrations of lysates extracted from cells were measured using Modified Lowry Protein Assay Kit (PIERCE). Serial dilutions of Bovine Serum Albumin (BSA) were made from the BSA standard solution (2 mg/ml, supplied by the Kit) as listed in Table 2.3,

Table 2.3 BSA standards preparation

Volume of standard solution (μl)	Distilled water (μl)	Final concentration ($\mu\text{g/ml}$)
0	200	0
1.56	198.44	15.63
3.13	196.87	31.25
6.25	193.75	62.5
12.5	187.5	125
25	175	250
50	150	500

10 μl of each lysate sample was diluted 20 folds with 190 μl of distilled water. 1 ml of Modified Lowry Protein Assay Reagent was added to each diluted sample or BSA standard and mixed gently. The mixture was incubated for exactly 10 minutes at room temperature. 2N Folin-Ciocalteu Reagent (supplied by the Modified Lowry Protein Assay Kit) was diluted 1/2 with distilled water to make the concentration of 1N. At the end of the 10 minute incubation, 100 μl of 1N Folin-Ciocalteu Reagent was added to each lysate sample or BSA standard and mixed gently. The mixture was incubated for 30 minutes at room temperature. Afterwards, the samples were measured using the UV/Visible Spectrophotometer Ultrospec 3100 Pro. Standard curve was plotted automatically by the machine based on absorbance readings against the concentrations of BSA standards. Readings of lysate samples were taken from the machine and concentrations were calculated by $\times 20$ of the values from the machine.

2.11 SDS-PAGE and protein blotting

Equal amount of total protein from lysate samples was normalized to the same volume using RIPA buffer. Appropriate volume of 6 × Sample Buffer (200 mM Tris, pH6.8, 60% glycerol, 12 mM EDTA, 12% SDS, 864 mM β-mercaptoethanol, 0.05% bromophenol blue) was added to the protein samples to reach the final concentration of 1 × SB. The mixture was heated at 95°C for 5 minutes. The denature protein samples were then ready to be loaded onto the sodium dodecyl sulphate (SDS)-polyacrylamide gel with appropriate concentration of acrylamide, depending on the size of the protein investigated. The recipe of SDS-polyacrylamide gel is listed in Table 2.3.

Table 2.4 Recipe of SDS-polyacrylamide gel

Resolving gel					
	6%	8%	10%	12%	14%
1 M Tris, pH8.8	3.75 ml				
30% Acrylamide	2 ml	2.67 ml	3.33 ml	4 ml	4.67 ml
H₂O	4.2 ml	3.53ml	2.87 ml	2.2 ml	1.53 ml
20% SDS	50 µl				
10% (APS)	100 µl				
TEMED	6 µl				

Table 2.4 Recipe of SDS-polyacrylamide gel (continued)

Stacking gel	
1 M Tris, pH 6.8	375 μ l
30% Acrylamide	374 μ l
H₂O	2.24 ml
20% SDS	15 μ l
10% APS	30 μ l
TEMED	5 μ l

For one SDS-polyacrylamide gel, around 8 ml of resolving gel solution was poured into the assembled Mini-PROTEAN III (Bio-Rad) gel cassette. When the resolving gel was set, stacking gel solution was prepared and poured onto the top of the resolving gel. The comb was placed into the stacking gel before the gel was set. When the whole gel was set, boiled protein samples were applied to the separated wells. 10 μ l of Rainbow Molecular Weight Marker (Amersham) was loaded as the reference for molecular sizes. The gel was subjected to electrophoresis using the Mini PRTOEAN III Electrophoresis System (Bio-Rad) at a constant current (20 mA per gel) in running buffer (25 mM Tris, 0.19 M glycine, 0.1% SDS) for 1-2 hours until the dye was running out from the bottom of the gel.

2.12 Western-blotting

Immediately after the SDS-PAGE, proteins on the SDS-polyacrylamide gel were electronically transferred onto a Polyvinylidene fluoride (PVDF) membrane (Millipore). The transfer sandwich, including the sponge, filter paper, gel and PVDF membrane, was assembled as illustrated below,



Every component of the transfer sandwich was rinsed in transfer buffer (25 mM Tris, HCl, 192 mM glycine, 20% methanol). The PVDF membrane was pre-wet in 100% methanol for 15 seconds and then rinsed in transfer buffer. The transfer sandwich was placed into the assembly tray of the Mini Trans-Blot Cell (Bio-Rad) which was filled with transfer buffer. The gel was closed to the cathode and the electrotransfer was carried out at a constant voltage of 20 V overnight at 4°C.

After electrotransfer, the membrane was rinsed briefly in PBS-Tween 20 (PBS-T, 0.1% Tween-20 in 1 × PBS) and blocked in 5% non-fat milk (in PBS-T) for 1 hour at room temperature. After blocking, the membrane was probed with 5 ml of appropriately diluted primary antibody (the details of antibodies used all through are listed in Table 2.4) in 1% non-fat milk (in PBS-T) and incubated for 1-2 hours at room temperature or overnight at 4 °C. After primary antibody incubation, the membrane was washed with PBS-T

for 2 minutes four times. After washing the membrane was incubated with 5 ml of appropriate horseradish peroxidase (HRP)-conjugated secondary antibody diluted in 1% non-fat milk (in PBS-T) for 1 hour. The membrane was then washed with PBS-T for 2 minutes four times and ready for enhance chemiluminescent (ECL) development.

The chemiluminescent signals were developed by Pierce ECL Western Blotting Substrate (PIERCE). Appropriate volume of mixture of Detection Reagents 1 and 2 at a 1:1 ratio was added to the membrane and incubated for 5 minutes at room temperature. The membrane was then placed between two sheets of transparency and set into a Kodak BioMax Cassette (Kodak). The membrane was exposed to X-ray films and the films were developed with developer and fixer solutions (Kodak).

Table 2.5 Antibody list

Against antigen	manufacturer	Catalogue no.	Dilution factor
Plexin-B1	Santa Cruz	sc-25642	1:1000
VSV tag	Sigma	V4888	1:1000
myc tag	Sigma	C3956	1:5000
plexin-B1 (C-terminal)	ECM	PP1841	1:1000
ErbB-2	Upstate	06-562	1:5000
Met	Santa Cruz	sc-161	1:1000
phospho-MEK1/2	Cell signaling	9154	1:1000
phospho-p44/42MAPK	Cell signaling	4377	1:1000
Akt	Cell signaling	9272	1:1000
phospho-Akt	Cell signaling	9271	1:1000
MEK1/2	Cell signaling	9122	1:1000

2.5 Antibody list (continued)

CD100	BD	61060	1:2000
beta-actin	Abcam	ab6276	1:5000
anti-Rabbit IgG-HRP	Santa Cruz	sc-2004	1:5000
anti-mouse IgG-HRP	Santa Cruz	sc-2005	1:5000

2.13 Immunoprecipitation

HEK293 cells were transfected with appropriate plasmids and cells were lysed as described in previous sections. 1 mg of total protein for each sample was used for each immunoprecipitation assay. Each sample lysate was normalized to the same volume of 1 ml. Sample lysate was then precleared by incubating with 20 μ l of Protein A agarose slurry (Invitrogen) by rotation at 4°C for 1 hour. The lysate was centrifuged at 12,000 rpm for 20 seconds and the supernatant was collected into a fresh eppendorf tube. 1 μ g of selective antibody against the targeted antigen was added into the precleared lysate and incubated for 3 hours at 4°C. the antigen-antibody complex was then mixed with 50 μ l of Protein-A agarose and incubated overnight at 4°C on a rocking platform. At the end of incubation, the antibody-sample complex with agarose was centrifuged at 12,000 rpm for 20 seconds at 4°C and the supernatant was removed by vacuum. The precipitated beads were then washed one with RIPA lysis buffer at 12,000 rpm for 20 seconds at 4°C. The second wash was carried out with high salt wash buffer (50 mM Tris-HCl, pH7.5, 500 mM NaCl, 0.1% TritonX-100) and the third wash was performed with low salt buffer

(50 mM Tris-HCl, pH7.5, 0.1% TritonX-100). After the wash, the agarose beads were pelleted and the last trace of wash buffer was removed. 40 µl of 1 × Sample Buffer was added to the bead pellet and mixed well gently. Proteins on the bound to the beads were released by heating at 95°C for 5 minutes. Samples were centrifuged and the supernatants were collected and ready to be analyzed by SDS-PAGE and immunoblotting.

2.14 Coomassie blue staining of SDS-polyacrylamide gel

At the end of SDS-PAGE, the SDS-polyacrylamide gel was fully immersed in the appropriate volume of Coomassie Plus Reagent (PIERCE) and incubated with mild shaking at room temperature for at least 1 hours. The stained gel was destained with distilled water for a couple of hours until blue protein bands were observed with good contrast with the blank gel. The gel was dried and preserved using Gel Drying Kit (Promega). Gel was soaked in gel drying solution (40% methanol, 10% glycerol, 7.5% acetic acid) for 3-5 minutes. Two sheets of Gel Drying Film (Promega) were rinsed briefly in the gel drying solution. After that the gel was placed in between of the two sheets and the films were clamped on the Gel Drying Frames and were left air-dry.

2.15 Inducing competence and transforming of BL21

The *E. coli* BL21 strain (Amersham) was used for expression of GST fusion proteins. Firstly BL21 cells were induced of competence. Lyophilized culture was resuspended in 1 ml of L-broth and grown overnight with shaking at 300 rpm at 37°C. the

overnight culture was then spread onto a L-broth medium plate and incubated for 12-16 hours at 37°C until colonies were formed. One single colony was picked and inoculated into 5 ml of LB medium and incubated overnight at 37°C with vigorous shaking at 300 rpm. 4 ml of the overnight culture was inoculated into 400 ml of LB medium and incubated at 37°C with vigorous shaking at 300 rpm until OD₅₉₀ was above 0.375. The culture was divided into eight portions and transferred into 50 ml pre-chilled tubes, followed by incubation on ice for 10 minutes. Bacterial cells were collected by centrifuge at 1,600 g for 7 minutes at 4°C. The cell pellets were re-suspended in 10 ml of ice-cold CaCl₂ solution (60 mM CaCl₂, 15% glycerol, 10 mM PIPES) and washed twice by centrifuge at 1,600 g for 7 minutes at 4°C. After washing steps, cells were suspended in 10 ml of ice-cold CaCl₂ solution and incubated on ice for 30 minutes. The bacterial cells were then precipitated by centrifuge at 1,100 g for 5 minutes at 4°C and the cell pellets were suspended in 2 ml of ice-cold CaCl₂ buffer. The competent BL21 cell solution was then divided into aliquots at 250 µl and stored at -80°C.

For transformation of BL21 cells with plasmids, 0.5 µg of plasmids was mixed gently with 250 µl of competent BL21 cells. The mixture was incubated on ice for 20 minutes and heat-shocked at 42°C for 1 minute. 300 µl of S.O.C. medium was then added to the bacterial cells and incubated at 37°C for 1 hour. 80-100 µl of the transformed cells was spread onto LB agar plates containing appropriate selective antibiotics (Ampicillin, 50 µg/ml, Sigma). The LB agar plates were incubated overnight at 37°C until colonies formed.

2.16 GST-cyto plexin-B1 purification

Plasmids pGEX-4T3 encoding GST-fused cyto-plexin-B1 wildtype or mutants were from previous group member Oscar Wong and described in his thesis. Competent BL21 cells were transformed with pGEX-cytoB1 WT/mutants as described in previous section. One single colony was inoculated into 200 ml of LB broth medium (ampicillin, 50 µg/ml) and incubated at 37°C with vigorous shaking at 300 rpm until OD₆₀₀ reached 0.6. Fusion protein expression was induced by adding 200 µl of 100 mM isopropyl β-D-thiogalactoside (IPTG) and the bacterial culture was incubated for additional 2 hours. The induced culture was centrifuged at 7,700 g for 10 minutes at 4°C and cell pellets were then lysed with 10 ml of CellLytic™ B buffer (Sigma) supplemented with 0.2 mg/ml lysozyme (Sigma), 50 µg/ml DNaseI (Sigma), 1 mM dithiothreitol (DTT), 10 µg/ml aprotinin, 10 µg/ml leupeptin, and 1 mM phenylmethylsulfonyl fluoride (PMSF). In alteration, cell pellets were lysed in 10 ml of lysis buffer (50 mM Tris, pH7.5, 1% Triton X-100, 150 mM NaCl, 5 mM MgCl₂, 1 mM DTT, 10 µg/ml aprotinin, 10 µg/ml leupeptin, and 1 mM PMSF). The lysed cells could be subjected to sonication on ice with a setting at 50% amplitude for six to eight times, 15 sec each using Sonic Vibra Cell. Lysed samples were kept on ice for 1-2 minutes between sonications.

The lysate was clarified by centrifugation at 14,000 rpm for 30 minutes at 4°C and the supernatant was collected. The supernatant containing the fused protein was then mixed with 200 µl of 50% slurry of Glutathione Sepharose 4B (Amersham) equilibrated with 1 × PBS and incubated on rotation overnight at 4°C. The matrix was centrifuged at 500 g for 5 minutes at 4°C and the supernatant was removed. The matrix was washed five

times with 1 ml of cold 1 × PBS by centrifuge. The matrix containing the GST-fused protein was then resuspended in 100 µl of 1 × PBS and used for GST-pull down assay. The matrix was stored at 4°C. 10 µl of the matrix was analyzed by SDS-PAGE (8% SDS-polyarylamide gel) and Coomassie blue staining to check the yield of GST-fused protein expression.

2.17 GST-pull down assay

Cell lysate expressing the target protein for interaction study was incubated with 20 µl of the matrix obtained in section 2.16 overnight with rotation at 4°C. The matrix was washed four times with cold 1 × PBS by centrifuge at 500 g for 5 minutes at 4°C. The supernatant was decanted and the sepharose beads were resuspended in 20 µl of 1 × sample buffer. Samples were heated at 95°C for 5 minutes and ready for analysis by SDS-PAGE and Western-blotting.

2.18 Generation and purification of Sema4D

COS7 cells were grown to 60% confluence in T-75 culture flasks and were transfected with plasmid encoding Sema4D-Fc using the Lipofectamine™ 2000 reagent. Cells were incubated in DMEM supplemented with 8% of low IgG FBS for 72 hours at 37°C for Sema4D-Fc secretion. Supernatant medium from 3 T-75 flasks was collected and centrifuged to get rid of cell debris. The Sema4D-Fc containing medium was

incubated with 2 ml of 50% slurry of Protein A Sepharose (Sigma) with rotation overnight at 4°C. Sepharose beads were precipitated by centrifuge and resuspended in 4 ml of cold 1 × PBS. The bead matrix was applied to a PBS equilibrated disposable column (Falcon) and left to drain by gravity flow. The column was washed with 15 ml of cold 1 × PBS. Sema4D-Fc was eluted using 2.5 ml of 100mM glycine, pH2.7, neutralized in 500 µl of 1M Tris, pH9.0. The eluted Sema4D-Fc was transferred into Amicon Ultra-4 Centrifugal filter Devices, 10K (Millipore) and concentrated by centrifuge at 3,000 rpm for 12 minutes. The Sema4D-Fc containing solute in the insert was collected and stored at -80°C. The yield of Sema4D-Fc was analyzed by SDS-PAGE and Coomassie blue staining.

In alteration, COS-7 cells were transfected with plasmid encoding GST-Sema4D-AP. After transfection and incubation, supernatant was clarified by centrifuge and applied to the matrix in a drained and washed Glutathione Sepharose 4B RediPack (GE Healthcare). The lysate was allowed to flow through by gravity flow. The fusion protein bound on the matrix was washed twice with 10 ml of cold 1 × PBS. After washing step, 1 ml of glutathione elution buffer (provided by the Kit) was added to the matrix and incubated for 10 minutes to elute the fusion protein. The elution step was repeated twice more and the three elutes were pooled together. The GST-Sema4D-Fc solute was analyzed by SDS-PAGE and Coomassie blue for quality check.

2.19 Dialysis of Sema4D concentrates

Sema4D concentrate was dialyzed to remove low molecular weight contaminant by using Slide-A-Lyzer Dialysis Cassette (Thermo scientific). The Slide-A-Lyzer Cassette was hydrated in dialysis buffer 1 × PBS for 1-2 minutes. Sema4D concentrate was added to the cassette by syringe injection. The sample was dialyzed for 2 hour at 4°C. After that the sample was dialyzed in fresh dialysis buffer for another 2 hours. Dialysis buffer was changed again and the dialysis was performed overnight at 4°C. The dialysis buffer was at 200-500 times the volume of the sample. After dialysis, the sample was collected by syringe and stored at -80°C.

2.20 Migration assay

Migration assays were performed using Transwell[®] Permeable Support System (Corning). Cells were serum starved overnight the day before migration assays and were detached from culture flasks using cell dissociation solution (Sigma). After dissociation step cells were suspended in culture medium without serum and 20,000 cells were seeded into each insert in the volume of 100 µl. The lower side of the inserts was coated with 15 µg/ml fibronectin (Sigma) for 2 hours at 37 °C before cell seeding. The wells of the lower plates were filled with the same culture medium as the inserts. Cells were incubated for 6 hours in the absence or presence of Sema4D. At the end of incubation, cells on the upper side of the inserts were removed using cotton buds and the cells on the lower sides were fixed with freshly prepared 4% paraformaldehyde for 15 minutes. Fixed cells were

stained with 0.5% crystal violet (in 20% ethanol) for 1 hour. The membrane was washed with distilled water and air dried. For each inserts, five different fields were randomly selected under the microscope at $100 \times$ magnifications and the cell numbers were counted. Relative cell migration was determined by the numbers of the migrated cells normalized to the number of control. Each experiment was repeated at least three times and the error bars indicated standard deviations.

2.21 Statistical analysis

For cell motility assays, P values were calculated using a two-Two-tailed Students *t*-test when comparing values of controls and treatments. $p < 0.05$ was considered statistically significant.

Chapter 3

Plexin-B1 expression in cancer cells

3.1 Introduction

Sema4D is expressed in a variety of tissues and organs, but strongly expressed mainly in lymphoid organs. In non-lymphoid organs, Sema4D is expressed at low levels. The receptor for Sema4D, plexin-B1, is reported to be ubiquitously distributed at mRNA level (Maestrini et al., 1996). In human cancer cell lines derived from colon, liver, pancreas, and gastric tumors, plexin-B1 protein is over-expressed (Conrotto et al., 2004). Recently, our lab has also demonstrated that plexin-B1 and Semaphorin 4D were over-expressed in primary prostate cancer (Wong et al., 2007). There is no report on expression of plexin-B1 in prostate cancer cell lines. This chapter aimed to reveal the expression profiles of plexin-B1 and Sema4D in human prostate cancer cell lines at both mRNA and protein levels. A wide range of human cell lines derived from tumors and other mammalian cell lines were also screened for endogenous plexin-B1 and Semaphorin 4D expressions at both mRNA and protein levels for a comparison.

3.2 Results

3.2.1 Expression of plexin-B1 and Sema4D at the mRNA level

RNA samples extracted from different cell lines were reverse transcribed to synthesize first strand cDNA and the products were amplified by PCR with specific primers for target genes. Figure 3.1 shows the expression of plexin-B1 and Sema4D at the mRNA level. All the human prostate cancer cell lines DU145, PC3, LNCaP, 1542CPT, 1532CPT, human benign prostate cell line 1542NPT, and human kidney

embryonic cells HEK293 exhibited plexin-B1 expression at the mRNA level except PC12 cell line. The absence of product in PC12 is due to the fact that the human primers used were not complementary to the rat plexin-B1 DNA sequence. There was no significant difference in plexin-B1 expression levels among all the human cell lines. Sema4D mRNA was also detected in human cells as shown by Figure 3.1. There was a rather weak band observed in PC3 cells indicating that the mRNA level of Sema4D in PC3 was relatively low compared to the rest of the human cell lines.

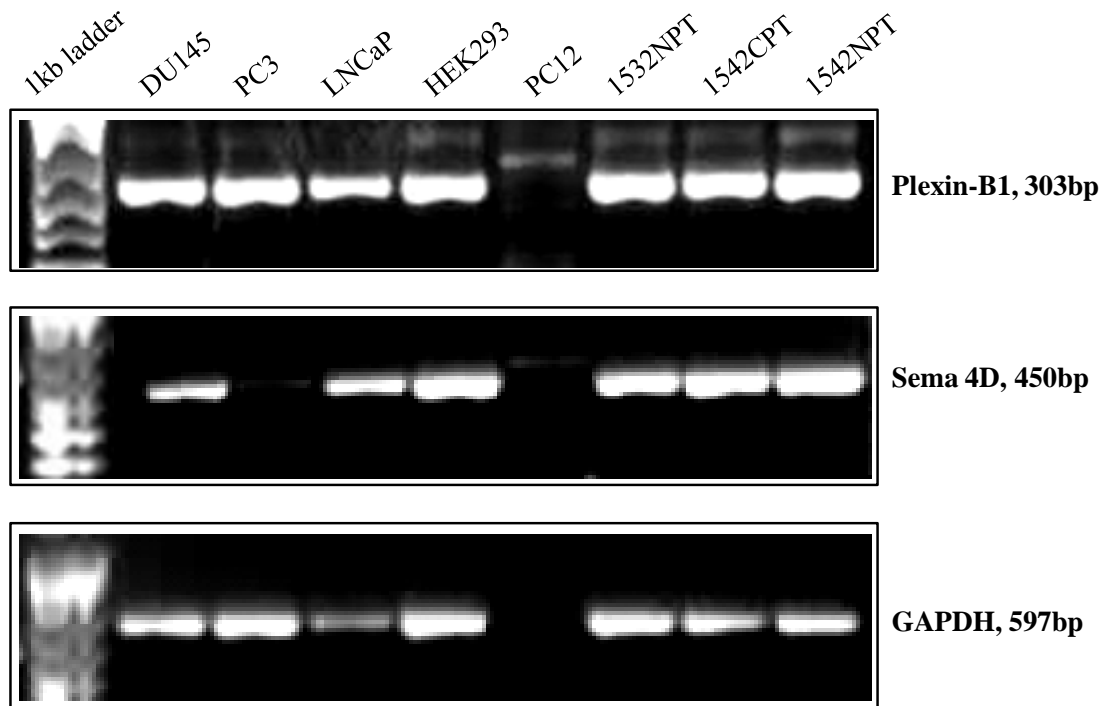


Figure 3.1 mRNA expression levels of plexin-B1 and Sema 4D in cell lines. RNA was extracted from cells and then subjected to RT-PCR. The PCR products were then analyzed using agarose electrophoresis. All the human cell lines tested expressed plexin-B1 mRNA. No plexin-B1 mRNA was detected in PC12 because the primers were not complementary to rat. Sema4D mRNA was detected in all the human cell lines. The Sema4D mRNA expression level in PC3 was relatively low compared to the rest of the cell lines. GAPDH was amplified as the control.

3.2.2 Expression of plexin-B1 and Sema4D at the protein level

To study the expression of plexin-B1 and Sema4D at protein level, a wide range of cell lines were investigated. Lysis buffer RIPA (radioimmunoprecipitation) was used to extract proteins as it gave least protein degradation compared to other compositions. Total lysates of different protein samples were analyzed by Western-blotting following SDS-PAGE. As shown in Figure 3.2.A, protein from HEK293 stably transfected with plexin-B1 was a positive control for plexin-B1 expression and it exhibited proteins with molecular sizes of 300 kDa and 200 kDa. Compared with the control, there was no observable signal of plexin-B1 expression in all the cell lines, even with 80 µg of total input proteins and over-night exposure. To find out if this missing expression of plexin-B1 was due to no or low level of target protein, protein samples were then concentrated by immunoprecipitation using anti-plexin-B1 antibody and then further analyzed using SDS-PAGE and Western-blotting. By using this enrichment step, plexin-B1 expression at the size of 300 kDa was detected in prostate cell lines DU145, LNCaP, PC3, 1542CPT and 1542NPT (Figure 3.2.B). In human kidney embryonic cells HEK293 and PC12 cells which are derived from a pheochromocytoma of the rat, there was no comparable signal detected.

The two pictures in Figure 3.2.C show the Western-blotting results of plexin-B1 expression using the same Santa Cruz anti-plexin-B1 antibody as Figure 3.2.A and Figure 3.2.B, but of a different batch number. In all the human epithelial cells from tumors, this new batch anti-plexin-B1 antibody recognized endogenous plexin-B1 with lower total protein input (40 µg) than those in Figures 3.2.A and 3.2.B. Endogenous plexin-B1

protein was present in two forms, a 300 kDa fragment and a predominantly expressed smaller fragment at the size of 200 kDa.

Sema4D expression was detected by Western-blotting using antibody anti-CD100 (Conrotto et al., 2005). Among the prostate cancer cell lines tested, 22RV1, LNCaP and DU145 expressed Sema4D with a molecular mass of 150 kDa. DU145 was low in expression of this protein compared with 22RV1 and LNCaP. In the PC3 cell line and the PC3-LN3 cell line that is derived from PC3, there was no obvious expression of Sema4D (Figure 3.2.B). HEK293 cells and COS7 cells (derived from kidney cells of African green monkey) both demonstrated Sema4D protein expression.

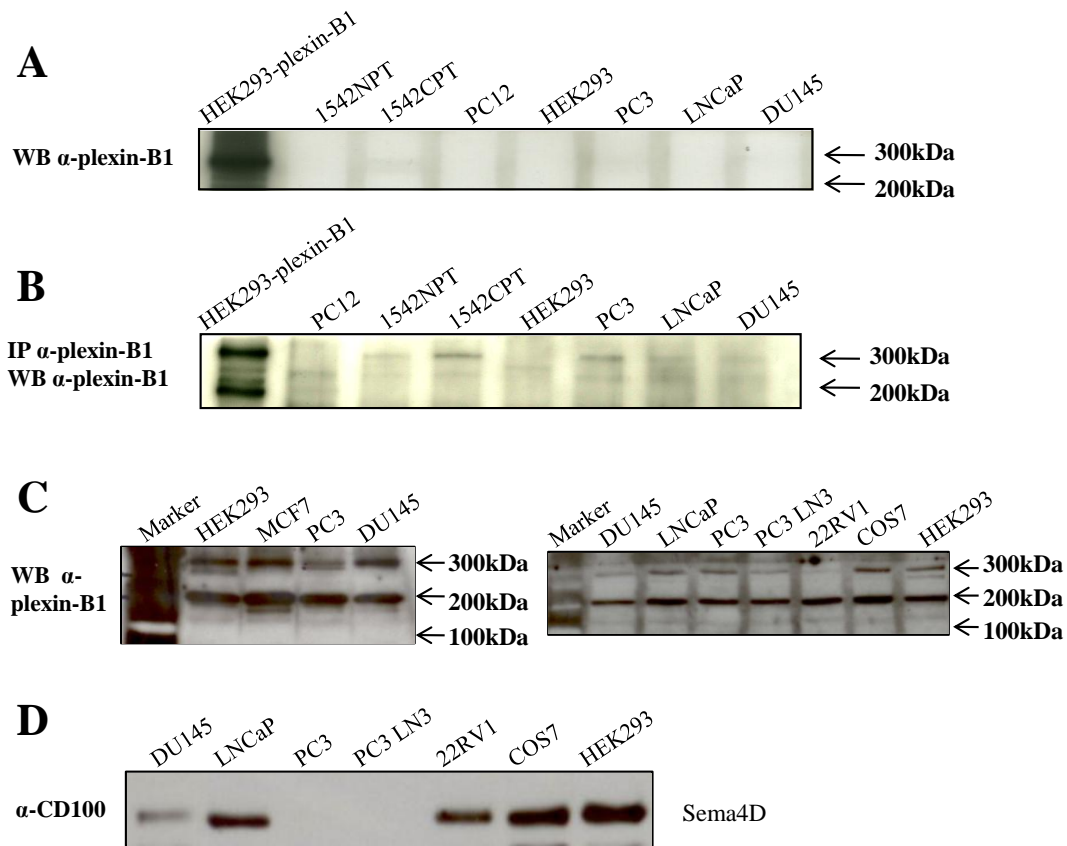


Figure 3.2 Plexin-B1 and Sema4D protein expressions in different cell lines. (A) Total lysates from different cell lines were analyzed for plexin-B1 protein. None of the cell line displayed detectable endogenous plexin-B1 protein using the first batch of anti-plexin-B1 antibody. (B) Cell lysates were enriched by immunoprecipitation with anti-plexin-B1 antibody (same batch as A). (C) Total lysates were resolved by SDS-PAGE and probed with anti-plexin-B1 antibody of different batch (batch no..10804). (D) Proteins from different cell lines were investigated for Sema4D expression through the Western-blotting method.

3.3 Discussion

As discussed in the beginning of this chapter, both Sema4D and its receptor plexin-B1 are reported to be expressed widely in different tissues and organs. Sema4D is high at mRNA level in skeletal muscle, peripheral blood lymphocytes, spleen, and thymus (Hall et al., 1996). In other non-lymphoid organs, including the testes, brain, kidney, small intestine, prostate, heart, placenta, lung and pancreas, the mRNA of Sema4D is expressed at low level (Hall et al., 1996). In this study, I found that mRNA of Sema4D was expressed in prostate cancer cell lines except PC3 cells which demonstrated rather weak signal compared with the rest. However to assay the mRNA levels more accurately, real-time PCR might be more informative and could be applied. At the protein level, Sema4D expression was not detectable in PC3 cells consistent with the RT-PCR results, but was present in other prostate cancer cell lines tested. These results demonstrated that epithelial cells from human prostate cancer are positive for Sema4D expression.

Plexin-B1 is predominantly expressed in fetal neural tissues (Maestrini et al., 1996). Recently research reported that over-expression of plexin-B1 was associated with cancer. In this part of study, I tested a variety of cell lines including human prostate cancer cell lines (DU145, PC3, LNCaP, 1542NPT, 1542CPT, 22RV1, PC3-LN3), human breast cancer cell line (MCF7), human embryonic kidney cell line (HEK293) and monkey kidney cell line (COS7). I found that all the cell lines tested were expressing detectable amount of plexin-B1 protein (Figure 3.2). My result have shown, for the first time, that plexin-B1 is endogenously expressed in prostate cancer cell lines. Artigiani and

her colleagues have demonstrated that plexin-B1 is predominantly found in a cleaved form in cells and tissues (Artigiani et al., 2003). The full length receptor plexin-B1 is a 300 kDa protein which is a single-chain precursor. By proteolytic processing, this protein is converted into a heterodimeric receptor consisting of a 200 kDa extracellular moiety and a 100 kDa that contains a portion of the transmembrane moiety and the cytoplasmic region (Artigiani et al., 2003). The Western-blotting result by anti-plexin-B1 antibody from Santa Cruz showed that there was a predominant expression of the 200 kDa extracellular domain of plexin-B1 in all the cell lines tested. However, the full length of plexin-B1 was low in amount relatively. There was no 100 kDa small fragment of plexin-B1 detected in all the cell lines studies. The intracellular domain of plexin-B1 consists of residues from 1512-2135. The Santa Cruz antibody recognizes amino acids 771-1070 region that locates in the extracellular domain of plexin-B1. Therefore this antibody could not bind to the 100kDa fragment of plexin-B1. Interestingly, the batch number of this antibody also affected the result. Results from different batches varied (Figure 3.2.A.). However, these results together showed that plexin-B1 was present in prostate cancer cell lines.

Sema4D can act either as membrane-bound or locally released protein to exert its regulatory effects. In this study protein plexin-B1 protein is expressed in both DU145 and PC3 cell lines. Sema4D protein expression is only observed in cell line DU145 but not in PC3. The different expression patterns of the two proteins in these two cell lines suggest that the signaling of Sema4D/plexin-B1 in these two cells lines might be different. In DU145 cell line plexin-B1 could initiate downstream pathways by binding with the autocrine production of Sema4D by DU145 cells. PC3 cells that lack Sema4D protein

expression may employ a paracrine signaling method in which plexin-B1 signals through Sema4D released by other cells.

In a summary, the results from this chapter revealed the expression of proteins plexin-B1 and Sema4D in prostate cancer cell lines. It also provided a relative comparison of the protein expression levels between prostate cancer cell lines and other human cell lines.

Chapter 4

Plexin-B1 mutation and tyrosine kinases

4.1 Introduction

Phosphorylation at tyrosine residues is thought to be an important way of plexin-B1 signaling. Plexin-B1 associates in a molecular complex with certain tyrosine kinases. Upon stimulation by Sema4D, both plexin-B1 and the associated tyrosine kinase are tyrosine phosphorylated (Giordano et al., 2002; Swiercz et al., 2004). The activation of the plexin-B1/RTK (receptor tyrosine kinase) complex results in multiple intracellular signaling pathways and subsequently regulation of cell functions.

Met (also known as c-met) and ErbB-2 are the main receptor tyrosine kinases which interact with plexin-B1 and are involved in plexin-B1/Sema4D signaling. Plexin-B1 binds to Met through their extracellular domains. Binding of Sema4D to plexin-B1 results in phosphorylation of the tyrosine residues in the cytoplasmic portions of both receptors (Conrotto et al., 2004; Giordano et al., 2002). This indirect activation of Met by Sema4D promotes Met-mediated invasive growth of cells consequently.

ErbB-2 associates with plexin-B1 into a complex through their extracellular domains (Swiercz et al., 2004). After ligand Sema4D binds to plexin-B1, the intrinsic tyrosine kinase activity of ErbB-2 is stimulated and this results in phosphorylation of both plexin-B1 and ErbB-2 (Swiercz et al., 2004). Plexin-B1 forms a complex with PDZ-RhoGEF/LARG and Sema4D/plexin-B1 signaling regulates RhoGEF-mediated RhoA activation (Hirotani et al., 2002; Perrot et al., 2002; Swiercz et al., 2002). ErbB-2 is critically involved in this signaling process. ErbB-2-mediated phosphorylation of plexin-B1 is essential for the Sema4D-induced activation of RhoA.

Interestingly, ErbB-2 and Met compete for plexin-B1 binding and have opposite effects on RhoA activation downstream of Sema4D/plexin-B1 signaling (Swiercz et al., 2008). Sema4D/plexin-B1 signaling inhibits RhoA activation in cells expressing Met, whereas in cell expressing ErbB-2, stimulation of the Sema4D/plexin-B1 pathway results in RhoA activation (Swiercz et al., 2008). Figure 4.1 illustrates the reciprocal roles of ErbB-2 and Met on plexin-B1 signalling based on Swiercz's findings.

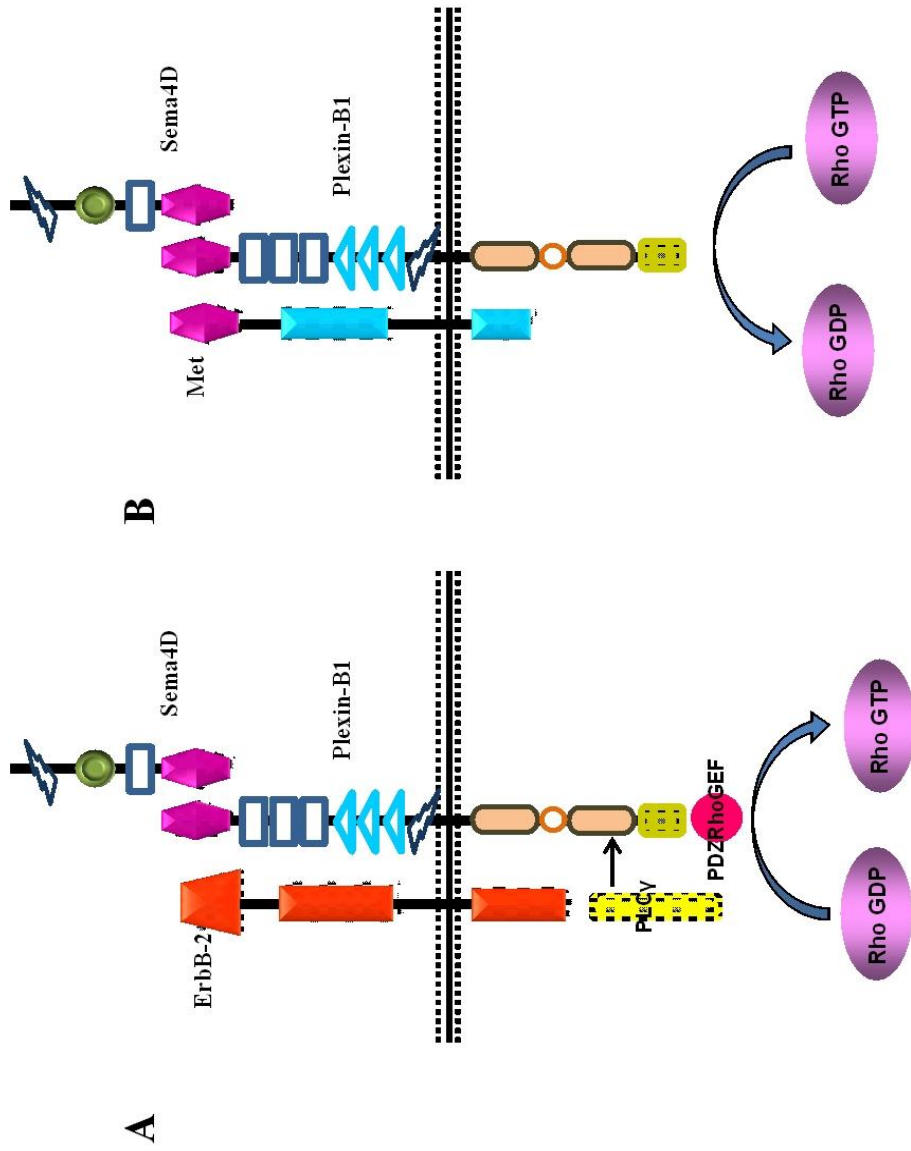


Figure 4.1 Reciprocal roles of ErbB-2 and Met on plexin-B1 signaling. (A) ErbB-2 binds to plexin-B1. Sema4D induces phosphorylation of both ErbB-2 and plexin-B1, resulting in recruitment of PLC γ to plexin-B1. Subsequently PDZ-Rho GEF is activated by PLC γ and activates Rho, leading to Akt phosphorylation and increased cell motility. (B) Met couples to plexin-B1. Sema4D stimulation results in phosphorylation of both Met and plexin-B1 and Rho inactivation. The mechanism responsible for Met/plexin-B1-regulated Rho inactivation is not known.

Plexin-B1 signaling pathways also involve non-receptor tyrosine kinases including the PI3K/Akt and MAPK pathways. In endothelial cells, the Sema4D/plexin-B1 signaling pathway promotes cell migration through activating phosphatidylinositol 3-kinase (PI3K)-Akt (Basile et al., 2005). Plexin-B1 associates with PYK2, the p85 subunit of PI3K and to a lesser extent with Src. Activation of plexin-B1 leads to phosphorylation of PYK2 which is necessary for consequent Src-dependent activation of the PI3K-Akt pathway and for plexin-B1 phosphorylation. The group lead by Dr. Guan has found that the MAPK pathway is activated downstream of Sema4D/plexin-B1 signaling through RhoA activation (Aurandt et al., 2006). Sema4D/plexin-B1 induces Rho activation and Rho co-operates with Ras to active Raf, which in turn stimulates ERK (extracellular-signal-regulated kinase) activation.

Given that tyrosine kinases are important signalling partner molecules for Sema4D/plexin-B1 signal transduction, it is important to know if the mutations have any impact on the pathways involving receptor/non-receptor tyrosine kinases. To achieve this, exogenous plexin-B1 expression was introduced into cells by transfection with cDNA plasmids encoding VSV-tagged plexin-B1 wildtype or mutants A5359G, A5653G and T5714C. Cells co-expressing targeted proteins were lysed and immunoprecipitated with specific antibodies and then analyzed by Western-blotting to study the interaction of plexin-B1 wildtype/mutants with ErbB-2 or with Met. Swiercz et al. has demonstrated that Sema4D induces or inhibits cell migration depending on the presence of ErbB-2 or Met in breast cancer cell lines. However, Conrotto et al. showed the opposite result in regulatory effect of Met on cell motility. Conrotto demonstrated that Met activation by Sema4D/plexin-B1 signaling promotes cell migration (Conrotto et al., 2005; Giacobini et

al., 2008; Giordano et al., 2002). These contradictory results may be due to the different cell types investigated. There is no previous report on how prostate cancer cells respond to Sema4D. The roles of ErbB-2 and Met on Sema4D/plexin-B1-mediated cell motility in prostate cancer cells are not known. In order to reveal the mechanism underlying the effect of Sema4D on cell motility in the context of ErbB-2 and Met expression in prostate cancer cells, I investigated the expressions of ErbB-2 and Met in prostate cancer cell lines and carried out cell migration assays with these cells. To study if the Akt and MAPK pathways are involved in Sema4D/plexin-B1 signaling in epithelial cells, I used HEK293 cells expressing exogenous plexin-B1 and studied the phosphorylation levels of the tyrosine kinases under the effect of Sema4D treatment.

4.2 Results

4.2.1 Interaction between plexin-B1 and ErbB-2

The HEK293 cell line was used for protein-protein interaction studies throughout my project. Before using HEK293 cells, prostate cancer cell lines DU145 and PC3 were transfected with exogenous plexin-B1 with the purpose of performing protein-protein interaction assays. However, I did not successfully establish prostate cancer cell lines expressing exogenous proteins because the transfection efficiency for DU145 and PC3 was very low. Therefore, I used HEK293 cells that are easy to work with and transfect. HEK293 cells were seeded in 6-well plates and each well was transfected with 4 μg of plasmids in total. The DNA components of each sample in Figure 4.2.A is listed as followed,

	Plexin-B1 plasmid (μg)	ErbB-2 plasmid (μg)	PDZ-RhoGEF plasmid (μg)
Lane 1	1 (pcDNA3)	1.5	1.5
Lane 2	2	-	2
Lane 3	1	1.5	1.5
Lane 4	2	2	-
Lane 5	1.33	1.33	1.33
Lane 6	2	1	1

The first panel of Figure 4.2.A shows the interaction of plexin-B1 with ErbB-2 by immunoprecipitation. Lane 1 was set as the control which was transfected with an empty vector instead of plexin-B1. The pull-down assay was performed with anti-VSV antibody

and the Western-blotting was performed with anti-ErbB2 antibody. It is expected to see no signal in Lane 1, since the empty vector is not VSV-tagged. No signal of interaction between plexin-B1 and ErbB-2 is observed as expected. This indicates that the immunoprecipitation is specific for VSV-tagged plexin-B1 protein or a protein complex containing VSV-plexin-B1. Lane 2 represents cells co-expressing VSV-plexin-B1 and PDZ-RhoGEF proteins and the weak band indicates the binding between VSV-plexin-B1 and endogenous ErbB-2. Lanes 3, 5 and 6 demonstrate the interaction between exogenous VSV-plexin-B1 and ErbB-2 at different ratios of transfected plasmids. Compared with the signal from lane 2, the binding signals in those lanes are much stronger, resulting from a relatively high level of exogenous ErbB-2 protein expression. Lane 4 is the protein immunoprecipitated from cells co-expressing plexin-B1 and ErbB-2 in the absence of PDZ-RhoGEF. Interaction between plexin-B1 and ErbB-2 is still observed and this indicates that PDZ-RhoGEF is not necessary for plexin-B1/ErbB-2 interaction. Lane 4 gives the strongest signal of plexin-B1/ErbB-2 binding. This is due to the higher DNA input at transfection, resulting in a relatively higher proportion of plexin-B1 and ErbB-2 in total lysates than those of the rest of the samples. The lower panels of Figure 4.2.A shows the expressions of exogenous proteins, indicating the input of protein for immunoprecipitation is equal among different lanes.

Figure 4.2.B is the mirror experiment of immunoprecipitation. Proteins from cells co-expressing plexin-B1 and ErbB-2 were extracted and immunoprecipitated with anti-ErbB-2. The Western-blotting result confirms the interaction between plexin-B1 and ErbB-2, as demonstrated by the left panel of the figure. The same membrane was stripped of antibodies and re-probed with anti-ErbB-2 antibody. The right panel shows the

expression of ErbB-2 in the cell lysate used in the immunoprecipitation, showing the level of ErbB2 input protein.

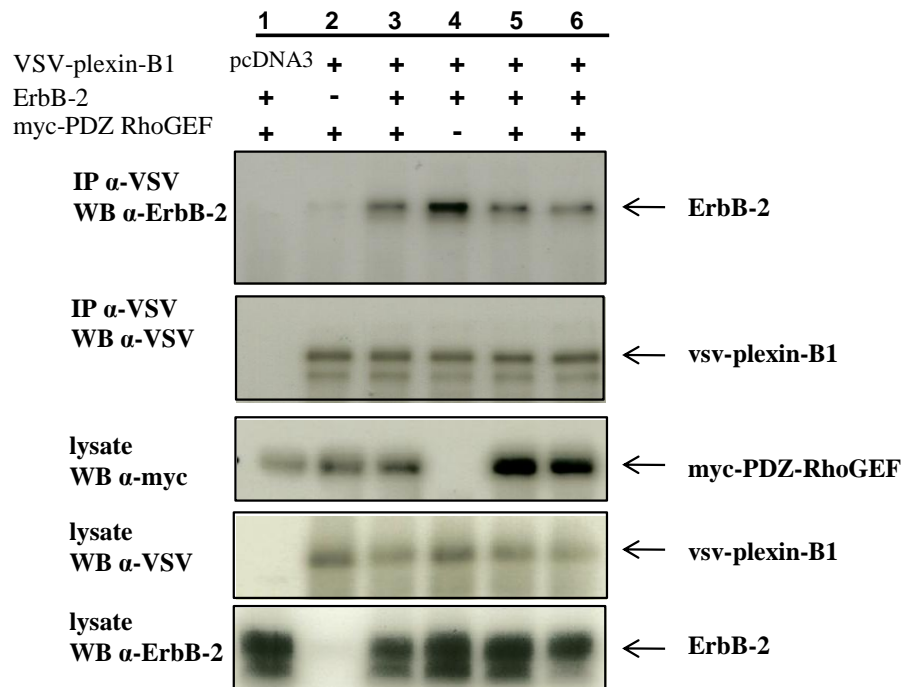
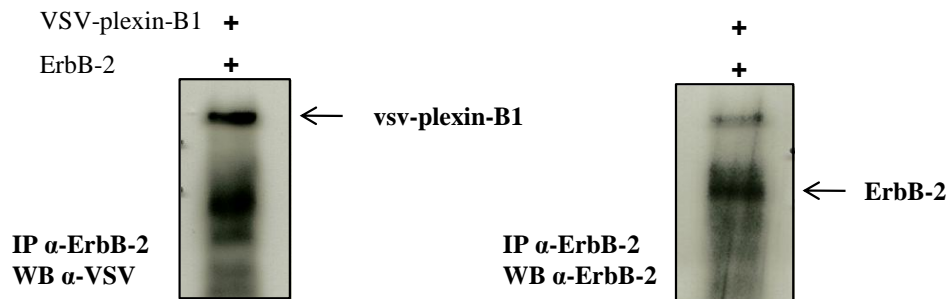
A**B**

Figure 4.2 Interaction between plexin-B1 and ErbB-2. HEK293 cells were co-transfected with different ratios of plasmid DNA encoding plexin-B1, PDZ-RhoGEF and ErbB-2 as indicated. Proteins were extracted with RIPA buffer and samples were immunoprecipitated with antibodies. (A) Cell lysates were immunoprecipitated with anti-VSV antibody and then probed with anti-ErbB-2 in Western-blotting. Different lanes of blots represent protein from cells transfected with different ratio of plasmid DNA (as shown in table above). (B) The mirror experiment of immunoprecipitation was performed using anti-ErbB-2 antibody and followed by anti-VSV antibody incubation in Western-blotting.

4.2.2 Interaction between ErbB-2 and mutated forms of plexin-B1

With the association of ErbB-2 and plexin-B1 confirmed, I then studied if the mutated forms of plexin-B1 had any effects on its binding to ErbB-2. Constructs of DNA expressing VSV-tagged plexin-B1 wildtype and mutated forms were from previous group member Oscar Wong and are described in his thesis. HEK293 were transiently co-transfected with wildtype/mutant plexin-B1 and ErbB-2. The upper blot in Figure 4.3 shows that plexin-B1 wildtype, mutants A5359G, A56553G, T5714C and C5060T all demonstrate binding to ErbB-2. There is no alteration in the interaction between plexin-B1 and ErbB-2 in any mutated form of plexin-B1 compared with the wildtype plexin-B1. The lower blot shows that the protein input for all samples is equal.

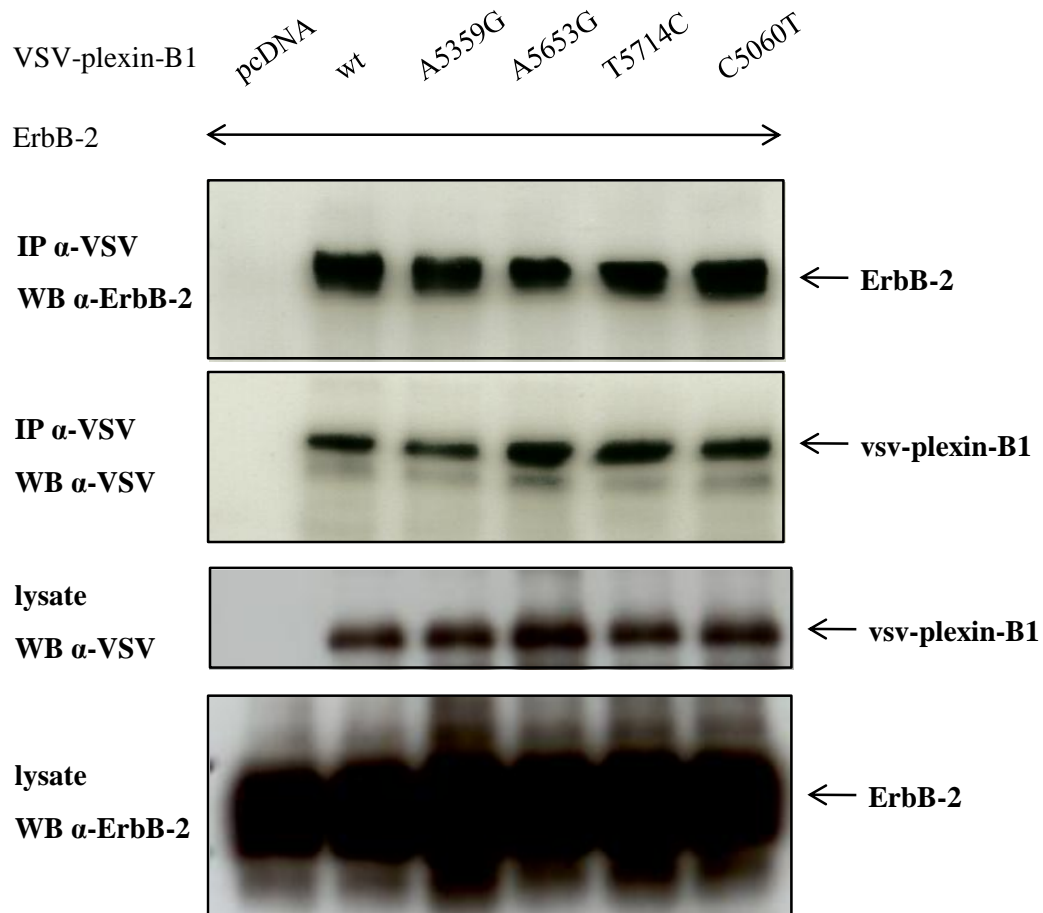


Figure 4.3 Effect of plexin-B1 mutations on ErbB-2 and plexin-B1 interaction. HEK293 cells were transiently transfected with plasmid DNA encoding ErbB-2 and plexin-B1 wildtype or mutated forms (VSV tagged). Lysates were cleared and immunoprecipiated with anti-VSV antibody. Samples were then analyzed by SDS-PAGE followed by Western-blotting with primary antibody anti-ErbB-2. All the mutated forms of plexin-B1 bind to ErbB-2 to the same extent as the wildtype does.

4.2.3 Interaction between plexin-B1 and Met

In order to study the binding of plexin-B1 and Met, HEK293 cells were transfected with plasmids encoding VSV-tagged plexin-B1 wildtype/mutants and full length Met. Cells were plated in 6-well plates and each well was transfected with 4 μg of DNA in total. The DNA composition of the samples in lanes in Figure 4.3 is listed below,

	Plexin-B1 plasmid (μg)	Met plasmid (μg)
Lane 1	2	2
Lane 2	3	1
Lane 3	1	3
Lane 4	2	-
Lane 5	-	2

The precursor of Met is a single-chain protein of 170 kDa. The precursor protein is glycosylated and then cleaved into an extracellular 50 kDa α -chain and a 145 kDa β -chain consisting of a large extracellular domain, the transmembrane segment and the intracellular tyrosine kinase region (Giordano et al., 1989; Mondino et al., 1991). The anti-Met antibody used in this study is to recognize the cytoplasmic domain of Met, i.e., the 170 kDa and 145 kDa forms. The Lane 4 of panel 2 in Figure 4.4 shows the expression of endogenous Met. The antibody recognizes the 145 kDa fragment of Met. In addition to the expression of 145 kDa form of Met, cells transfected with the Met plasmid express the Met precursor with a molecular mass of 170 kDa. Cell lysates were then immunoprecipitated with anti-VSV antibody to investigate the interaction between plexin-B1 and Met. In control sets, cells were either transfected with plexin-B1 alone

(lane 4) or Met alone (lane 5) respectively. There is no sign of pull-down of Met with anti-VSV antibody in lanes 4 and 5 showing that the bands in the other lanes (from cells transfected with both plasmids) are specific for Met and VSV-plexin-B1 binding. In cells transfected with both plasmids, 170 kDa Met is immunoprecipitated indicating the interaction between plexin-B1 and Met. There is no sign of interaction between plexin-B1 and the 145 kDa Met in the first two lanes (lanes 1 and 2), whereas in cells expressing relative high Met (3 μ g DNA, lane 3) immunoprecipitation result shows 145 kDa Met also interacts with plexin-B1. Cell lysate from Lane 3 contained higher proportion of Met in total protein than Lanes 1 and 2. These results suggest that plexin-B1 couples with 170 kDa Met. However, the 145 kDa Met binds to plexin-B1 to a lesser extent in comparison with precursor form of Met. Interaction between plexin-B1 and the 145 kDa fragment of Met is observed only in the case of high over-expression of Met, indicating that plexin-B1 binds predominantly to the N-terminal extracellular region of Met and more weakly with 145 kDa fragment.

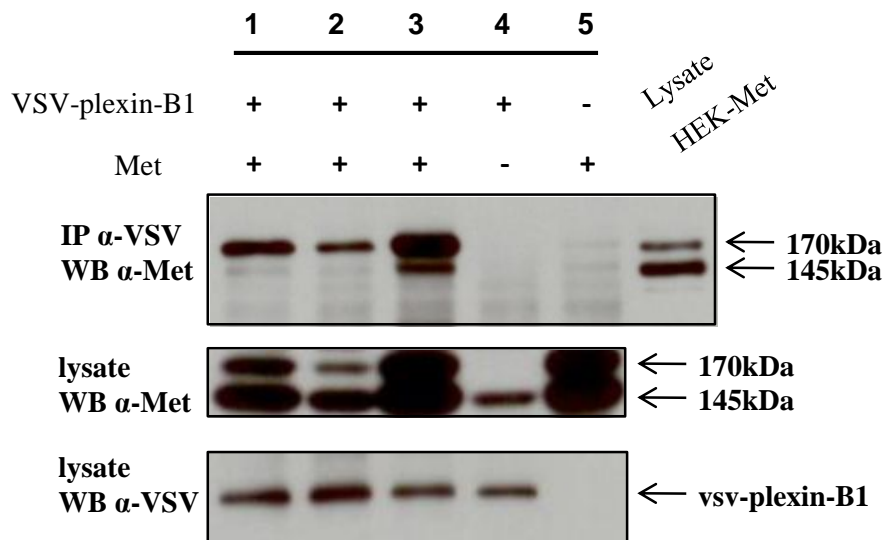


Figure 4.4 Interaction between plexin-B1 and Met. HEK293 cells were transiently transfected with different ratio of Met and VSV-plexin-B1 plasmid DNA (shown in table above). Proteins were extracted and immunoprecipitated with anti-VSV antibody and then analyzed by Western-blotting.

4.2.4 Interaction between Met and mutated forms of plexin-B1

To study the effect of plexin-B1 mutations on plexin-B1 binding to Met, I co-transfected HEK293 cells with VSV-tagged plexin-B1 wildtype/mutants and Met plasmids. Cells were plated in 6-well-plates and each well was co-transfected with 2 µg of Met and 2 µg of plexin-B1 or vector control. The Western-blotting result of total lysate shows that when co-expressed with plexin-B1, the expression of Met (170 kDa) is suppressed compared with the vector control (Figure 4.5, 3rd panel). In immunoprecipitation assays, 170 kDa Met was found to be co-precipitated with all the mutated forms of plexin-B1 (A5359G, A56553G, T5714C) and wildtype plexin-B1 by anti-VSV antibody as shown in Figure 4.4. There is no interaction of 145 kDa Met and plexin-B1 detected. This suggests that mutated forms of plexin-B1 interact with Met at the same extent as wildtype plexin-B1 to Met. Mutations of plexin-B1 have no effect on its binding to Met.

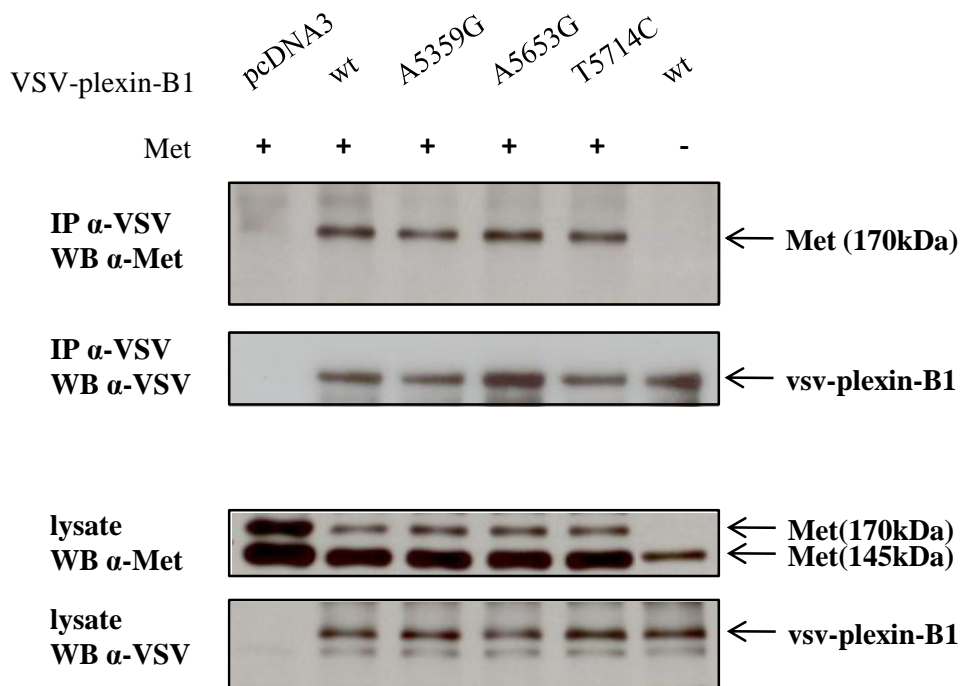


Figure 4.5 Effect of plexin-B1 mutations on Met and plexin-B1 interaction. HEK293 cells were transiently transfected with plasmid DNA encoding Met and plexin-B1 wildtype or mutated forms (VSV tagged). Lysates were cleared and immunoprecipiated with anti-VSV antibody. Samples were then resolved by SDS-PAGE and analyzed by Western-blotting with primary antibody anti-Met. All the mutations bind to Met (170kDa) to the same extent as wildtype plexin-B1 does.

4.2.5 Effect of ErbB-2 and Met expression on cell migration in prostate cancer cells

As mentioned in the introduction to this section, the response of cells to Sema4D/plexin-B1 signaling is cell specific and is dependent on the ratio of Met and ErbB-2 expression in the responding cells (reviewed in 4.1 of Chapter 4). To study the regulatory functions of these two tyrosine kinases in prostate cancer cells, I firstly screened prostate cancer cells for expression levels of ErbB-2 and Met. As shown in Figure 4.6.A, several human epithelial cell lines and monkey cells COS7 were investigated for the expression of ErbB-2 and Met. Of all the cell lines tested, prostate cancer cell lines PC3 and PC3-LN3 exhibit much stronger expression of Met compared to the rest. LNCaP cells show null expression of Met. MCF7 is not expressing Met which is consistent with a previous report (Swiercz et al., 2008). In comparison, PC3 and LNCaP cells demonstrate different patterns of ErbB-2 expression (Figure 4.6.A). LNCaP cell line is strongly expressing ErbB-2, whereas ErbB-2 is expressed at relatively low levels in PC3 cells. These results demonstrate that the stoichiometry of Met and ErbB-2 in LNCaP and PC3 cells is different from each other. Based on this finding, I then studied the motility of these cells.

Previously, my supervisor Dr. Magali Williamson has demonstrated that Sema4D treatment increases the motility of LNCaP cells compared with the control untreated cells (Figure 4.6.S). In this section, I performed transwell migration assays with PC3 cells. Cells were treated with or without Sema4D concentrate. Sema4D was added to the lower wells of the transwell chamber. The cell seeding efficiency for each experiment was different, resulting in a great variance of starting cell numbers between trials. Therefore

the number of cells migrated through with Sema4D treatment was normalized to that of the migrated cells in the control. The relative cell migration was calculated. I found that Sema4D treatment decreases the cell motility in PC3 cells (Figure 4.6.B). These results suggest that in prostate cancer cells Sema4D induces cell migration in the presence of ErbB-2, whereas Sema4D inhibits cell migration when Met expression is dominant. This finding is consistent with the results observed in breast cancer cells reported by Swiercz (Swiercz et al., 2008).

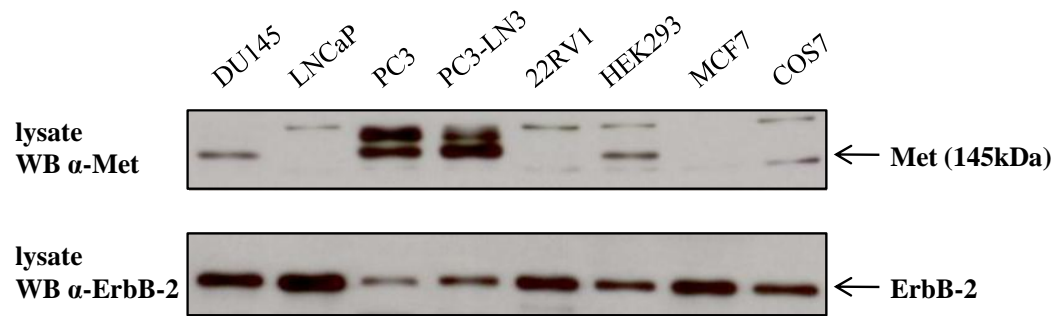
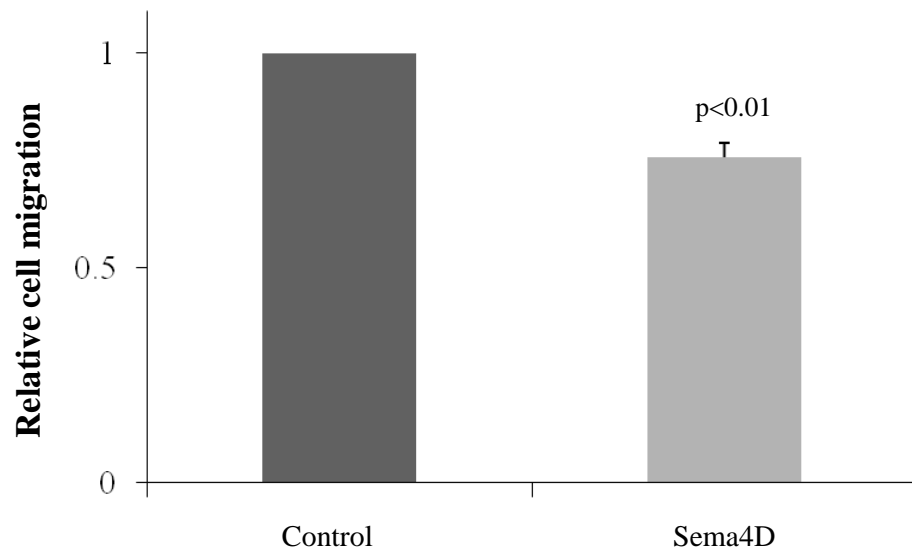
A**B**

Figure 4.6 Effect of Sema4D on PC3 cell motility. (A) Expression levels of Met and ErbB-2 in different cells detected by Western-blotting. (B) PC3 cells were plated in the transwell inserts which were coated with fibronectin on the lower side. Cells were incubated for 8 hours with or without Sema4D. At the end of incubation, cells on the lower side of the inserts were fixed and stained with crystal violet. Relative migration ability was measured as cells migrated normalized to that in the control (The raw data is presented in Appendix 3). The experiment was repeated at least three times and SEM was indicated as the error bar.

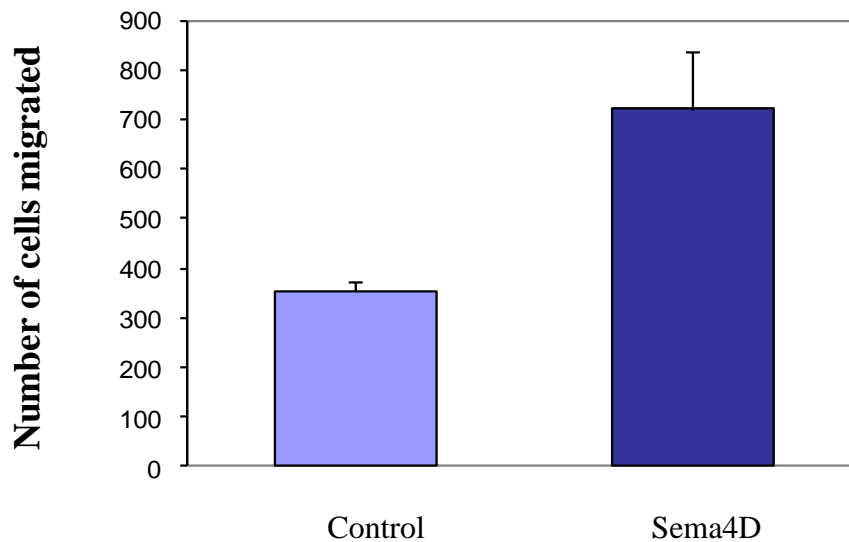


Figure 4.6S. Sema4D increases the motility of LNCaP cells. Transwell migration assays were performed using 24-well, 0.8 mm transwell chambers (BD) with LNCaP cells (2×10^4 per insert) in the upper chamber incubated with RPMI +/- Sema4D (100 ng/ml) in lower chamber. After 6hrs, cells on underside were fixed, stained with crystal violet and counted. Assays performed 4 times in triplicate. Error bars represent SEM, ($p=0.002$, 2 tailed T-test). (from Dr. Magali Williamson)

4.2.6 Plexin-B1 and Akt/MAPK pathways in epithelial cells

To study the downstream pathways involved in Sema4D/plexin-B1 signaling, recombinant Sema4D-Fc was produced. Sema4D-Fc was generated and purified as described in Chapter 2. Sema4D-Fc concentrate was then resolved by SDS-PAGE and stained with coomassie blue. Serial dilutions of BSA were loaded as the standards for protein amount. Sema3A-Fc (R&D) was loaded as a semaphorin protein control. Figure 4.7.A shows the yield of Sema4D-Fc. Sema4D-Fc demonstrates two fragments at the sizes of around 150 kDa and 120 kDa. The concentrate of Sema4D-Fc could be estimated by comparing the band to those of BSA standards.

HEK293 cells were transfected with plexin-B1 plasmid or control vector for 48 hours. Cells were serum starved overnight and incubated with Sema4D (200 ng/ml) for 15 minutes. LPA (200 ng/ml) treatment was applied as the positive control for MAPK activation (Ediger et al., 2003). Proteins were then extracted and proteins involved in PI3K/Akt or MAPK pathways were analyzed for their phosphorylation levels. HEK293 is null in PYK2 expression as shown in the Western-blotting of Figure 4.7.B. There is a basic level of phosphorylated Akt in HEK293 cells. No alteration in expression level of the phosphorylated form of Akt is observed in samples incubated with Sema4D. However MEK1/2, which is part of MAPK signaling pathway, is activated. Like LPA, Sema4D increases the expression of phosphorylated MEK1/2 both in cells transfected with plexin-B1 or vector control. This suggests that endogenous plexin-B1 in HEK293 cells are responsible for Sema4D-induced MEK1/2 phosphorylation. The phosphor-MEK1/2 in cells transfected with plexin-B1 is slightly higher than the vector-transfected cells,

suggesting that over-expression of plexin-B1 makes cells respond to Sema4D at higher magnitude. These preliminary results suggest that Sema4D may have some effect on MAPK pathway activation in epithelial cells.

I then treated cells either with increasing concentrations of Sema4D or with increasing incubation times with Sema4D to further study the MAPK pathway. In cells transfected with plexin-B1, Sema4D induces MEK1/2 phosphorylation at the concentration 100 ng/ml and with increasing concentrations the MEK1/2 phosphorylation level stays elevated (Figure 4.7.C). However, there is a drop at the dose of 800 ng/ml. In the time-dependent study, phosphorylation level of MEK1/2 induced by Sema4D increases at time point 5 minutes and is slightly higher at time point 10 minutes. The elevated level of phosphorylated MEK1/2 is still observed at 30 minutes. Erk1/2, which is downstream of MEK1/2, is also activated by Sema4D as shown in Figure 4.6.D. The increased level of Erk1/2 appears at time point 5 and peaks at time point 10. After 30 minutes incubation, there is an obvious drop of phospho-Erk1/2 compared with earlier time points. These results show that Sema4D promotes MAPK pathway proteins activation in epithelial cells.

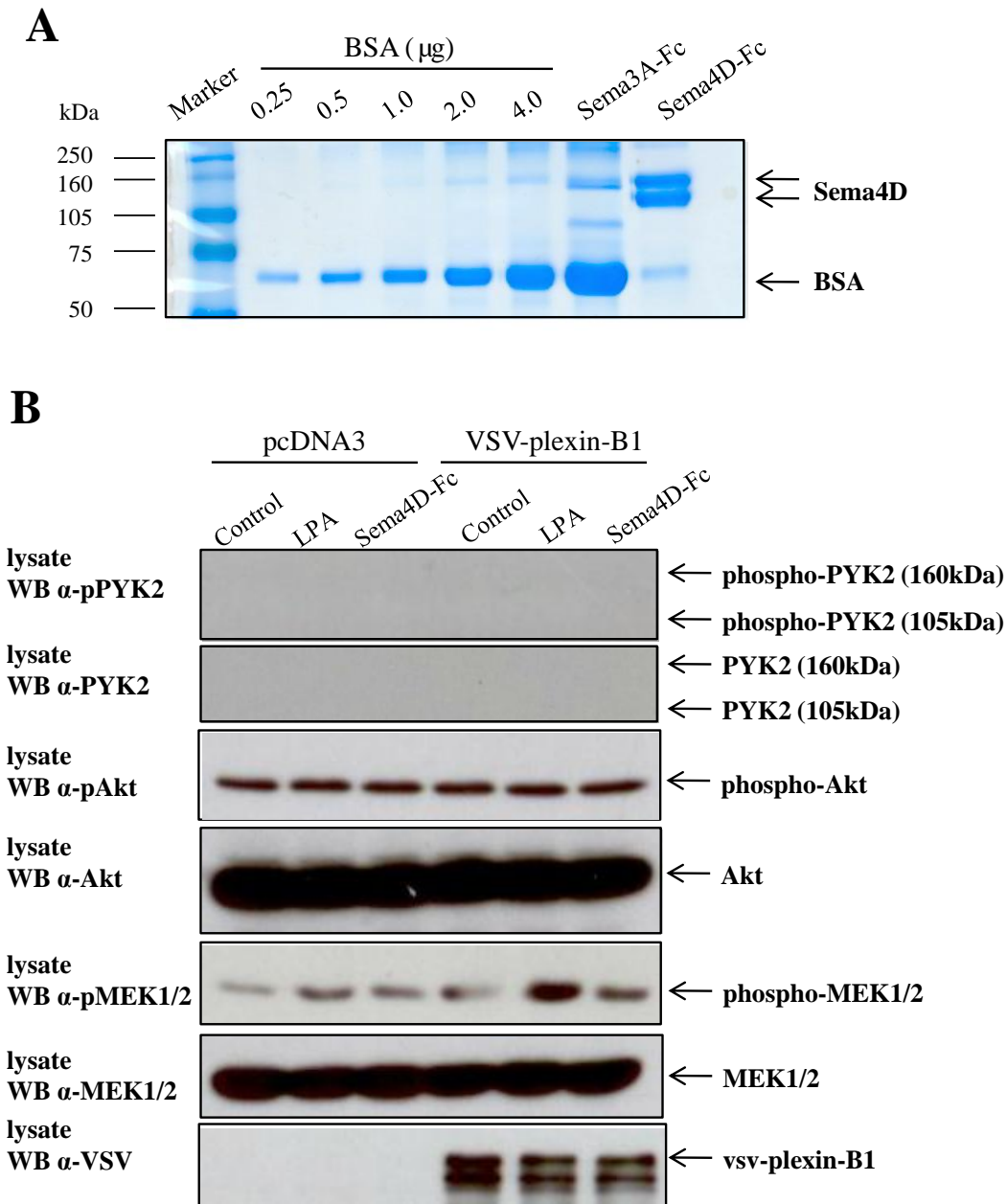


Figure 4.7 Akt and MAPK pathways under the effect of Sema4D. (A) Purified Sema4D was generated as described in Chapter 2. 15 μ l of Sema4D concentrate was analyzed by SDS-PAGE and coomassie blue staining. The amount of Sema4D protein loaded could be estimated according to the staining of BSA standard. Approximate concentration of Sema4D could be calculated. (B) HEK293 transfected with VSV-tagged plexin-B1 or empty vector was serum starved overnight and then incubated with LPA (200 ng/ml) or Sema4D (200 ng/ml) for 15 minutes. Lysates were analyzed for Akt and MAPK pathway proteins using specific antibodies.

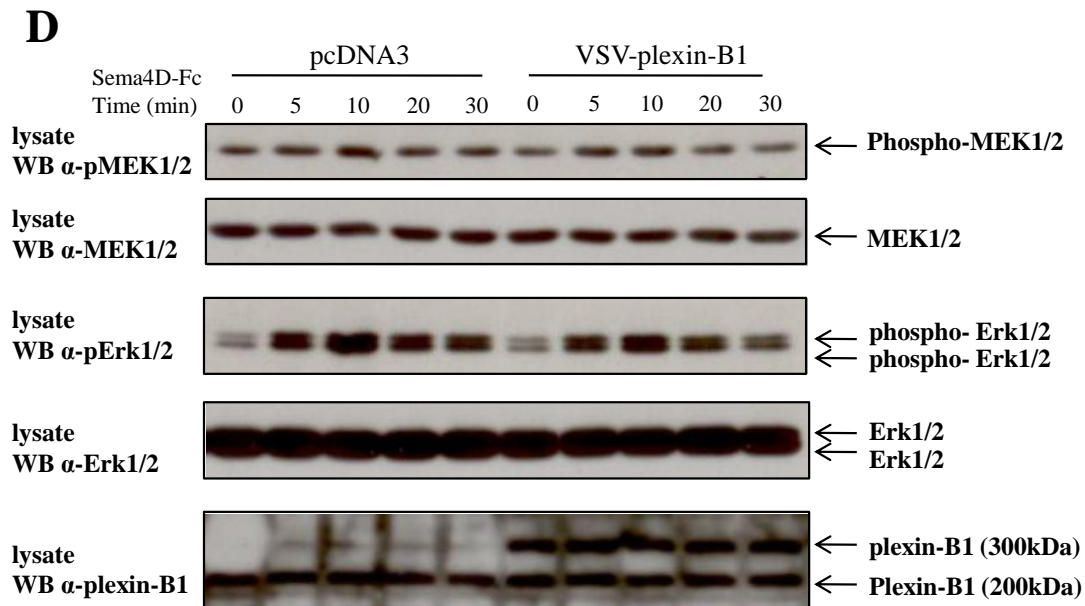
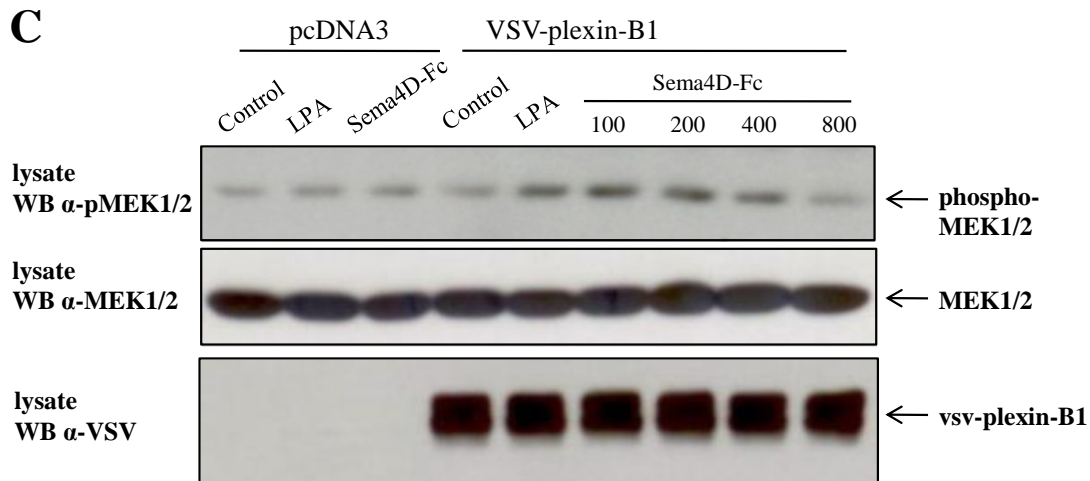


Figure 4.7 Akt and MAPK pathways under the effect of Sema4D. (C) HEK293 cells expressing exogenous plexin-B1 were treated with Sema4D with different concentrations for 15 minutes and analyzed for MEK activation status. (D) HEK293 cells transfected with exogenous plexin-B1 were incubated with Sema4D (200 ng/ml) with increasing time intervals. Cells transfected with empty vector were set as the control. Proteins of interest were then examined by Western-blotting.

In the experiments in the previous sections, glycine (neutralized with Tris) was used as the vehicle for Sema4D delivery. To further confirm the MAPK activation, cells treated with vehicle control glycine (neutralized by Tris) were used as a proper control. HEK293 cells transfected with plexin-B1 or vector control were either treated with Sema4D concentrate or with neutralized glycine (of the same volume as Sema4D) with different incubation time intervals. Both glycine and Sema4D concentrate induces MAPK activation (MEK1/2 and Erk1/2 phosphorylation) as shown in Figure 4.8.A. To eliminate the effect of glycine on MAPK activation, Sema4D-AP eluted with glutathione was applied to the cells and glutathione was set as the vehicle control. Figure 4.8.B illustrates the Sema4D-AP protein by Coomassie blue staining following SDS-PAGE. Glutathione alone induces MAPK activation as glycine does (Figure 4.8.C). These results suggest that both glycine and glutathione have positive effect on MAPK activation and this effect may mask the effect of Sema4D. Therefore, I performed dialysis with the eluted Sema4D concentrate using PBS as the dialysis buffer. The same experiment was carried out and cells were incubated with either PBS or PBS-dialyzed Sema4D. Again PBS exhibits a positive effect on promoting activation of MAPK, the same as glycine and glutathione (Figure 4.8.D). Conditioned medium containing Sema4D was used instead of purified Sema4D. Cells were either incubated with Sema4D-containing medium or medium from cells transfected with vector only (MOCK). Figure 4.8.E shows that cells demonstrate increased phosphorylation level of MAPK in both MOCK and conditioned medium.

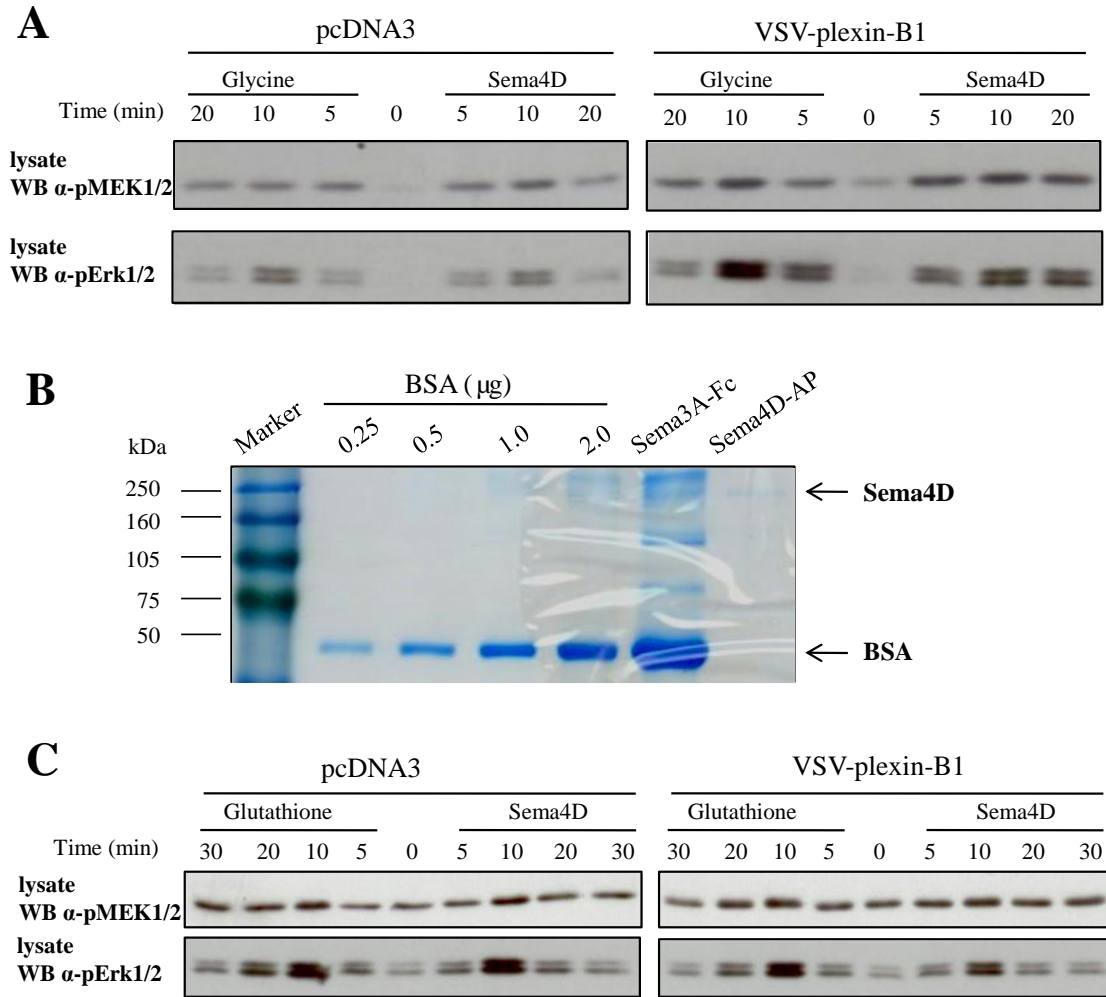


Figure 4.8 Effect of Sema4D in different solvents on MAPK activation. (A) HEK293 transfected with VSV-tagged plexin-B1 or empty vector was serum starved overnight and then incubated with Sema4D (200 ng/ml) or glycine (the same volume as Sema4D) for different time intervals. Lysates were analyzed for Akt and MAPK pathway proteins using specific antibodies. (B) Purified Sema4D-AP was generated as described in Chapter 2. 15 μ l of Sema4D concentrate was analyzed by SDS-PAGE and coomassie blue staining. The amount of Sema4D protein loaded could be estimated according to the staining of BSA standards. Approximate concentration of Sema4D could be calculated. (C) HEK293 cells expressing plexin-B1 or carrying empty vector were incubated with Sema4D-AP (200 ng/ml) or glutathione with different time intervals and analyzed for MAPK activation.

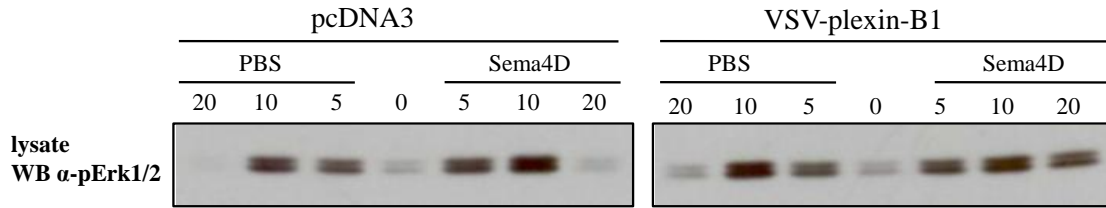
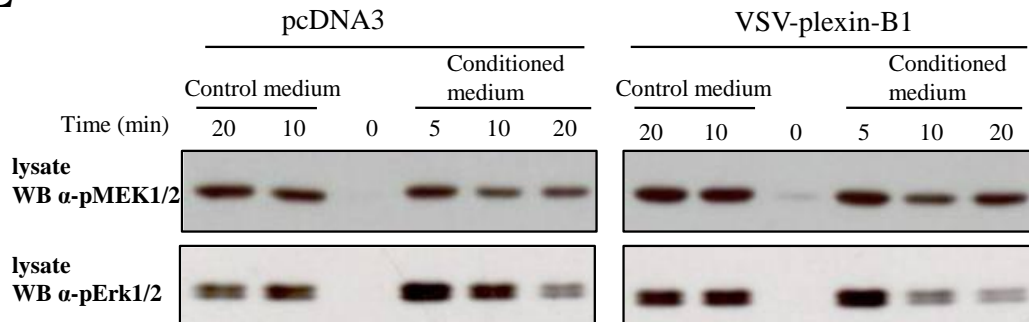
D**E**

Figure 4.8 Effect of Sema4D in different solvents on MAPK activation. (D) HEK293 cells expressing exogenous plexin-B1 were incubated with dialyzed Sema4D (200 ng/ml) or PBS for different time intervals. Cells with empty vector were set as the control. Proteins of interest were the examined by Western-blotting. (E) Conditioned medium containing Sema4D was generated as described in Chapter 2. Cells were serum starved overnight and incubated with conditioned medium or medium from cells transfected with empty vector. MAPK pathway proteins were analyzed by Western-blotting.

4.2.7 Plexin-B1 mutations and MAPK pathway

In order to study if mutations of plexin-B1 have any impact on Sema4D-induced activation of Akt pathway proteins, HEK293 cells were over-expressed with plexin-B1 wildtype or mutants. As shown in Figure 4.9, Sema4D induces MEK1/2 activation in cells expressing plexin-B1 wildtype. In cells expressing mutated forms of the protein, the magnitude of elevation of phospho-MEK1/2 induced by Sema4D is not different from the wildtype. Although, as suggested in the previous section, the effect of Sema4D on MEK1/2 phosphorylation is masked by the effect of the vehicle solution, the finding in this section suggests that the mutated forms of plexin-B1 have no impact on the Sema4D/plexin-B1 induced MAPK activation or the alteration by mutation could not overcome the masking effect of other factors.

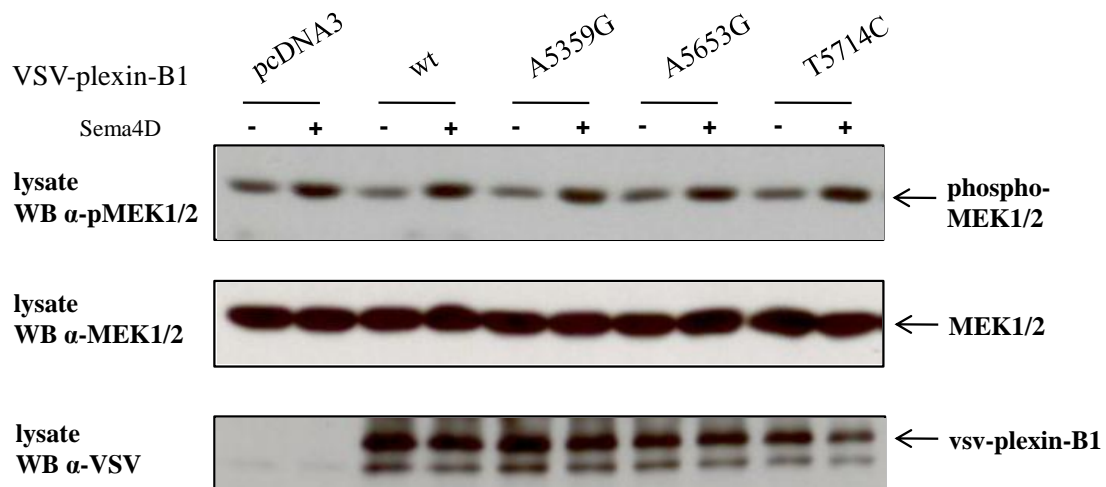


Figure 4.9 MAPK activation in cells expressing plexin-B1 wildtype/mutants. HEK293 cells were transfected with plexin-B1 wildtype/mutants. On the second day of transfection, cells were serum starved overnight and then incubated with Sema4D (200 ng/ml) for 15 minutes. Cells were harvested and proteins were extracted. The protein of interest was the examined by Western-blotting.

4.3 Discussion

4.3.1 Plexin-B1 mutations and receptor tyrosine kinases

Met belongs to the scatter factor receptor family. Met, plexin-B1 and Sema4D all share homology in their extracellular domain, and contain a conserved sequence of ~500 amino acids called the Sema domain (Maestrini et al., 1996). Met elicits a complex sequence of events resulting in invasive growth in cells upon HGF binding. ErbB-2 is notable for its role in breast cancer progression and over-expression of ErbB-2 is also found in ovarian cancer, stomach cancer in addition to breast cancer. There is no ligand known for ErbB-2 and it can only be activated by dimerization with other members of ErbB family (Olayioye et al., 2000). Both Met and ErbB-2 have recently been implicated in Sema4D/plexin-B1 signaling by coupling with plexin-B1. In the first part of this chapter, interaction between the receptor tyrosine kinases Met/ErbB-2 and plexin-B1 was studied. Using immunoprecipitation, I confirmed that plexin-B1 interacts with ErbB-2 and Met. Plexin-B1 binds to either ErbB-2 or Met through their extracellular domains (Swiercz et al., 2004). The mutated forms of plexin-B1, A5359G, A5653G and T5714C, are all site mutated in the cytoplasmic domain. There is no alteration of plexin-B1/ErbB-2 or plexin-B1/Met binding in all the mutated forms of plexin-B1. These results suggest that mutations of plexin-B1 located in the cytoplasmic domain do not have any effect on its extracellular portions and do not induce any changes of its binding ability to these two receptor tyrosine kinases.

Different groups have reported that plexin-B1 interacts with receptor tyrosine kinases and both Met and ErbB-2 are involved in the Sema4D/plexin-B1 regulated cell

function. However, there are controversial findings about the cell responses regulated by RTK/plexin-B1 signaling. The Italian group has shown that Sema4D induces invasive growth by coupling with Met via plexin-B1 (Conrotto et al., 2004; Conrotto et al., 2005; Giordano et al., 2002). By applying scatter assays, transwell motility assays, soft agar growth assays and 3-D growth assays in collagen type I, they observed consistent increased cell metastatic behavior in mouse epithelial liver cells MLP29, human endothelial cells HUVECs and mouse fibroblast cells NIH 3T3 (Conrotto et al., 2004; Giacobini et al., 2008; Giordano et al., 2002). The German group also reported the involvement of Met in Sema4D/plexin-B1 signaling (Swiercz et al., 2008). In cell models established in breast cancer cells, they found ErbB-2 and Met have opposite effects on cell motility after Sema4D activation. Sema4D promotes cell motility through activation of RhoA which is dependent on ErbB-2. Whereas, Sema4D inhibits cell migration through inactivation of RhoA via Met. Combining results from these two groups, the role of Met in regulation of cell movement through Sema4D/plexin-B1 signaling is contradictory. ErbB-2 and Met compete for plexin-B1 (Swiercz et al., 2008). The controversial role of Met in cell motility regulation might be determined by the stoichiometry of ErbB-2, Met and plexin-B1 expression in each cell type. This is also consistent with the dual role of Sema4D as an attractive or repulsive cue in regulating cell movement. Based on these findings, I investigated the role of Met and ErbB-2 in Sema4D-induced cell migration in prostate cancer cells. LNCaP cells express ErbB-2 but are null in Met expression. In comparison, PC3 cells express Met and exhibits relatively low level of ErbB-2 expression. Previously, our group has demonstrated that Sema4D increased cell migration ability in LNCaP cells using transwell migration assays. In this

study, it is shown that Sema4D inhibits PC3 cells from migrating through the membrane of transwells. Taken together, these findings are the first to suggest the reciprocal roles of ErbB-2 and Met on cell motility via plexin-B1 within prostate cancer cells. In LNCaP cells Sema4D increases cell motility in the presence of ErbB-2 expression. In PC3, Sema4D decreases cell motility suggesting that Met has overcome the effect of ErbB-2 and exhibits an inhibitory effect on cell motility. These results are consistent with the theory of opposite roles of ErbB-2 and Met on cell motility via plexin-B1 by Swiercz group.

Due to time limitation, further study was not carried on. siRNA targeting Met could be applied in prostate cancer cell line PC3 to study if the Sema4D-induced suppression of cell motility could be abolished. In the same way siRNA against ErbB-2 could be infected into LNCaP cells and meanwhile Met could be introduced to LNCaP cells. Migration assays could be carried out in these cells to investigate if the Sema4D-induced increase of cell motility is suppressed. To further confirm the regulatory role of Met/ErbB-2 on Sema4D/plexin-B1 induced RhoA inactivation/activation in prostate cancer cells, RhoA inactivation/activation in response to Sema4D in both PC3 and LNCaP cells could also be examined.

4.3.2 Plexin-B1 mutations and the Akt/MAPK pathways

In endothelial cells, Sema4D induces activation of the PI3K-Akt pathway. In this study, I aimed to study if Sema4D/plexin-B1 signaling had any effect on PI3K-Akt

pathway in epithelial cells. There is no Sema4D-induced activation of Akt in epithelial cells, suggesting that Sema4D-induced activation of PI3K-Akt pathway might be restricted to endothelial cells. MAPK activation is observed in growth cone in response to axon guidance molecules (Campbell and Holt, 2003; Pasterkamp et al., 2003). Sema4D acts as axon guidance cue and could also activate MAPK pathway. In epithelial cells I found that Sema4D also activates MEK1/2 and Erk1/2. However, control experiment shows that the effect of Sema4D on MAPK has been masked by Sema4D carrying vehicles such as glycine and glutathione. There has been reported that glycine could indirectly induced MAPK activation (Campbell and Holt, 2003). To avoid the masking effect of Sema4D by other factors, I dialyzed Sema4D concentrate to get rid of the vehicle molecules. Surprisingly MAPK activation is still observed in PBS control samples. MAPK activation is induced by many factors and it is directly downstream of Sema4D/plexin-B1 signaling. Therefore the effect of Sema4D on MAPK could be affected by many factors. As shown in this chapter, the interfering factors could not be completely subtracted. I also investigated the MAPK response to Sema4D in cells expressing mutated forms of plexin-B1. I did not observe any alteration in MAPK activation between the mutants and wildtype in response to Sema4D treatment. If mutated forms of plexin-B1 had lower capacity in activating MAPK, the effect of interfering factors on MAPK activation could be strong enough to cover the alteration. If the mutated forms had increased ability to stimulated MAPK, it is also possible this effect could not be observed because the interfering factors have made the phosphorylated forms of MEK1/2 or Erk1/2 saturated. A conclusion could not be drawn as to whether mutated forms of plexin-B1 have any effect on MAPK activation.

Chapter 5

Mutation of plexin-B1 and cell migration

5.1 Introduction

Three of the mutated forms of plexin-B1 investigated in this thesis were found in the metastases of clinical prostate cancer tissues (mutant A5653G, T5714C) or prostate cancer cell lines (A5359G, only in LNCaP cells), also the frequency of plexin-B1 mutations were higher in metastases than primary tumors (Wong et al., 2007). Previously our group members Dr. Oscar Wong and Dr. Tharani Nitkunan have demonstrated that mutated forms of plexin-B1 have changed cell phenotypes using cell spreading, cell invasion, and cell collapse assays. These results suggest that the mutated forms of plexin-B1 results in increased metastatic abilities. In this chapter, I carried out experiments aiming to find out if mutated forms of plexin-B1 have any effect on cell motility. HEK293 cells stably over-expressing plexin-B1 wildtype/mutants were subjected to migration assays using a transwell system.

5.2 Results

Pools of HEK293 cells stably expressing plexin-B1 wildtype/mutants were obtained from Dr. Magali Williamson. Firstly I performed Western-blotting to confirm the plexin-B1 protein expression. Figure 5.1.A shows that all the transfectant pools express plexin-B1 protein at 300 kDa. These cells were then applied to migration assays. The graph in Figure 5.1.B shows that cells expressing wildtype plexin-B1 has lower motility relative to vector control, suggesting that wildtype plexin-B1 may have an inhibitory effect on motility. The motility of cells expressing mutants A5359G and

A5653G is significantly higher relative to both wildtype and vector control cells, indicating a gain of function. Mutant T5714C shows higher motility than the wildtype at a less threshold compared with the other mutants and the same motility as the vector control, suggesting a loss of inhibitory function of wildtype plexin-B1. Sema4D did not initiate statistically significant change of motility compared to untreated cells.

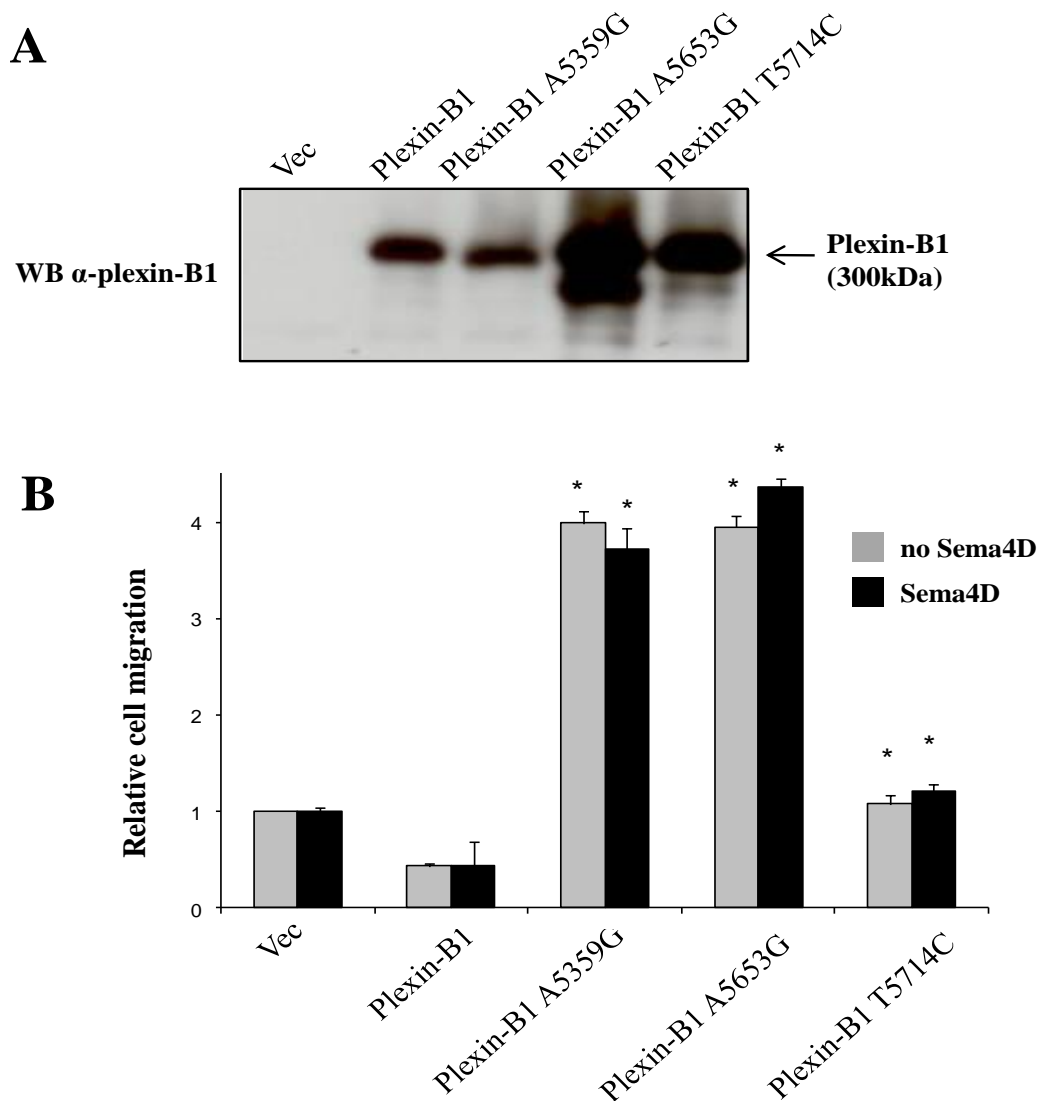


Figure 5.1 The motility of cells expressing plexin-B1 wildtype/mutants.

(A) HEK293 cells were stably expressing plexin-B1 wildtype/mutants. Cells were lysed and proteins were resolved by SDS-PAGE. Western blotting result was performed by using anti-plexin-B1 antibody as the primary antibody. (B) Cells expressing plexin-B1 wildtype/mutants were applied to transwells for migration assays. Cells were treated with or without Sema4D (400 ng/ml). The bottom cells were fixed and stained at the end of migration assay. The relative migration of cells were calculated as the cells migrated relative to vector control (The raw data is presented in Appendix 3). All the experiments were repeated at least three times and the error bars stand for the standard error of the mean.

5.3 Discussion

Plexin-B1 has been implicated in the regulation of a variety of cell functions including cell migration, axon guidance and neurite outgrowth. The ultimate aim of this project is to find out how the mutations affect cell signalling and cell functions. By using migration assays I found that cells expressing mutated forms of plexin-B1 exhibit increased motility relative to cells expressing wildtype plexin-B1. This result is consistent with the time-lapse experiment of Dr. Tharani Nitkunan (Wong et al., 2007). She did the assays without Sema4D, therefore the effect could be autocrine Sema4D/plexin-B1 signalling for her experiment. In this study, I looked at the effect of externally applied Sema4D. However, I did not observe the difference between untreated and Sema4D treated cells. It has been suggested that over-expression of plexin-B1 results in constitutively active plexin-B1 (Conrotto et al., 2004). Over-expressed plexin-B1 wildtype/mutants in HEK293 cells could be constitutively active and mediate cell motility independent of Sema4D. Also HEK293 cells express Sema4D (Figure 3.2). The increase in motility resulting from mutations of plexin-B1 could be due to a number of factors. The loss of R-Ras GAP activity and the loss of inhibition on Rac activity for mutants will both result in an increase in cell motility. Met and ErbB-2 also regulate cell motility. The increased motility of plexin-B1 mutants is probably due to a balance between all these factors. My group member Dr. Magali Williamson and Dr. Oscar Wong have also found that mutated forms of plexin-B1 expressing cells demonstrate other metastatic phenotypes. All the three mutated forms of plexin-B1, A5359G, A5653G and T5714C confer an increased capacity to spread and invade. This evidence supports the

hypothesis that mutation of plexin-B1 promotes the progression of cells to more metastatic and malignant state.

Chapter 6

Plexin-B1 mutation and RhoD GTPase

6.1 Introduction

The Rho subfamily of small GTPases including Rac and Cdc42 are important regulators for actin reorganization. Recently small Rho GTPases have been shown to be highly involved in plexin-B1 signaling transduction. Plexin-B1 signaling mediated by several Rho GTPases, regulates many actin-driven processes such as growth cone collapse, axon guidance and cell migration. Activation of Rac results in lamellipodia formation. GTP-bound Rac binds to a CRIB-like motif in the non-conserved region of the cytoplasmic domain of plexin-B1 (Tong et al., 2007). In this way plexin-B1 sequesters Rac1 from its downstream effector PAK and inhibits actin polymerization (Vikis et al., 2002). Rho mediates the formation of stress fibers. Rho switches from inactive GDP-bound form into the active GTP-bound state by guanine nucleotide exchange factors (GEFs), including PDZ-RhoGEF, leukemia-associated RhoGEF (LARG) (Boguski and McCormick, 1993). Plexin-B members possess a PDZ-binding motif in their carboxyl terminal through which plexin-B1 binds to the PDZ domain of PDZ-RhoGEF/LARG, resulting in Rho activation and subsequent neurite retraction and growth cone collapse in response to Sema4D (Hirotsani et al., 2002; Perrot et al., 2002; Swiercz et al., 2002). Rnd1, a member of Rho family, is critically involved in this plexin-B1-mediated Rho activation in COS7 cells. Rnd1 binds to cytoplasmic domain of plexin-B1 and this interaction enhances the interaction between PDZ-RhoGEF and plexin-B1, potentiating PDZ-RhoGEF-mediated RhoA activation (Oinuma et al., 2003).

The research group led by Dr. M. Buck demonstrates consistent result of interaction between plexin-B1 and small GTPases proteins using NMR spectroscopy and

x-ray crystallographic solutions. They identified the region consisting of 120 amino acids located in cytoplasmic domain of plexin-B1 that directly binds to Rac1, Rnd1, and RhoD (Tong et al., 2007). Previously my group colleague Dr. Oscar Wong has demonstrated that mutant plexin-B1 T5714C has lost its binding ability to Rac1 GTPase. This suggests that mutation of plexin-B1 results in conformation change in its cytoplasmic region responsible for small GTPase binding. Combining these facts and findings, I hypothesized that the mutations of plexin-B1 might also affect its interaction with RhoD, the other small GTPase which is reported to interact with plexin-B1. I generated GST-fused cyto-plexin-B1 wildtype/mutants proteins and performed GST-pull down assay to study if the interaction between plexin-B1 and RhoD was altered by plexin-B1 mutations.

6.2 Results

6.2.1 Interaction between RhoD and full length plexin-B1

Plasmids encoding dominant negative or constitutively active forms of RhoD were introduced to HEK293 cells by Lipofectamine transfection. The amount of DNA for each well of six-well plates is indicated in Figure 6.1.A. Myc-tagged Rac L61/N17 plasmids were used as positive control for gradient increasing expressions of myc-tagged protein in HEK293 cells. The upper panel of Figure 6.1.A shows that myc-tagged RhoD T31K is 26 kDa and myc-tagged RhoD G26V is 22 kDa as expected (personal communication with Dr. Endo). At a low DNA input at transfection, the expression of RhoD T31K or G26V is not detectable at a short exposure time (lanes 1, 2, 4 and 5). The

lower panel of Figure 6.1.A illustrates the expression of RhoD T31K/G26V and plexin-B1 in HEK293 cells co-transfected with these two plasmids. The DNA amounts labeled in the figure indicates the quantity of plasmids per transfection for each well of 6-well plates. As shown in the figure, the transfection efficiency of plasmid encoding RhoD T31K is lower than that of RhoD G26V, given the same transfection conditions. According to these results, the optimal ratio of plasmids for transfection was determined.

As implied by Tong et al. RhoD interacts with the cytoplasmic region of plexin-B1 at the same site as that to which Rac1 binds to (Tong et al., 2007). Therefore HEK293 cells were co-transfected with plexin-B1 and RhoD T31K/G26V and immunoprecipitation was carried out to study the interaction between RhoD and full length of plexin-B1. There are no positive bands indicating the interaction between full length plexin-B1 and either active or inactive form of RhoD in the blots.

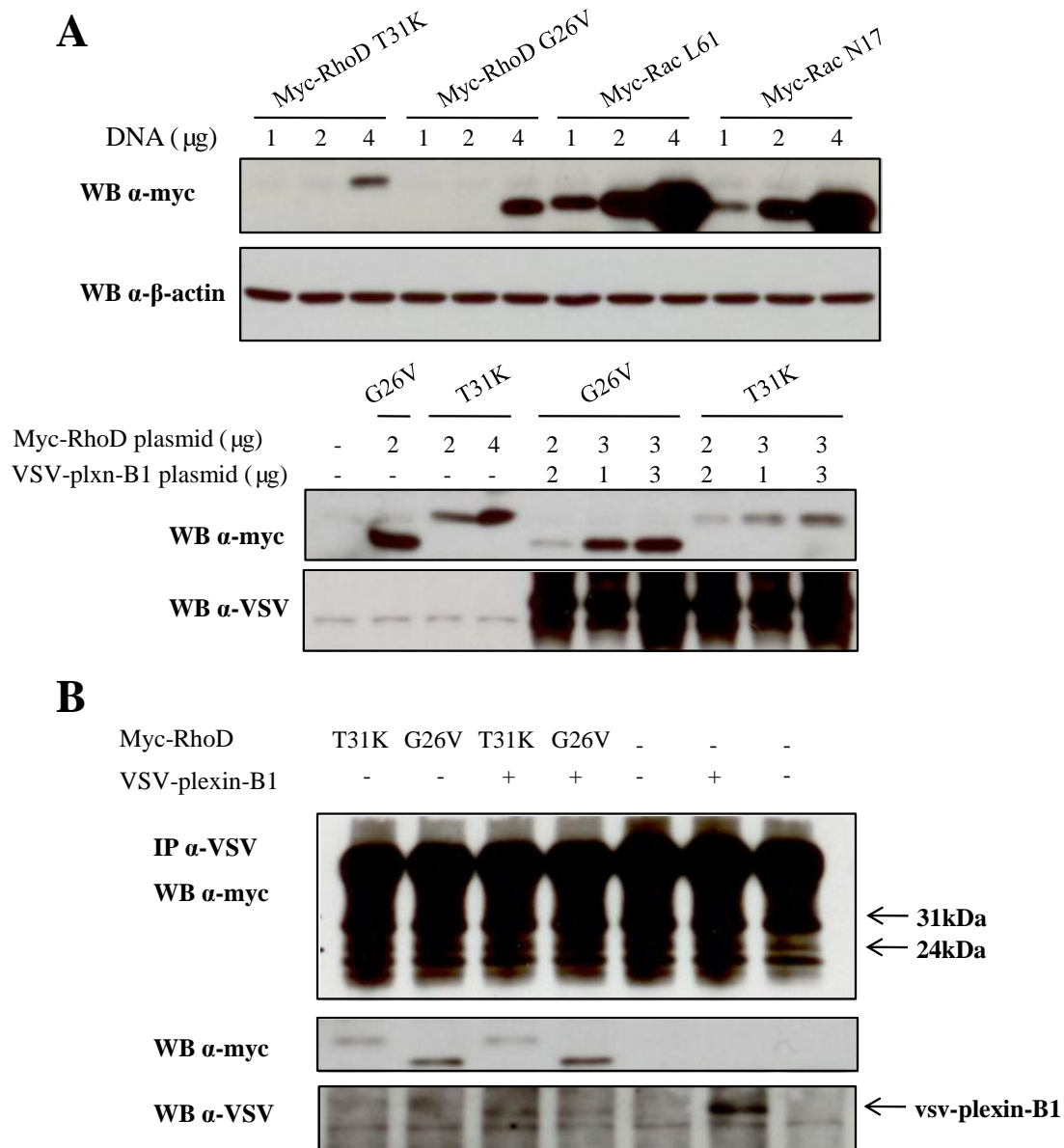


Figure 6.1 Interaction between RhoD and full length plexin-B1. (A) HEK293 cells were co-transfected with different quantities of plasmid DNA encoding constitutively negative (T31K) or active (G26V) RhoD and lysates were analyzed by Western-blotting. Lower panel shows the titration of DNA for transfection when co-expressing RhoD T31K/G26V and plexin-B1. Cells expressing myc-Rac were used as a relative indicator of myc expression. (B) HEK293 cells were co-expressed RhoD T31K/G26V and plexin-B1/pcDNA3. Lysates were immunoprecipitated with anti-VSV antibody and probed with anti-myc antibody to investigate the binding between RhoD and plexin-B1.

6.2.2 Interaction between RhoD and cyto-plexin-B1 wildtype/mutants

Since I could not manage to get positive results in immunoprecipitation assay aiming to investigate the interaction between full length plexin-B1 and RhoD, I used cytoplasmic plexin-B1 as an alternative to investigate the binding of RhoD and plexin-B1. Expression of GST fusion proteins of the cytoplasmic plexin-B1 wildtype/mutants were induced in BL21 bacterial cells. The fusion proteins were then extracted and purified by incubation with glutathione sepharose 4B matrix. Figure 6.2.A shows the coomassie blue staining results of GST fusion proteins before GST purification and of the supernatant after purification. All the lanes of the figure were labeled by the name of the plasmid with which the BL21 cells were transformed. A control was set as BL21 cells transformed with pGEX cyto-plexin-B1 without inducer IPTG. During the GST purification step, only GST fusion protein binds to the matrix. Figure 6.2.B illustrates the yield of purified GST fusion protein of cytoplasmic plexin-B1 wildtype/mutants. Clear blue bands at the size of 80 are the GST-fused protein products. There is no equivalent band in GST control which originated from cells transformed with pGEX4T3. In the control without IPTG inducer there is a very weak band indicating that there was a leak of non-specific induction of GST protein during the process. However, this faint band provides evidence of the good yield of specific GST fusion protein.

I then incubated the GST fusion protein of cyto-plexin-B1 wildtype/mutants with lysates from HEK293 expressing either dominant negative RhoD (T31K) or constitutively active RhoD (G26V). A GST pull-down assay revealed that there is no interaction between plexin-B1 with RhoD T31K that encodes inactive form of RhoD

(Figure 6.3). Plexin-B1 binds to the active form of RhoD and further more mutants A5359G and A5653G exhibit an increased binding capability to active RhoD compared with cytoplasmic plexin-B1 wildtype. Mutant T5714C also shows increased binding; though to a lesser extent relative to the other mutants. These results provide evidence that mutated forms of plexin-B1 have an increased binding affinity to active RhoD.

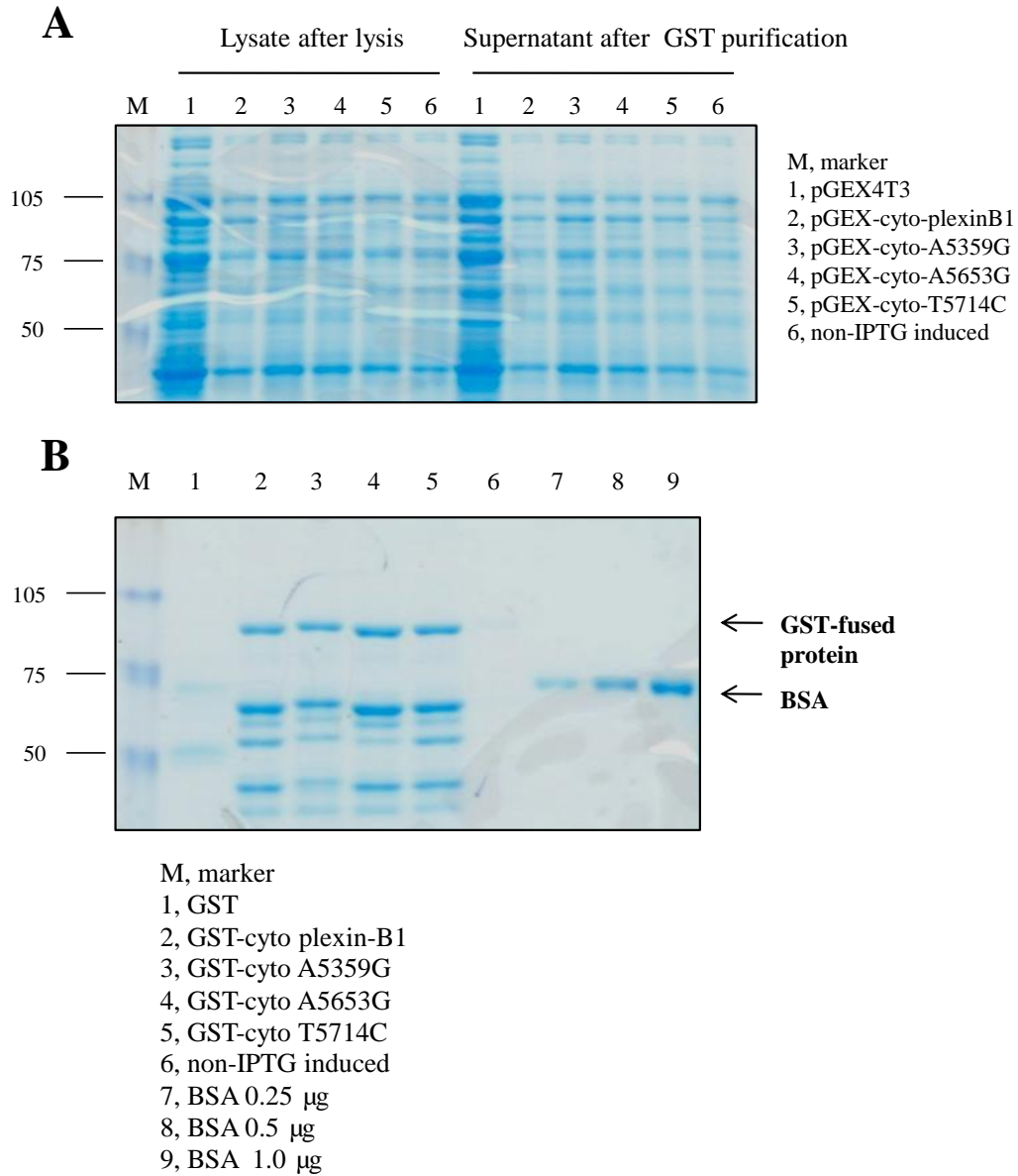


Figure 6.2 Coomassie blue staining of GST-fused products. Vectors encoding cytoplasmic portion of plexin-B1 wildtype/mutants were introduced to BL21 cells and GST fusion proteins were induced by adding IPTG. Cells were lysed and lysates were resolved by SDS-PAGE and followed by Coomassie blue staining. (A) Cell lysates before purification with Glutathione sepharose 4B beads and after GST purification were visualized by electrophoreses for quality check. (B) 5 µl of GST-purified protein matrix was resolved by SDS-PAGE.

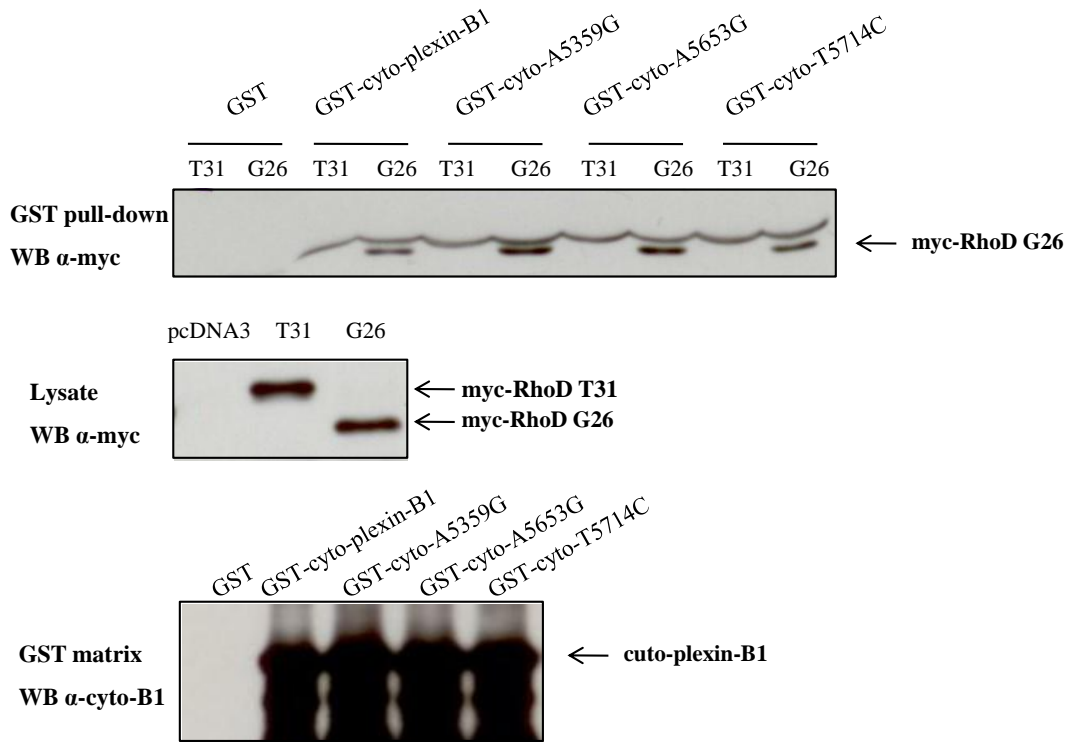


Figure 6.3 Interaction between RhoD and cyto plexin-B1 wildtype/mutants. GST fusion protein of cytoplasmic plexin-B1 wildtype/mutants were induced in *E. coli* bacterial cells and GST pull-down assay was performed with HEK293 lysates expressing constitutively inactive (T31) or active (G26) RhoD. Mutants A5359G and A5653G demonstrated increased binding ability to active RhoD (G26) compared with wildtype cyto-plexin-B1, whereas mutant T5714C exhibited a lesser extent of elevated ability. This is representative of three repeats.

6.3 Discussion

Previously my group member Dr. Oscar Wong has found that plexin-B1 mutant T5714C has lost the binding affinity to active Rac. This consequently results in the inhibition of Rac-dependent plexin-B1 trafficking to the cell surface and loss of inhibition of lamellipodia formation (Geewan Wong, The effects of prostate cancer-related plexin-B1 mutations on protein function, Thesis submitted in 2008, University College London). Given the evidence that the region of plexin-B1 for Rac binding is the same site as for RhoD interaction, I carried on the research on the effects of plexin-B1 mutation on RhoD binding. Using full-length plexin-B1, I did not manage to get positive result of interaction between plexin-B1 wildtype and RhoD. The same problem happened with Dr. Wong when he was dealing with full-length plexin-B1/Rac interaction assay. The suggested explanation for this failure to pull down small Rho GTPases with full-length plexin-B1 might be the massive size of the full-length plexin-B1 protein (300 kDa). This may make the yield of immunoprecipitated RhoD or Rac too low to be detected.

By using GST fusion protein of cytoplasmic plexin-B1 I have successfully demonstrated that plexin-B1 wildtype binds to RhoD, and this is consistent to the spectroscopy and x-ray crystallography results by Tong et. al. (Tong et al., 2007). However, Tong did not indicate if the binding between plexin-B1 and RhoD GDPase is GTP-dependent. In this chapter, I have been the first to show that plexin-B1 specifically binds to RhoD GTPase but not RhoD GDPase. In contrast to the finding of loss of binding function of plexin-B1 mutants to Rac, the mutations confer a gain of binding function of plexin-B1 to RhoD. Mutated forms of plexin-B1 demonstrate stronger

binding affinity to RhoD G26V than wildtype cyto-plexin-B1 does. In Chapter 5 it is presented that cells over-expressing mutated forms of plexin-B1 demonstrate increased migration ability compared with cells with plexin-B1 wildtype. Combining these findings, increased RhoD GTPase binding is correlated to increased migration ability. RhoD is a member of the Rho GTPase subfamily but it possesses unique functions among the Rho family. Over-expression of constitutively active RhoD disassembles stress fibers and focal adhesions, resulting in decreased cell migration in fibroblasts (Tsubakimoto et al., 1999). It is likely that by binding to RhoD GTPase, wildtype plexin-B1 sequesters active RhoD and inhibits the suppressive effect on migration by RhoD. Mutated forms of plexin-B1 exhibit stronger binding affinity to RhoD, suggesting that plexin-B1 mutants sequester more RhoD than the wildtype does and consequently lessen the inhibitory effect of RhoD on migration to a greater extent. Therefore, cells over-expressing mutated forms of plexin-B1 demonstrate higher motility than cells over-expressing wildtype plexin-B1. In this way expression of mutated forms of plexin-B1 may increase the motility of cells.

Zanata et al. has reported the antagonistic effects of Rnd1 and RhoD GTPases on Sema3A-induced cytoskeletal collapse (Zanata et al., 2002). Both Rnd1 and RhoD bind to the cytoplasmic domain of plexin-A1, which is the receptor for Sema3A. Sema3A induces cytoskeletal collapse in a Rnd1-dependent way. RhoD blocks this Rnd1-dependent Sema3A-induced collapse (Zanata et al., 2002). Given the fact that the cytoplasmic domain of plexins is highly conserved among all the members, it is possible that binding of RhoD to plexin-B1 antagonizes Rnd-induced collapse. Our group member, Dr. Tharani Nitkunan, has revealed that cells expressing mutated forms of plexin-B1

exhibit decreased Sema4D-induced cytoskeletal collapse compared with the cells expressing wildtype. This phenotype of the mutants is correlated with increased binding affinity to RhoD GTPase as demonstrated in this chapter. Taken Zanata's theory and our findings, we propose the model that RhoD mediates Sema4D/plexin-B1 signalling by antagonizing Rnd. The Sema4D induced R-Ras GAP activity of plexin-B1 is mediated by Rnd. Binding of RhoD to wildtype plexin-B1 antagonizes Rnd and results in a decrease in Rnd-mediated R-Ras GAP activity. Mutated forms of plexin-B1 couple more RhoD GTPase relative to wildtype plexin-B1 and have increased antagonism to Rnd, resulting in loss of R-Ras GAP activity and block of Rnd1-dependent cell collapse induced by Sema4D. Zanata did not show if Rnd1 and RhoD compete for plexin-A1 binding. Previously our group has shown that mutants A5359G and A5653G bind to Rnd, and mutant T5714C has lost the ability to bind to Rnd1 (Wong et al., 2007). However mutant T5714C has only a small increase in RhoD binding compared to mutants A5359G and A5653G. This suggests that Rnd and RhoD may not compete for plexin-B1 binding. This should be confirmed by further analysis if given more time. The mutated site for mutant T5714C is in the Rac-binding domain of plexin-B1, while mutants A5359G and A5653G are outside of this domain (Tong et al., 2008). Mutant T5714C has lost Rac binding ability, whereas the other two mutants have gained ability to bind to RhoD. Therefore the mutated region of mutants A5359G and A5653G are more important in RhoD binding. Mutants A5359G and A5653G possibly result in conformation change, suggested by Dr. Matthias Buck (personal communication). This conformation change may explain the increased RhoD binding ability.

RhoD is unique among Rho family members that it regulates the motility of early endosomes (Murphy et al., 1996). The effectors of RhoD have not been extensively studied. hDia2C protein is the first identified effector for RhoD and it induces alignment of early endosomes along actin filaments and inhibits endosome motility in a c-Src kinase-dependent way (Gasman et al., 2003). Src is necessary for Sema4D-induced Akt/PI3K pathway activation in endothelial cells. These together may imply that Src may crosslink the RhoD and Akt/PI3K pathways through Sema4D/plexin-B1 activation. On the other side, this hypothesis is likely dependent on cell types since Akt pathway activation through Sema4D is only reported in endothelial cells. If given more time, I would further explore the downstream of RhoD in context with Sema4D/plexin-B1 signaling. To determine the effects of increased RhoD binding observed in the mutants, inhibition of RhoD activity assays may be performed to further investigate cell functions.

Chapter 7

Discussion

7.1 Significance of this study

Our group has been the first to report plexin-B1 mutations in prostate cancer. Of all the mutated forms identified in both clinical samples and prostate cancer cell lines, we have been focusing on mutants A5359G, A5653G, and T5714C and have revealed that cells expressing these mutated forms of plexin-B1 exhibit more metastatic features compared with cells expressing wildtype plexin-B1 (Wong et al., 2007). In this study I continued the study on molecular characterization of plexin-B1 mutation and explored how these mutated forms affect cell signalling and cell functions. My studies on tyrosine kinases ErbB-2, Met and small GTPase RhoD completed the blank spaces of Table 1.1 in Chapter 1 and are summarized in Table 7.1.

Table 7.1 Protein function changes of the plexin-B1 mutations relative to wildtype

	Rac binding	Rnd binding	R-Ras binding	RhoD binding	ErbB-2 binding	Met binding	PDZ-RhoGEF binding
wt	binds	binds	binds	binds	binds	binds	binds
A5359G	reduced	binds	lost	increased	binds	binds	binds
A5653G	reduced	binds	lost	increased	binds	binds	binds
T5714C	lost	lost	lost	increased	binds	binds	binds

Due to the lack of intrinsic tyrosine kinase activity of plexin-B1, the signal transduction pathways initiated by Sema4D/plexin-B1 involves extrinsic tyrosine kinases. Several tyrosine kinases such as Met, ErbB2, and PI3K/Akt have been extensively studied in Sema4D/plexin-B1 signalling and play crucial roles either upstream or downstream of plexin-B1. Whether mutations of plexin-B1 have any effect on tyrosine

kinase-regulated plexin-B1 signalling was not previously known. My study on tyrosine kinases has unveiled this aspect. Met and ErbB-2 are the two main receptor tyrosine kinases that interact with plexin-B1 and regulate cell movement. All three mutants, A5359G, A5653G, and T5714C bind to either Met or ErbB-2 to the same extent as wildtype plexin-B1 does. Therefore mutations located in the cytoplasmic portion of plexin-B1 do not change the protein's binding ability to Met or ErbB-2 through the extracellular domain.

The effects of Met and ErbB-2 on Sema4D/plexin-B1-regulated cell motility have been contradictory according to the reports of different research groups. Swiercz et al. have shown that treatment of breast cancer cells co-expressing plexin-B1 and ErbB-2 with Sema4D results in increased migration, whereas treatment of cells co-expressing plexin-B1 and Met results in decreased migration (Swiercz et al., 2008). Other groups have shown that the interaction of Met and plexin-B1 enhances migration (Giordano et al., 2002). The study on Met/plexin-B1 and ErbB2/plexin-B1 using prostate cancer cell lines LNCaP and PC3 show consistent results with Swiercz's. My group leader Dr. Williamson has demonstrated Sema4D increases cell motility in the LNCaP cell line. I have found that Sema4D decreases cell motility in PC3 cells. Western-blotting analysis shows that these two cell lines exhibit special patterns of Met/ErbB-2 expression that fit the theory of the reciprocal roles of Met and ErbB-2 on Sema4D/plexin-B1-regulated motility (Swiercz et al., 2008). LNCaP expresses ErbB-2 but not Met, while PC3 expresses Met and a relatively low level of ErbB-2. These findings suggest that the cell motility response stimulated by Sema4D through endogenous plexin-B1 in prostate cancer cells depends on the stoichiometry of plexin-B1, ErbB-2 and Met. Sema4D could initiate

diverse cell responses depending on the composition of the heteromultimeric receptor complexes formed by plexin-B1 and other receptor tyrosine kinases. Further evidence for a link between the identity of the receptor tyrosine kinase with which plexin-B1 couples and the response to Sema4D could be provided by screening other prostate cancer cell lines for Met/ErbB-2 expression and for increased or decreased Sema4D-induced motility. To determine if the opposite effects of Sema4D on PC3 and LNCaP are due to plexin-B1 signalling via Met and ErbB-2 respectively, expression of these two tyrosine kinases could be reversed. This would be achieved by reducing ErbB-2 activity with inhibitors or siRNA in conjunction with exogenous expression of Met in LNCaP. In a similar way, Met could be inhibited and ErbB-2 over-expressed in PC3. Motility in response to Sema4D could then be assayed. It remains unclear how the RhoA activity downstream of Sema4D/plexin-B1 signalling is regulated by ErbB-2 and Met in prostate cancer cell lines. In addition, it is not clear whether the mutated forms of plexin-B1 have any impact on ErbB-2/Met-regulated RhoA activation in prostate cancer cells. The answers to these questions will help with the characterization of the molecular mechanism underlying the contribution of plexin-B1 mutations to prostate cancer progression. After I had completed my work, Swiercz et al. have newly found that ErbB-2 phosphorylates plexin-B1 in response to Sema4D at different tyrosine residues from Met, leading to binding of phospholipase C γ (PLC γ) to plexin-B1 and activation of PDZ-RhoGEF (Swiercz et al., 2009). The difference in the position of the phosphorylation sites in plexin-B1 that are phosphorylated by ErbB-2 and Met, and presumably the different adaptor proteins which bind to these phosphorylated tyrosines, may explain the opposite effects on RhoA regulation downstream of Sema4D/plexin-B1.

PI3K/Akt and MAPK pathways are two important pathways that have been extensively studied in cancer and other human diseases. Both of the pathways have been implicated in Sema4D/plexin-B1 signalling. Different research groups have reported contradictory findings for the response of PI3K/Akt under the regulation of Sema4D/plexin-B1 (Basile et al., 2005; Ito et al., 2006; Swiercz et al., 2004). These opposite results of PI3K/Akt phosphorylation status in response to Sema4D/plexin-B1 signalling may depend on different cell types and the corresponding cellular context. My study on PI3K/Akt and MAPK aimed to identify if mutated forms of plexin-B1 have any effect on activation of these kinases compared to wildtype. Ito et al. has reported that PI3K/Akt is downstream of plexin-B1/Rnd1-regulated R-Ras GAP activity and is decreased in activity in response to Sema4D (Ito et al., 2006). Our group has previously found that all the three mutants A5359G, A5653G, and T5714C have lost the binding ability to R-Ras and the R-Ras GAP activity. Combining these findings, it is possible that plexin-B1 mutants may affect downstream PI3K/Akt activity in response to Sema4D relative to wildtype. Swiercz et al. also found that Sema4D/plexin-B1 signaling via ErbB-2 increased Akt phosphorylation (Swiercz et al., 2004). However, no alteration in Akt phosphorylation has been observed under the effect of Sema4D in HEK293 cells expressing plexin-B1 wildtype/mutants in this study. Plexin-B1 wildtype and mutants do not show any differences in Akt phosphorylation in response to Sema4D. Cells expressing mutant plexin-B1 do not show any difference in the magnitude of activation of MEK and Erk. However, any change in phosphorylation of these proteins in response to Sema4D may have been masked by phosphorylation resulting from treatment with the vehicle solution for Sema4D. As described in Chapter 4, many efforts have been made in

order to get rid of the masking effects on MAPK activation. The complexity and number of different signalling pathways that result in activation of PI3K/Akt and MAPK also increases the difficulty of revealing the molecular linkage between Sema4D/plexin-B1 and PI3K/Akt and MAPK pathways. It is possible that plexin-B1 together with many other proteins mediate PI3K/Akt and MAPK pathways and the mechanism of this remains to be elucidated.

Small GTPases such as Rnd1 and Rac1 are the other class of proteins that are critically involved in plexin-B1 signal transduction. Plexin-B1 sequesters Rac from PAK by interaction with Rac. Rnd1 is required for plexin-B1-mediated R-Ras GAP activity. Previously our group have reported that mutant T5714C has lost the ability to bind to Rnd1 and Rac1 compared to the wildtype plexin-B1. Although mutants A5359G and A5653G do not show any alteration in binding to Rnd1, these two mutated forms have decreased ability of sequestering active Rac1. Since Rac, Rnd and RhoD bind to plexin-B1 at the same region between C1 and C2 domains according to Tong et al., it was though possible that mutated forms of plexin-B1 affect RhoD binding. I have newly confirmed the binding of wildtype plexin-B1 and active RhoD using an immunoprecipitation approach, and this finding is consistent with that of Tong using crystallographic and structural solutions. All the three mutants exhibit increased binding ability towards active RhoD. Mutants A5359G and A5653G exhibit stronger interaction with RhoD than mutant T5714C does. Combining these results, we could come to the conclusion that the three site mutations within the small GTPase binding motif of plexin-B1 severely alter the association between small GTPases and plexin-B1. My group members and I have performed cell invasion assays and migration assays on cells stably

expressing plexin-B1 wildtype/mutants and have found that mutants A5359G, A5653G, and T5714C show increased motility compared to wildtype. Given that mutations of plexin-B1 are frequent in prostate cancer metastases, the three mutants are very likely correlated with tumor progression. Our findings on the altered binding ability to Rac, Rnd and RhoD of plexin-B1 mutants provide possible molecular mechanism responsible for the increased metastatic features. The proposed model of how RhoD contributes to plexin-B1-mediated cell motility has been discussed in Chapter 6. Binding of active RhoD to plexin-B1 may inhibit the suppressive effect of RhoD on cell motility. The interaction of plexin-B1 and RhoD also antagonizes the Rnd1-mediated cell collapse, leading to increased cell motility. Although this proposed theory needs to be further tested, my project together with our group members' findings, establish the basic molecular characterization of the role of plexin-B1 mutations on prostate cancer progression. The detailed discussion of how plexin-B1 mutations contribute to cancer invasion and metastasis via those affected pathways will be introduced in next section of this chapter.

7.2 Contribution of plexin-B1 mutations to the progression of prostate cancer

Based on the knowledge on Sema4D/plexin-B1 signalling pathways, the network of plexin-B1 is summarized into a diagram as shown in Figure 1.5 in Chapter 1. Plexin-B1 couples oncogene ErbB-2 and activates ErbB-2 in response to Sema4D, which in turn phosphorylates plexin-B1 and activates RhoA, resulting in an increase in cell motility and promotion of the invasive phenotype. On the other side, plexin-B1 sequesters Rac1 and

inactivates R-Ras GTP, resulting in decreased adhesion and increased cell collapse. Interaction of plexin-B1 and RhoD suppresses the inhibitory effect of RhoD on cell migration. RhoD binding also antagonizes Rnd and inhibits plexin-B1/Rnd-mediated cell collapse induced by Sema4D. These pathways work together to regulate cell movement and the net effect of these pathways determines the cells motility. Plexin-B1 mutations alter the way that the plexin-B1 protein functions and the cumulative effect of mutations on the various affected pathways is manifested as an increase in metastatic characteristics. Given the findings of our research work, we propose a model of how prostate cancer-related mutations of plexin-B1 contribute to the progression of prostate cancer (Figure 7.1). The mutations may selectively inhibit plexin-B1 inhibitory pathways (via R-Ras, Rac and RhoD) while retaining activation of promoting pathways (ErbB-2, Met), resulting in an increase in adhesion, motility and invasion relative to wildtype plexin-B1. In addition to the high frequency of somatic missense mutations in the plexin-B1 gene in both localized and metastatic prostate cancer, we also observed over-expression of plexin-B1 protein in primary prostate cancers. Tumor progression occurs by enhanced Sema4D/plexin-B1 signalling via ErbB-2 for wildtype and mutant plexin-B1. I have shown that plexin-B1 mutants retain the ability of ErbB2-mediated cell motility. On top of this, plexin-B1 mutants do not bind and sequester Rac and has lost R-Ras GAP activity, leading to a loss of inhibitory effects on metastatic phenotypes. Expression of mutated forms of plexin-B1 results in increased adhesion and decreased cell collapse. In addition plexin-B1 mutants enhance the binding to RhoD, resulting in suppression on the inhibitory effect of RhoD on cell migration. The increased binding ability of mutants to RhoD may also release the suppressive effect of Rnd-mediated R-Ras GAP, leading to

reduced cell collapse. The cumulative effects result in a net increase in motility by mutants. Therefore, mutations may confer a gain of metastatic phenotypes to the cell through inactivation of inhibitory pathways on cell motility, leading to tumor progression.

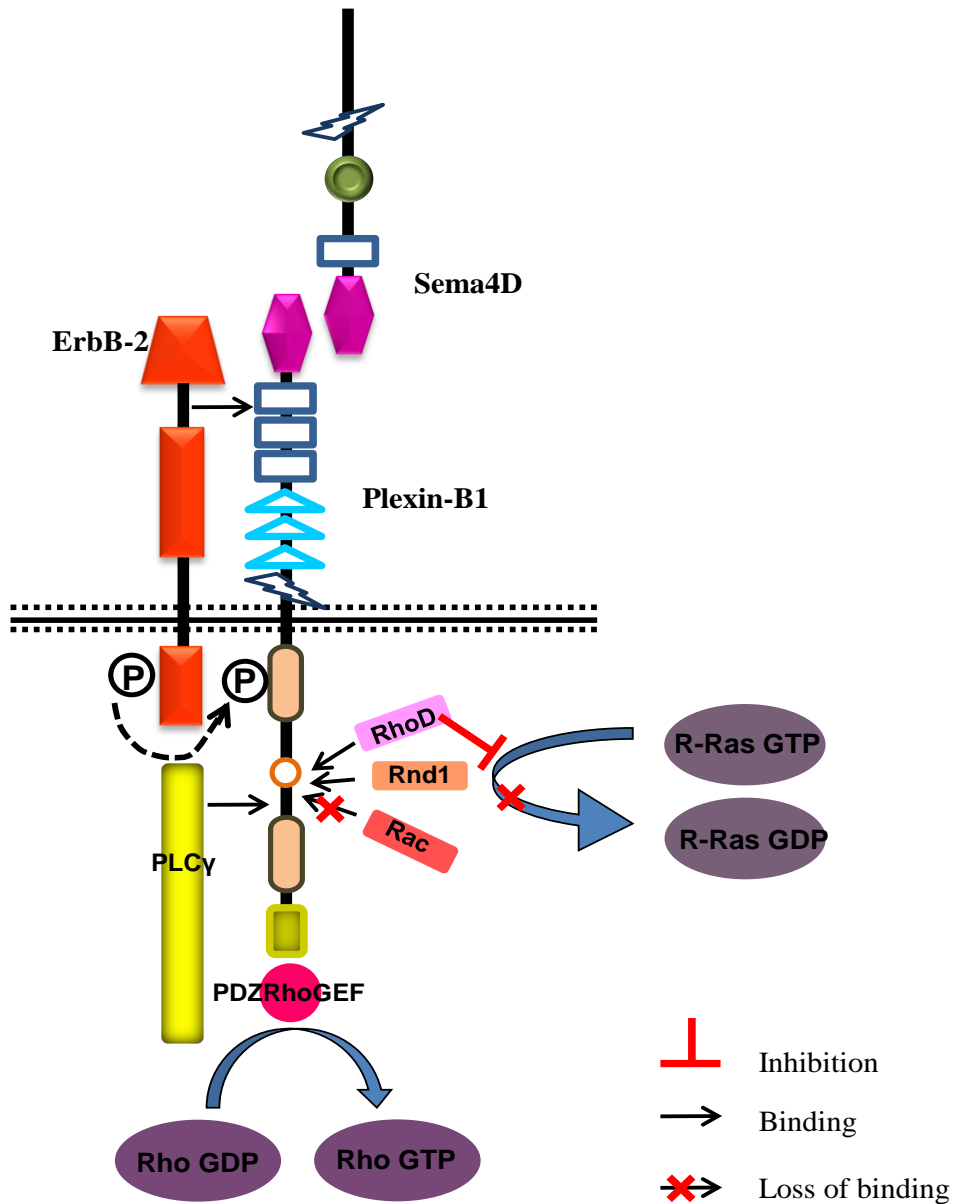


Figure 7.1 Proposed model of how plexin-B1 mutations affect cell signaling and contribute to increased cell motility. Sema4D/plexin-B1 transduces its signal through coupling with other proteins and forms a complex signaling network. Mutated forms of plexin-B1 retain the ability to bind to ErbB-2, Met and PDZ-RhoGEF which positively regulate cell migration. The mutations inhibit Rac, Rnd1 and R-Ras binding and R-Ras GAP activity. The mutated forms of plexin-B1 have therefore lost the ability to sequester Rac, leading to increased lamellipodia formation and cell spreading. In addition, the plexin-B1 mutants no longer bind to R-Ras and have lost the R-Ras GAP activity. My results have shown that the plexin-B1 mutants have increased RhoD binding ability. RhoD binding may antagonize the plexin-B1/Rnd-induced R-Ras GAP activity, resulting in loss of R-Ras inhibition and subsequent increased cell motility relative to the wildtype. The net result is an increase in motility.

7.3 Future work

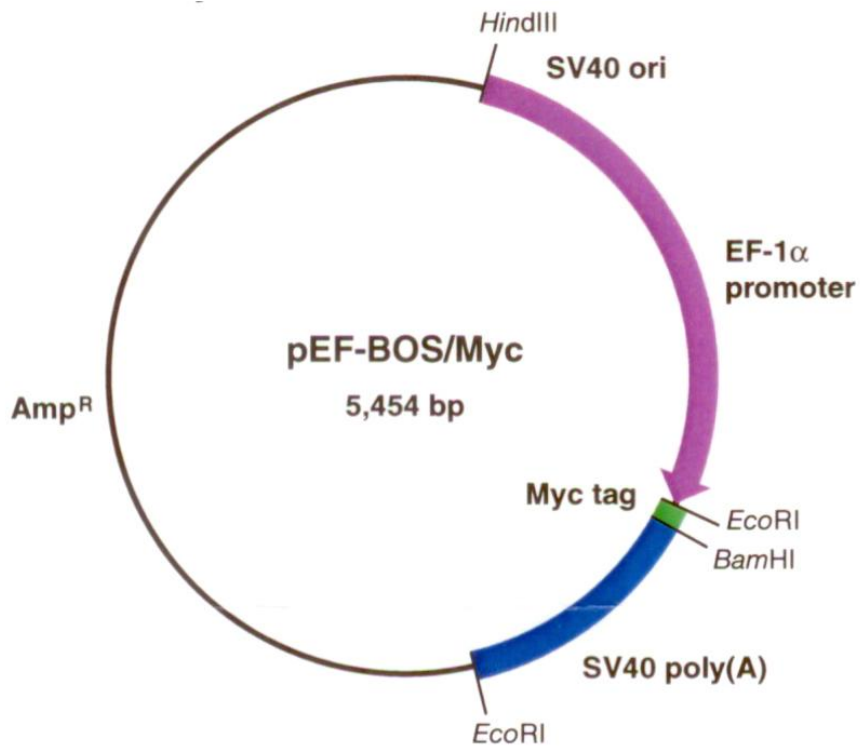
A high frequency of mutations in the plexin-B1 gene has been found in prostate cancer metastasis. Some of the mutations are also present in other tumors such as breast cancer. These findings suggest that plexin-B1 may be a potential oncogene. Our research on three mutants A5359G, A5653G and T5714C has led to a proposed model of how plexin-B1 mutations contribute to cancer progression. More work is needed to test this model. So far we mainly used non-prostate cells to determine if the mutations were functionally significant. However response to Sema4D is highly dependent on cell types and cellular context. Therefore, prostate cancer cell lines should be applied to determine the effect of mutant/wildtype plexin-B1 expression in response to Sema4D. During the time this thesis was drafted, our group has found plexin-B1 may play a role in cell proliferation. LNCaP cells treated with siRNA targeting at plexin-B1 demonstrated slower proliferation rate than the control (personal communication with Dr. Williamson). These preliminary results suggest that plexin-B1 may also control cell proliferation in addition to its role in cell movement. In our proposed model, RhoD may increase cell motility and suppress cell collapse through inhibiting the Rnd-induced R-Ras GAP activity. Further evidence is needed to confirm that the loss of R-Ras GAP activity in the three mutants is partly due to elevated RhoD binding to plexin-B1. To further test this, we could use siRNA to inhibit RhoD expression to investigate if the R-Ras GAP activity in plexin-B1 wildtype expressing cells is higher than the control. In cells expressing plexin-B1 mutants, we could inhibit RhoD expression to study if suppression of RhoD restores the R-Ras GAP activity in mutants A5359G and A5653G. There should be no

change for mutant T5714C as it does not bind Rnd and has lost the R-Ras GAP activity completely.

My findings on cell lines have revealed the role of plexin-B1 mutations on the metastatic phenotype *in vitro*. It is also important to know the functions of wildtype/mutant plexin-B1 *in vivo*. Xenografts of prostate cancer cells expressing wildtype/mutant plexin-B1 and prostate cancer cell lines in which plexin-B1 expression has been knocked out, could be applied to determine the role of plexin-B1 and its mutations in tumorigenicity. Transgenic mouse models in which mutant plexin-B1 is expressed in prostate only may provide insight on the effects of mutations on the process of metastasis of prostate cancer. To achieve this, a transgenic mouse could be generated with mutant plexin-B1 cDNA downstream of a Cre-inducible promoter. Crossing this mouse with a Probasin-Cre transgenic mouse would generate offspring in which mutant plexin-B1 is expressed in prostate epithelial cells only. This would be a good model to fully explore the promoting role of plexin-B1 mutations in prostate cancer development. Although there is much work to be done in further characterizing the significance of plexin-B1 mutations in prostate cancer progression, our research work has revealed the role of plexin-B1 in cancer metastasis and identified it as a potential therapeutic target in the future.

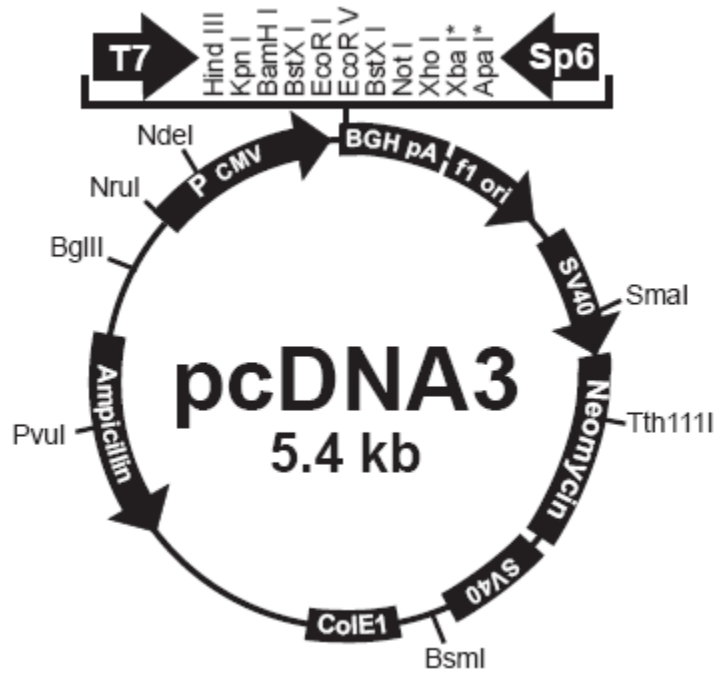
APPENDIX 1

pEF-BOS/Myc vector



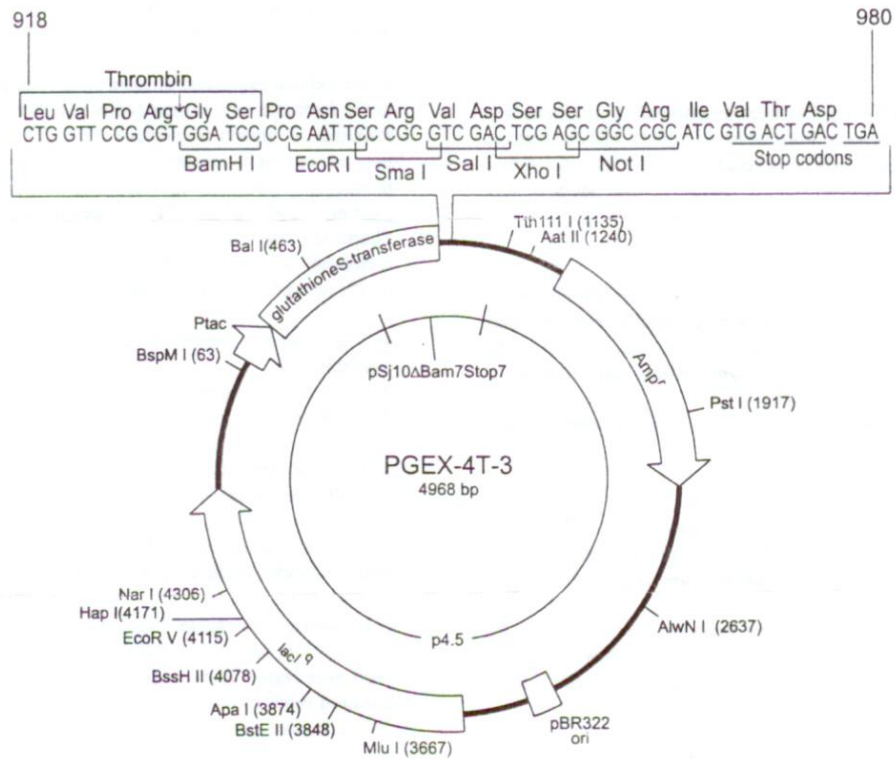
Plasmids DNA encoding pEF-BOS/Myc-RhoD (G26V) and pEF-BOS/Myc-Rhod (T31K) were gift from Professor Endo (Chiba University). cDNA encoding G26V/T31K was subcloned into the vector at the *HindIII* and *EcoRI* sites. The plasmid is ampicillin resistant. (The figure was adapted from Professor Endo's information.)

pcDNA3 vector



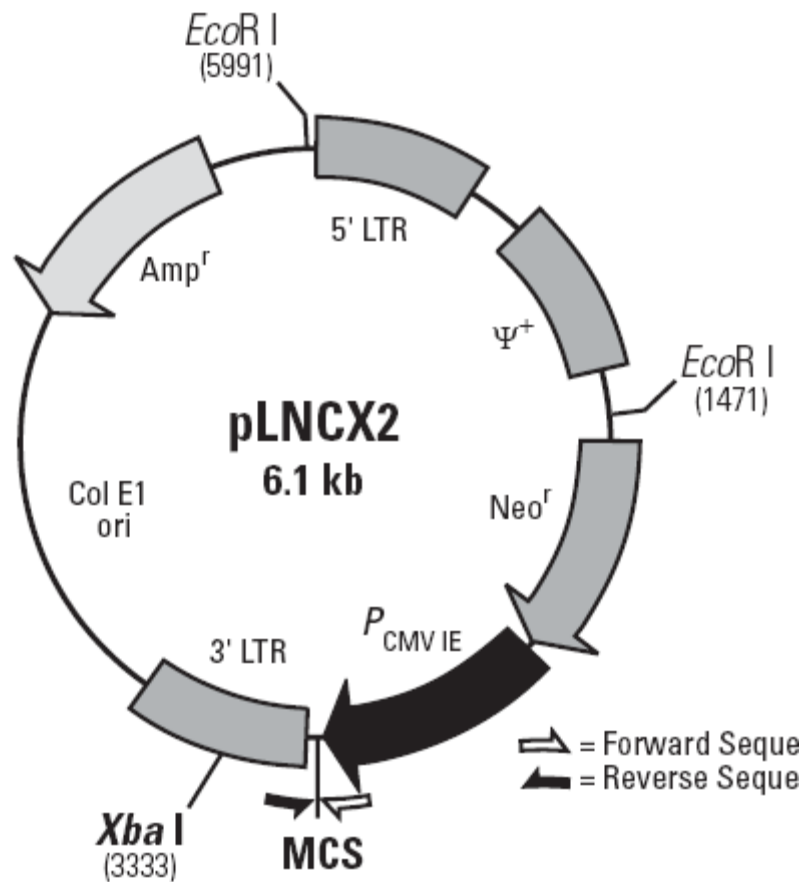
Plasmid DNA encoding vsv-tagged plexin-B1 was a gift from Dr. Tamagnone (University of Torino School of Medicine, Italy). cDNA encoding VSV-tagged plexin-B1 (5.6 kb) was subcloned into pcDNA3 vector at the Hind III and EcoR I sites. VSV was tagged at the N-terminal of plexin-B1. The plasmid is ampicillin resistant. (The figure was adapted from Invitrogen data sheet.)

PGEX-4T-3 vector



Plasmid DNA encoding GST-fused cyto-plexin-B1 wildtype/mutants were constructed with pGEX-4T-3 vector. cDNA encoding the cytoplasmic region of plexin-B1 (aa 1512-2135) was subcloned into the vector at the Sal I and Xho I sites. The plasmid is ampicillin resistant. (The picture was adapted from Amersham data sheet.)

pLNCX2 vector



Plasmid DNA encoding ErbB-2 was a gift from Dr. Swiercz (University of Heidelberg, Germany). Full length ErbB-2 was subcloned into pLNCX2 vector. The plasmid is ampicillin resistant.

Met plasmid

The plasmid encoding full length Met was a gift from Dr. Tamagnone and was labeled as PRRL2SinPPTthCMVMCSpre. It was specifically designed vector by his group and was compatible for lentivirus infection as well.

APPENDIX 2

List of reagents and Kits

Name	Company	Catalogue no.
Albumin from bovine serum	Sigma-Aldrich	A8806
Amicon Centricon YM-10	Millipore	4205
Benzonase nuclease	Sigma-Aldrich	E1014-25K
CellLytic B cell lysis reagent	Sigma-Aldrich	B7435-500
Complete mini protease cocktail	Roche	04693124001
Coomassie Plus-the better bradford assay reagent	Pierce	23238
Costar transwells 0.8µm	Sigma-Aldrich	CLS 3422
DNase I	Sigma-Aldrich	D4527-40KU
Fetal bovine serum ultra-low IgG	Invitrogen	16250-086
Fibronectin (0.1%) from human	Sigma-Aldrich	F0895
Full-range rainbow molecular weight markers	Amersham	RPN800E
Glutathione Sepharose 4B	Amersham	17-0756-01
Lipofectamine 2000 Transfection reagent	Invitrogen	11668-019
LPA sodium salt	Sigma-Aldrich	L7260
Modified lowry protein assay kit	Pierce	23240
PBS,pH 7.4 sterile	Invitrogen	10010
Protein A agarose	Invitrogen	15918-014
Redipack GST purification module	GE healthcare	27-4570-02
Recombinant human semaphorin 3A-Fc chimera	R&D systems	1250-S3

APPENDIX 3

Numbers of PC3 cells migrated in migration assays for Figure 4.6

	control	Sema4D
Experiment 1	2908	2816
Experiment 2	1972	1813
Experiment 3	1331	1139
Experiment 4	1917	1452
Experiment 5	1375	912

Numbers of cells migrated in migration assays for Figure 5.1

Experiment 1

	control	Sema4D
Vector	333	342
Wildtype	132	124
A5359G	1270	1345
A5653G	1219	1300
T5714C	332	311

Experiment 2

	control	Sema4D
Vector	466	431
Wildtype	165	158
A5359G	1728	1242
A5653G	1785	1789
T5714C	647	665

Experiment 3

	control	Sema4D
Vector	406	311
Wildtype	216	181
A5359G	1799	1350
A5653G	1765	1584
T5714C	335	363

Reference List

- Adams,R.H., Lohrum,M., Klostermann,A., Betz,H., and Puschel,A.W.** (1997). The chemorepulsive activity of secreted semaphorins is regulated by furin-dependent proteolytic processing. *EMBO J.* **16**, 6077-6086.
- Antipenko,A., Himanen,J.P., van,L.K., Nardi-Dei,V., Lesniak,J., Barton,W.A., Rajashankar,K.R., Lu,M., Hoemme,C., Puschel,A.W. et al.** (2003). Structure of the semaphorin-3A receptor binding module. *Neuron.* **39**, 589-598.
- Argast,G.M., Croy,C.H., Coutts,K.L., Zhang,Z., Litman,E., Chan,D.C., and Ahn,N.G.** (2009). Plexin B1 is repressed by oncogenic B-Raf signaling and functions as a tumor suppressor in melanoma cells. *Oncogene.* **28**, 2697-2709.
- Artigiani,S., Barberis,D., Fazzari,P., Longati,P., Angelini,P., van de Loo,J.W., Comoglio,P.M., and Tamagnone,L.** (2003). Functional regulation of semaphorin receptors by proprotein convertases. *J. Biol. Chem.* **278**, 10094-10101.
- Aurandt,J., Li,W., and Guan,K.L.** (2006). Semaphorin 4D activates the MAPK pathway downstream of plexin-B1. *Biochem. J.* **394**, 459-464.
- Aurandt,J., Vikis,H.G., Gutkind,J.S., Ahn,N., and Guan,K.L.** (2002). The semaphorin receptor plexin-B1 signals through a direct interaction with the Rho-specific nucleotide exchange factor, LARG. *Proc. Natl. Acad. Sci. U. S. A.* **99**, 12085-12090.
- Bagnard,D., Lohrum,M., Uziel,D., Puschel,A.W., and Bolz,J.** (1998). Semaphorins act as attractive and repulsive guidance signals during the development of cortical projections. *Development.* **125**, 5043-5053.
- Bagri,A., Cheng,H.J., Yaron,A., Pleasure,S.J., and Tessier-Lavigne,M.** (2003). Stereotyped pruning of long hippocampal axon branches triggered by retraction inducers of the semaphorin family. *Cell.* **113**, 285-299.
- Barberis,D., Artigiani,S., Casazza,A., Corso,S., Giordano,S., Love,C.A., Jones,E.Y., Comoglio,P.M., and Tamagnone,L.** (2004). Plexin signaling hampers integrin-based adhesion, leading to Rho-kinase independent cell rounding, and inhibiting lamellipodia extension and cell motility. *FASEB J.* **18**, 592-594.
- Barberis,D., Casazza,A., Sordella,R., Corso,S., Artigiani,S., Settleman,J., Comoglio,P.M., and Tamagnone,L.** (2005). p190 Rho-GTPase activating protein

associates with plexins and it is required for semaphorin signalling. *J. Cell Sci.* **118**, 4689-4700.

Basile,J.R., Afkhami,T., and Gutkind,J.S. (2005). Semaphorin 4D/plexin-B1 induces endothelial cell migration through the activation of PYK2, Src, and the phosphatidylinositol 3-kinase-Akt pathway. *Mol. Cell Biol.* **25**, 6889-6898.

Basile,J.R., Barac,A., Zhu,T., Guan,K.L., and Gutkind,J.S. (2004). Class IV semaphorins promote angiogenesis by stimulating Rho-initiated pathways through plexin-B. *Cancer Res.* **64**, 5212-5224.

Basile,J.R., Castilho,R.M., Williams,V.P., and Gutkind,J.S. (2006). Semaphorin 4D provides a link between axon guidance processes and tumor-induced angiogenesis. *Proc. Natl. Acad. Sci. U. S. A.* **103**, 9017-9022.

Basile,J.R., Gavard,J., and Gutkind,J.S. (2007). Plexin-B1 utilizes RhoA and Rho kinase to promote the integrin-dependent activation of Akt and ERK and endothelial cell motility. *J. Biol. Chem.* **282**, 34888-34895.

Behar,O., Golden,J.A., Mashimo,H., Schoen,F.J., and Fishman,M.C. (1996). Semaphorin III is needed for normal patterning and growth of nerves, bones and heart. *Nature.* **383**, 525-528.

Bielenberg,D.R., Hida,Y., Shimizu,A., Kaipainen,A., Kreuter,M., Kim,C.C., and Klagsbrun,M. (2004). Semaphorin 3F, a chemorepellent for endothelial cells, induces a poorly vascularized, encapsulated, nonmetastatic tumor phenotype. *J. Clin. Invest.* **114**, 1260-1271.

Boguski,M.S. and McCormick,F. (1993). Proteins regulating Ras and its relatives. *Nature.* **366**, 643-654.

Bookstein,R., MacGrogan,D., Hilsenbeck,S.G., Sharkey,F., and Allred,D.C. (1993). p53 is mutated in a subset of advanced-stage prostate cancers. *Cancer Res.* **53**, 3369-3373.

Bork,P., Doerks,T., Springer,T.A., and Snel,B. (1999). Domains in plexins: links to integrins and transcription factors. *Trends Biochem. Sci.* **24**, 261-263.

Brawley,O.W., Knopf,K., and Thompson,I. (1998). The epidemiology of prostate cancer part II: the risk factors. *Semin. Urol. Oncol.* **16**, 193-201.

Brouns,M.R., Matheson,S.F., Hu,K.Q., Delalle,I., Caviness,V.S., Silver,J., Bronson,R.T., and Settleman,J. (2000). The adhesion signaling molecule p190

RhoGAP is required for morphogenetic processes in neural development. *Development*. **127**, 4891-4903.

Campbell,D.S. and Holt,C.E. (2003). Apoptotic pathway and MAPKs differentially regulate chemotropic responses of retinal growth cones. *Neuron*. **37**, 939-952.

Castro-Rivera,E., Ran,S., Thorpe,P., and Minna,J.D. (2004). Semaphorin 3B (SEMA3B) induces apoptosis in lung and breast cancer, whereas VEGF165 antagonizes this effect. *Proc. Natl. Acad. Sci. U. S. A.* **101**, 11432-11437.

Chen,H., Chedotal,A., He,Z., Goodman,C.S., and Tessier-Lavigne,M. (1997). Neuropilin-2, a novel member of the neuropilin family, is a high affinity receptor for the semaphorins Sema E and Sema IV but not Sema III. *Neuron*. **19**, 547-559.

Chodak,G.W., Keane,T., and Klotz,L. (2002). Critical evaluation of hormonal therapy for carcinoma of the prostate. *Urology* **60**, 201-208.

Christensen,C.R., Klingelhofer,J., Tarabykina,S., Hulgaard,E.F., Kramerov,D., and Lukanidin,E. (1998). Transcription of a novel mouse semaphorin gene, M-semaH, correlates with the metastatic ability of mouse tumor cell lines. *Cancer Res.* **58**, 1238-1244.

Coen,J.J., Zietman,A.L., Thakral,H., and Shipley,W.U. (2002). Radical radiation for localized prostate cancer: local persistence of disease results in a late wave of metastases. *J. Clin. Oncol.* **20**, 3199-3205.

Conrotto,P., Corso,S., Gamberini,S., Comoglio,P.M., and Giordano,S. (2004). Interplay between scatter factor receptors and B plexins controls invasive growth. *Oncogene*. **23**, 5131-5137.

Conrotto,P., Valdembri,D., Corso,S., Serini,G., Tamagnone,L., Comoglio,P.M., Bussolino,F., and Giordano,S. (2005). Sema4D induces angiogenesis through Met recruitment by Plexin B1. *Blood*. **105**, 4321-4329.

Cooke,P.S., Young,P., and Cunha,G.R. (1991). Androgen receptor expression in developing male reproductive organs. *Endocrinology* **128**, 2867-2873.

Cunha,G.R., Alarid,E.T., Turner,T., Donjacour,A.A., Boutin,E.L., and Foster,B.A. (1992a). Normal and abnormal development of the male urogenital tract. Role of androgens, mesenchymal-epithelial interactions, and growth factors. *J. Androl* **13**, 465-475.

Cunha,G.R., Alarid,E.T., Turner,T., Donjacour,A.A., Boutin,E.L., and Foster,B.A. (1992b). Normal and abnormal development of the male urogenital tract. Role of androgens, mesenchymal-epithelial interactions, and growth factors. *J. Androl* **13**, 465-475.

Cunha,G.R. and Young,P. (1991b). Inability of Tfm (testicular feminization) epithelial cells to express androgen-dependent seminal vesicle secretory proteins in chimeric tissue recombinants. *Endocrinology* **128**, 3293-3298.

Cunha,G.R. and Young,P. (1991a). Inability of Tfm (testicular feminization) epithelial cells to express androgen-dependent seminal vesicle secretory proteins in chimeric tissue recombinants. *Endocrinology* **128**, 3293-3298.

Danilkovitch-Miagkova,A. and Zbar,B. (2002). Dysregulation of Met receptor tyrosine kinase activity in invasive tumors. *J. Clin. Invest.* **109**, 863-867.

De Marzo,A.M., Nelson,W.G., Meeker,A.K., and Coffey,D.S. (1998). Stem cell features of benign and malignant prostate epithelial cells. *J. Urol.* **160**, 2381-2392.

Dearnaley,D.P. (1995). Radiotherapy for prostate cancer: the changing scene. *Clin. Oncol. (R. Coll. Radiol.)* **7**, 147-150.

Delaire,S., Billard,C., Tordjman,R., Chedotal,A., Elhabazi,A., Bensussan,A., and Boumsell,L. (2001). Biological activity of soluble CD100. II. Soluble CD100, similarly to H-SemaIII, inhibits immune cell migration. *J. Immunol.* **166**, 4348-4354.

Donjacour,A.A. and Cunha,G.R. (1993). Assessment of prostatic protein secretion in tissue recombinants made of urogenital sinus mesenchyme and urothelium from normal or androgen-insensitive mice. *Endocrinology* **132**, 2342-2350.

Driessens,M.H., Hu,H., Nobes,C.D., Self,A., Jordens,I., Goodman,C.S., and Hall,A. (2001). Plexin-B semaphorin receptors interact directly with active Rac and regulate the actin cytoskeleton by activating Rho. *Curr. Biol.* **11**, 339-344.

Driessens,M.H., Olivo,C., Nagata,K., Inagaki,M., and Collard,J.G. (2002). B plexins activate Rho through PDZ-RhoGEF. *FEBS Lett.* **529**, 168-172.

Ediger,T.L., Schulte,N.A., Murphy,T.J., and Toews,M.L. (2003). Transcription factor activation and mitogenic synergism in airway smooth muscle cells. *Eur. Respir. J.* **21**, 759-769.

Feilotter,H.E., Nagai,M.A., Boag,A.H., Eng,C., and Mulligan,L.M. (1998). Analysis of PTEN and the 10q23 region in primary prostate carcinomas. *Oncogene* **16**, 1743-1748.

Feiner,L., Webber,A.L., Brown,C.B., Lu,M.M., Jia,L., Feinstein,P., Mombaerts,P., Epstein,J.A., and Raper,J.A. (2001). Targeted disruption of semaphorin 3C leads to persistent truncus arteriosus and aortic arch interruption. *Development*. **128**, 3061-3070.

Foster,R., Hu,K.Q., Lu,Y., Nolan,K.M., Thissen,J., and Settleman,J. (1996). Identification of a novel human Rho protein with unusual properties: GTPase deficiency and in vivo farnesylation. *Mol. Cell Biol.* **16**, 2689-2699.

Fukuhara,S., Chikumi,H., and Gutkind,J.S. (2000). Leukemia-associated Rho guanine nucleotide exchange factor (LARG) links heterotrimeric G proteins of the G(12) family to Rho. *FEBS Lett.* **485**, 183-188.

Fukuhara,S., Chikumi,H., and Gutkind,J.S. (2001). RGS-containing RhoGEFs: the missing link between transforming G proteins and Rho? *Oncogene*. **20**, 1661-1668.

Fukuhara,S., Murga,C., Zohar,M., Igishi,T., and Gutkind,J.S. (1999). A novel PDZ domain containing guanine nucleotide exchange factor links heterotrimeric G proteins to Rho. *J. Biol. Chem.* **274**, 5868-5879.

Gasman,S., Kalaidzidis,Y., and Zerial,M. (2003). RhoD regulates endosome dynamics through Diaphanous-related Formin and Src tyrosine kinase. *Nat. Cell Biol.* **5**, 195-204.

Gaudino,G., Follenzi,A., Naldini,L., Collesi,C., Santoro,M., Gallo,K.A., Godowski,P.J., and Comoglio,P.M. (1994). RON is a heterodimeric tyrosine kinase receptor activated by the HGF homologue MSP. *EMBO J.* **13**, 3524-3532.

Gherardi,E., Love,C.A., Esnouf,R.M., and Jones,E.Y. (2004). The sema domain. *Curr. Opin. Struct. Biol.* **14**, 669-678.

Giacobini,P., Messina,A., Morello,F., Ferraris,N., Corso,S., Penachioni,J., Giordano,S., Tamagnone,L., and Fasolo,A. (2008). Semaphorin 4D regulates gonadotropin hormone-releasing hormone-1 neuronal migration through PlexinB1-Met complex. *J. Cell Biol.* **183**, 555-566.

Giordano,S., Corso,S., Conrotto,P., Artigiani,S., Gilestro,G., Barberis,D., Tamagnone,L., and Comoglio,P.M. (2002). The semaphorin 4D receptor controls invasive growth by coupling with Met. *Nat. Cell Biol.* **4**, 720-724.

Giordano,S., Di Renzo,M.F., Narsimhan,R.P., Cooper,C.S., Rosa,C., and Comoglio,P.M. (1989). Biosynthesis of the protein encoded by the c-met proto-oncogene. *Oncogene*. **4**, 1383-1388.

Gittes,R.F. (1991). Carcinoma of the prostate. *N. Engl. J. Med.* **324**, 236-245.

Gleason,D.F. (1977). Histologic grading and clinical staging of prostatic carcinoma. In *Urologic Pathology: The Prostate*. (ed. Tannenbaum M), Philadelphia: Lea & Febiger.

Gleason,D.F. (1992). Histologic grading of prostate cancer: a perspective. *Hum. Pathol.* **23**, 273-279.

Grant,D.S., Kleinman,H.K., Goldberg,I.D., Bhargava,M.M., Nickoloff,B.J., Kinsella,J.L., Polverini,P., and Rosen,E.M. (1993). Scatter factor induces blood vessel formation in vivo. *Proc. Natl. Acad. Sci. U. S. A.* **90**, 1937-1941.

Gu,C., Yoshida,Y., Livet,J., Reimert,D.V., Mann,F., Merte,J., Henderson,C.E., Jessell,T.M., Kolodkin,A.L., and Ginty,D.D. (2005). Semaphorin 3E and plexin-D1 control vascular pattern independently of neuropilins. *Science*. **307**, 265-268.

Hall,K.T., Bousmell,L., Schultze,J.L., Boussiotis,V.A., Dorfman,D.M., Cardoso,A.A., Bensussan,A., Nadler,L.M., and Freeman,G.J. (1996). Human CD100, a novel leukocyte semaphorin that promotes B-cell aggregation and differentiation. *Proc. Natl. Acad. Sci. U. S. A.* **93**, 11780-11785.

Han,M., Partin,A.W., Pound,C.R., Epstein,J.I., and Walsh,P.C. (2001). Long-term biochemical disease-free and cancer-specific survival following anatomic radical retropubic prostatectomy. The 15-year Johns Hopkins experience. *Urol. Clin. North Am.* **28**, 555-565.

Hanks,G.E., Asbell,S., Krall,J.M., Perez,C.A., Doggett,S., Rubin,P., Sause,W., and Pilepich,M.V. (1991). Outcome for lymph node dissection negative T-1b, T-2 (A-2,B) prostate cancer treated with external beam radiation therapy in RTOG 77-06. *Int. J. Radiat. Oncol. Biol. Phys.* **21**, 1099-1103.

He,Z. and Tessier-Lavigne,M. (1997). Neuropilin is a receptor for the axonal chemorepellent Semaphorin III. *Cell*. **90**, 739-751.

Hirotsu,M., Ohoka,Y., Yamamoto,T., Nirasawa,H., Furuyama,T., Kogo,M., Matsuya,T., and Inagaki,S. (2002). Interaction of plexin-B1 with PDZ domain-containing Rho guanine nucleotide exchange factors. *Biochem. Biophys. Res. Commun.* **297**, 32-37.

Hood,J.D. and Cheresh,D.A. (2002). Role of integrins in cell invasion and migration. *Nat. Rev. Cancer.* **2**, 91-100.

Hynes,N.E. and Lane,H.A. (2005). ERBB receptors and cancer: the complexity of targeted inhibitors. *Nat. Rev. Cancer.* **5**, 341-354.

Ishida,I., Kumanogoh,A., Suzuki,K., Akahani,S., Noda,K., and Kikutani,H. (2003). Involvement of CD100, a lymphocyte semaphorin, in the activation of the human immune system via CD72: implications for the regulation of immune and inflammatory responses. *Int. Immunol.* **15**, 1027-1034.

Ito,Y., Oinuma,I., Katoh,H., Kaibuchi,K., and Negishi,M. (2006). Sema4D/plexin-B1 activates GSK-3beta through R-Ras GAP activity, inducing growth cone collapse. *EMBO Rep.* **7**, 704-709.

Jaehne,J., Urmacher,C., Thaler,H.T., Friedlander-Klar,H., Cordon-Cardo,C., and Meyer,H.J. (1992). Expression of Her2/neu oncogene product p185 in correlation to clinicopathological and prognostic factors of gastric carcinoma. *J. Cancer Res. Clin. Oncol.* **118**, 474-479.

Kanda,T., Yoshida,Y., Izu,Y., Nifuji,A., Ezura,Y., Nakashima,K., and Noda,M. (2007). PlexinD1 deficiency induces defects in axial skeletal morphogenesis. *J. Cell Biochem.* **101**, 1329-1337.

Keely,P.J., Rusyn,E.V., Cox,A.D., and Parise,L.V. (1999). R-Ras signals through specific integrin alpha cytoplasmic domains to promote migration and invasion of breast epithelial cells. *J. Cell Biol.* **145**, 1077-1088.

Kessler,O., Shraga-Heled,N., Lange,T., Gutmann-Raviv,N., Sabo,E., Baruch,L., Machluf,M., and Neufeld,G. (2004). Semaphorin-3F is an inhibitor of tumor angiogenesis. *Cancer Res.* **64**, 1008-1015.

Kigel,B., Varshavsky,A., Kessler,O., and Neufeld,G. (2008). Successful inhibition of tumor development by specific class-3 semaphorins is associated with expression of appropriate semaphorin receptors by tumor cells. *PLoS. One.* **3**, e3287.

Kimmelman,A.C., Nunez,R.N., and Chan,A.M. (2002). R-Ras3/M-Ras induces neuronal differentiation of PC12 cells through cell-type-specific activation of the mitogen-activated protein kinase cascade. *Mol. Cell Biol.* **22**, 5946-5961.

Kinbara,K., Goldfinger,L.E., Hansen,M., Chou,F.L., and Ginsberg,M.H. (2003). Ras GTPases: integrins' friends or foes? *Nat. Rev. Mol. Cell Biol.* **4**, 767-776.

Kitsukawa,T., Shimizu,M., Sanbo,M., Hirata,T., Taniguchi,M., Bekku,Y., Yagi,T., and Fujisawa,H. (1997). Neuropilin-semaphorin III/D-mediated chemorepulsive signals play a crucial role in peripheral nerve projection in mice. *Neuron*. **19**, 995-1005.

Klostermann,A., Lohrum,M., Adams,R.H., and Puschel,A.W. (1998). The chemorepulsive activity of the axonal guidance signal semaphorin D requires dimerization. *J. Biol. Chem.* **273**, 7326-7331.

Kobayashi,H., Koppel,A.M., Luo,Y., and Raper,J.A. (1997). A role for collapsin-1 in olfactory and cranial sensory axon guidance. *J. Neurosci.* **17**, 8339-8352.

Kolodkin,A.L., Levensgood,D.V., Rowe,E.G., Tai,Y.T., Giger,R.J., and Ginty,D.D. (1997). Neuropilin is a semaphorin III receptor. *Cell*. **90**, 753-762.

Kolodkin,A.L., Matthes,D.J., and Goodman,C.S. (1993). The semaphorin genes encode a family of transmembrane and secreted growth cone guidance molecules. *Cell*. **75**, 1389-1399.

Kolodkin,A.L., Matthes,D.J., O'Connor,T.P., Patel,N.H., Admon,A., Bentley,D., and Goodman,C.S. (1992). Fasciclin IV: sequence, expression, and function during growth cone guidance in the grasshopper embryo. *Neuron*. **9**, 831-845.

Konishi,N., Hiasa,Y., Matsuda,H., Tao,M., Tsuzuki,T., Hayashi,I., Kitahori,Y., Shiraishi,T., Yatani,R., Shimazaki,J. et al. (1995). Intratumor cellular heterogeneity and alterations in ras oncogene and p53 tumor suppressor gene in human prostate carcinoma. *Am. J. Pathol.* **147**, 1112-1122.

Kourlas,P.J., Strout,M.P., Becknell,B., Veronese,M.L., Croce,C.M., Theil,K.S., Krahe,R., Ruutu,T., Knuutila,S., Bloomfield,C.D. et al. (2000). Identification of a gene at 11q23 encoding a guanine nucleotide exchange factor: evidence for its fusion with MLL in acute myeloid leukemia. *Proc. Natl. Acad. Sci. U. S. A.* **97**, 2145-2150.

Kumanogoh,A., Marukawa,S., Suzuki,K., Takegahara,N., Watanabe,C., Ch'ng,E., Ishida,I., Fujimura,H., Sakoda,S., Yoshida,K. et al. (2002). Class IV semaphorin Sema4A enhances T-cell activation and interacts with Tim-2. *Nature*. **419**, 629-633.

Kumanogoh,A., Shikina,T., Suzuki,K., Uematsu,S., Yukawa,K., Kashiwamura,S., Tsutsui,H., Yamamoto,M., Takamatsu,H., Ko-Mitamura,E.P. et al. (2005). Nonredundant roles of Sema4A in the immune system: defective T cell priming and Th1/Th2 regulation in Sema4A-deficient mice. *Immunity*. **22**, 305-316.

Kumanogoh,A., Watanabe,C., Lee,I., Wang,X., Shi,W., Araki,H., Hirata,H., Iwahori,K., Uchida,J., Yasui,T. et al. (2000). Identification of CD72 as a lymphocyte receptor for the class IV semaphorin CD100: a novel mechanism for regulating B cell signaling. *Immunity*. **13**, 621-631.

Kuroki,T., Trapasso,F., Yendamuri,S., Matsuyama,A., Alder,H., Williams,N.N., Kaiser,L.R., and Croce,C.M. (2003). Allelic loss on chromosome 3p21.3 and promoter hypermethylation of semaphorin 3B in non-small cell lung cancer. *Cancer Res.* **63**, 3352-3355.

Lantuejoul,S., Constantin,B., Drabkin,H., Brambilla,C., Roche,J., and Brambilla,E. (2003). Expression of VEGF, semaphorin SEMA3F, and their common receptors neuropilins NP1 and NP2 in preinvasive bronchial lesions, lung tumours, and cell lines. *J. Pathol.* **200**, 336-347.

Love,C.A., Harlos,K., Mavaddat,N., Davis,S.J., Stuart,D.I., Jones,E.Y., and Esnouf,R.M. (2003). The ligand-binding face of the semaphorins revealed by the high-resolution crystal structure of SEMA4D. *Nat. Struct. Biol.* **10**, 843-848.

Luo,Y., Raible,D., and Raper,J.A. (1993). Collapsin: a protein in brain that induces the collapse and paralysis of neuronal growth cones. *Cell.* **75**, 217-227.

Maestrini,E., Tamagnone,L., Longati,P., Cremona,O., Gulisano,M., Bione,S., Tamanini,F., Neel,B.G., Toniolo,D., and Comoglio,P.M. (1996). A family of transmembrane proteins with homology to the MET-hepatocyte growth factor receptor. *Proc. Natl. Acad. Sci. U. S. A.* **93**, 674-678.

Maggiara,P., Marchio,S., Stella,M.C., Giai,M., Belfiore,A., De,B.M., Di Renzo,M.F., Costantino,A., Sismondi,P., and Comoglio,P.M. (1998). Overexpression of the RON gene in human breast carcinoma. *Oncogene.* **16**, 2927-2933.

Martin-Satue,M. and Blanco,J. (1999). Identification of semaphorin E gene expression in metastatic human lung adenocarcinoma cells by mRNA differential display. *J. Surg. Oncol.* **72**, 18-23.

McNeal,J.E. (1969). Origin and development of carcinoma in the prostate. *Cancer* **23**, 24-34.

McNeal,J.E. (1983a). Relationship of the origin of benign prostatic hypertrophy to prostatic structure of man and other mammals. In *Benign Prostatic Hypertrophy*. (ed. Hininan,F.J.), pp. 152-166. Berlin: Springer.

McNeal,J.E. (1983b). The prostate gland: morphology and pathology. *Monogr Urology* **4**, 3-33.

McNeal,J.E. and Bostwick,D.G. (1986). Intraductal dysplasia: a premalignant lesion of the prostate. *Hum. Pathol.* **17**, 64-71.

McNeal,J.E., Redwine,E.A., Freiha,F.S., and Stamey,T.A. (1988). Zonal distribution of prostatic adenocarcinoma. Correlation with histologic pattern and direction of spread. *Am. J. Surg. Pathol.* **12**, 897-906.

Messersmith,E.K., Leonardo,E.D., Shatz,C.J., Tessier-Lavigne,M., Goodman,C.S., and Kolodkin,A.L. (1995). Semaphorin III can function as a selective chemorepellent to pattern sensory projections in the spinal cord. *Neuron.* **14**, 949-959.

Mitsui,N., Inatome,R., Takahashi,S., Goshima,Y., Yamamura,H., and Yanagi,S. (2002). Involvement of Fes/Fps tyrosine kinase in semaphorin3A signaling. *EMBO J.* **21**, 3274-3285.

Moeller,H., Blank,B., Lander,K., and Mates,G. (1987). Ontogeny of the androgen receptor in rat ventral prostate during sexual development. *Res. Exp. Med. (Berl)* **187**, 287-294.

Mondino,A., Giordano,S., and Comoglio,P.M. (1991). Defective posttranslational processing activates the tyrosine kinase encoded by the MET proto-oncogene (hepatocyte growth factor receptor). *Mol. Cell Biol.* **11**, 6084-6092.

Murphy,C., Saffrich,R., Grummt,M., Gournier,H., Rybin,V., Rubino,M., Auvinen,P., Lutcke,A., Parton,R.G., and Zerial,M. (1996). Endosome dynamics regulated by a Rho protein. *Nature.* **384**, 427-432.

Murphy,C., Saffrich,R., Olivo-Marin,J.C., Giner,A., Ansorge,W., Fotsis,T., and Zerial,M. (2001). Dual function of rhoD in vesicular movement and cell motility. *Eur. J. Cell Biol.* **80**, 391-398.

Nakamura,F., Kalb,R.G., and Strittmatter,S.M. (2000). Molecular basis of semaphorin-mediated axon guidance. *J. Neurobiol.* **44**, 219-229.

Naldini,L., Weidner,K.M., Vigna,E., Gaudino,G., Bardelli,A., Ponzetto,C., Narsimhan,R.P., Hartmann,G., Zarnegar,R., Michalopoulos,G.K. et al. (1991). Scatter factor and hepatocyte growth factor are indistinguishable ligands for the MET receptor. *EMBO J.* **10**, 2867-2878.

Nasarre,P., Constantin,B., Rouhaud,L., Harnois,T., Raymond,G., Drabkin,H.A., Bourmeyster,N., and Roche,J. (2003). Semaphorin SEMA3F and VEGF have opposing effects on cell attachment and spreading. *Neoplasia*. **5**, 83-92.

Navone,N.M., Labate,M.E., Troncoso,P., Pisters,L.L., Conti,C.J., von Eschenbach,A.C., and Logothetis,C.J. (1999). p53 mutations in prostate cancer bone metastases suggest that selected p53 mutants in the primary site define foci with metastatic potential. *J. Urol.* **161**, 304-308.

Nobes,C.D., Lauritzen,I., Mattei,M.G., Paris,S., Hall,A., and Chardin,P. (1998). A new member of the Rho family, Rnd1, promotes disassembly of actin filament structures and loss of cell adhesion. *J. Cell Biol.* **141**, 187-197.

Oinuma,I., Ishikawa,Y., Katoh,H., and Negishi,M. (2004a). The Semaphorin 4D receptor Plexin-B1 is a GTPase activating protein for R-Ras. *Science*. **305**, 862-865.

Oinuma,I., Katoh,H., Harada,A., and Negishi,M. (2003). Direct interaction of Rnd1 with Plexin-B1 regulates PDZ-RhoGEF-mediated Rho activation by Plexin-B1 and induces cell contraction in COS-7 cells. *J. Biol. Chem.* **278**, 25671-25677.

Oinuma,I., Katoh,H., and Negishi,M. (2004b). Molecular dissection of the semaphorin 4D receptor plexin-B1-stimulated R-Ras GTPase-activating protein activity and neurite remodeling in hippocampal neurons. *J. Neurosci.* **24**, 11473-11480.

Oinuma,I., Katoh,H., and Negishi,M. (2006). Semaphorin 4D/Plexin-B1-mediated R-Ras GAP activity inhibits cell migration by regulating beta(1) integrin activity. *J. Cell Biol.* **173**, 601-613.

Olayioye,M.A., Neve,R.M., Lane,H.A., and Hynes,N.E. (2000). The ErbB signaling network: receptor heterodimerization in development and cancer. *EMBO J.* **19**, 3159-3167.

Parker,S.L., Tong,T., Bolden,S., and Wingo,P.A. (1996). Cancer statistics, 1996. *CA Cancer J. Clin.* **46**, 5-27.

Pasterkamp,R.J., Peschon,J.J., Spriggs,M.K., and Kolodkin,A.L. (2003). Semaphorin 7A promotes axon outgrowth through integrins and MAPKs. *Nature*. **424**, 398-405.

Perrot,V., Vazquez-Prado,J., and Gutkind,J.S. (2002). Plexin B regulates Rho through the guanine nucleotide exchange factors leukemia-associated Rho GEF (LARG) and PDZ-RhoGEF. *J. Biol. Chem.* **277**, 43115-43120.

Petrylak,D.P., Tangen,C.M., Hussain,M.H., Lara,P.N., Jr., Jones,J.A., Taplin,M.E., Burch,P.A., Berry,D., Moinpour,C., Kohli,M. et al. (2004). Docetaxel and estramustine compared with mitoxantrone and prednisone for advanced refractory prostate cancer. *N. Engl. J. Med.* **351**, 1513-1520.

Prins,G.S. and Birch,L. (1995). The developmental pattern of androgen receptor expression in rat prostate lobes is altered after neonatal exposure to estrogen. *Endocrinology* **136**, 1303-1314.

Rabacchi,S.A., Solowska,J.M., Kruk,B., Luo,Y., Raper,J.A., and Baird,D.H. (1999). Collapsin-1/semaphorin-III/D is regulated developmentally in Purkinje cells and collapses pontocerebellar mossy fiber neuronal growth cones. *J. Neurosci.* **19**, 4437-4448.

Renzi,M.J., Wexler,T.L., and Raper,J.A. (2000). Olfactory sensory axons expressing a dominant-negative semaphorin receptor enter the CNS early and overshoot their target. *Neuron.* **28**, 437-447.

Reuther,G.W., Lambert,Q.T., Booden,M.A., Wennerberg,K., Becknell,B., Marcucci,G., Sondek,J., Caligiuri,M.A., and Der,C.J. (2001). Leukemia-associated Rho guanine nucleotide exchange factor, a Dbl family protein found mutated in leukemia, causes transformation by activation of RhoA. *J. Biol. Chem.* **276**, 27145-27151.

Roche,J., Boldog,F., Robinson,M., Robinson,L., Varella-Garcia,M., Swanton,M., Waggoner,B., Fishel,R., Franklin,W., Gemmill,R. et al. (1996). Distinct 3p21.3 deletions in lung cancer and identification of a new human semaphorin. *Oncogene.* **12**, 1289-1297.

Rohm,B., Rahim,B., Kleiber,B., Hovatta,I., and Puschel,A.W. (2000). The semaphorin 3A receptor may directly regulate the activity of small GTPases. *FEBS Lett.* **486**, 68-72.

Rolny,C., Capparuccia,L., Casazza,A., Mazzone,M., Vallario,A., Cignetti,A., Medico,E., Carmeliet,P., Comoglio,P.M., and Tamagnone,L. (2008). The tumor suppressor semaphorin 3B triggers a prometastatic program mediated by interleukin 8 and the tumor microenvironment. *J. Exp. Med.* **205**, 1155-1171.

Ross,J.S., Nazeer,T., Church,K., Amato,C., Figge,H., Rifkin,M.D., and Fisher,H.A. (1993). Contribution of HER-2/neu oncogene expression to tumor grade and DNA content analysis in the prediction of prostatic carcinoma metastasis. *Cancer* **72**, 3020-3028.

Rosser,C.J., Reyes,A.O., Vakar-Lopez,F., Levy,L.B., Kuban,D.A., Hoover,D.C., Lee,A.K., and Pisters,L.L. (2003). Bcl-2 is significantly overexpressed in localized

radio-recurrent prostate carcinoma, compared with localized radio-naive prostate carcinoma. *Int. J. Radiat. Oncol. Biol. Phys.* **56**, 1-6.

Ruijter,E.T., Miller,G.J., van de Kaa,C.A., van,B.A., Bussemakers,M.J., Debruyne,F.M., Ruiten,D.J., and Schalken,J.A. (1999). Molecular analysis of multifocal prostate cancer lesions. *J. Pathol.* **188**, 271-277.

Saito,Y., Oinuma,I., Fujimoto,S., and Negishi,M. (2009). Plexin-B1 is a GTPase activating protein for M-Ras, remodelling dendrite morphology. *EMBO Rep.* **10**, 614-621.

Sakr,W.A., Macoska,J.A., Benson,P., Grignon,D.J., Wolman,S.R., Pontes,J.E., and Crissman,J.D. (1994). Allelic loss in locally metastatic, multisampled prostate cancer. *Cancer Res.* **54**, 3273-3277.

Santen,R.J. (1992). Clinical review 37: Endocrine treatment of prostate cancer. *J. Clin. Endocrinol. Metab* **75**, 685-689.

Sasaki,Y., Cheng,C., Uchida,Y., Nakajima,O., Ohshima,T., Yagi,T., Taniguchi,M., Nakayama,T., Kishida,R., Kudo,Y. et al. (2002). Fyn and Cdk5 mediate semaphorin-3A signaling, which is involved in regulation of dendrite orientation in cerebral cortex. *Neuron.* **35**, 907-920.

Sato,K., Qian,J., Slezak,J.M., Lieber,M.M., Bostwick,D.G., Bergstralh,E.J., and Jenkins,R.B. (1999). Clinical significance of alterations of chromosome 8 in high-grade, advanced, nonmetastatic prostate carcinoma. *J. Natl. Cancer Inst.* **91**, 1574-1580.

Semaphorin Nomenclature Committee (1999). Unified nomenclature for the semaphorins/collapsins. Semaphorin Nomenclature Committee. *Cell.* **97**, 551-552.

Sethi,T., Ginsberg,M.H., Downward,J., and Hughes,P.E. (1999). The small GTP-binding protein R-Ras can influence integrin activation by antagonizing a Ras/Raf-initiated integrin suppression pathway. *Mol. Biol. Cell.* **10**, 1799-1809.

Shepherd,I., Luo,Y., Raper,J.A., and Chang,S. (1996). The distribution of collapsin-1 mRNA in the developing chick nervous system. *Dev. Biol.* **173**, 185-199.

Shi,W., Kumanogoh,A., Watanabe,C., Uchida,J., Wang,X., Yasui,T., Yukawa,K., Ikawa,M., Okabe,M., Parnes,J.R. et al. (2000). The class IV semaphorin CD100 plays nonredundant roles in the immune system: defective B and T cell activation in CD100-deficient mice. *Immunity.* **13**, 633-642.

Slamon,D.J., Clark,G.M., Wong,S.G., Levin,W.J., Ullrich,A., and McGuire,W.L. (1987). Human breast cancer: correlation of relapse and survival with amplification of the HER-2/neu oncogene. *Science*. **235**, 177-182.

Song,H. and Poo,M. (2001). The cell biology of neuronal navigation. *Nat. Cell Biol.* **3**, E81-E88.

Sun,P., Watanabe,H., Takano,K., Yokoyama,T., Fujisawa,J., and Endo,T. (2006). Sustained activation of M-Ras induced by nerve growth factor is essential for neuronal differentiation of PC12 cells. *Genes Cells*. **11**, 1097-1113.

Suzuki,K., Okuno,T., Yamamoto,M., Pasterkamp,R.J., Takegahara,N., Takamatsu,H., Kitao,T., Takagi,J., Rennert,P.D., Kolodkin,A.L. et al. (2007). Semaphorin 7A initiates T-cell-mediated inflammatory responses through alpha1beta1 integrin. *Nature*. **446**, 680-684.

Swiercz,J.M., Kuner,R., Behrens,J., and Offermanns,S. (2002). Plexin-B1 directly interacts with PDZ-RhoGEF/LARG to regulate RhoA and growth cone morphology. *Neuron*. **35**, 51-63.

Swiercz,J.M., Kuner,R., and Offermanns,S. (2004). Plexin-B1/RhoGEF-mediated RhoA activation involves the receptor tyrosine kinase ErbB-2. *J. Cell Biol.* **165**, 869-880.

Swiercz,J.M., Worzfeld,T., and Offermanns,S. (2008). ErbB-2 and met reciprocally regulate cellular signaling via plexin-B1. *J. Biol. Chem.* **283**, 1893-1901.

Swiercz,J.M., Worzfeld,T., and Offermanns,S. (2009). Semaphorin 4D signalling requires the recruitment of phospholipase C{gamma} into the plexin-B1 receptor complex. *Mol. Cell Biol.*

Takagi,S., Hirata,T., Agata,K., Mochii,M., Eguchi,G., and Fujisawa,H. (1991). The A5 antigen, a candidate for the neuronal recognition molecule, has homologies to complement components and coagulation factors. *Neuron*. **7**, 295-307.

Takahashi,T. and Strittmatter,S.M. (2001). Plexin1 autoinhibition by the plexin sema domain. *Neuron*. **29**, 429-439.

Takeda,H. and Chang,C. (1991). Immunohistochemical and in-situ hybridization analysis of androgen receptor expression during the development of the mouse prostate gland. *J. Endocrinol.* **129**, 83-89.

Takegahara,N., Takamatsu,H., Toyofuku,T., Tsujimura,T., Okuno,T., Yukawa,K., Mizui,M., Yamamoto,M., Prasad,D.V., Suzuki,K. et al. (2006). Plexin-A1 and its interaction with DAP12 in immune responses and bone homeostasis. *Nat. Cell Biol.* **8**, 615-622.

Tamagnone,L., Artigiani,S., Chen,H., He,Z., Ming,G.I., Song,H., Chedotal,A., Winberg,M.L., Goodman,C.S., Poo,M. et al. (1999). Plexins are a large family of receptors for transmembrane, secreted, and GPI-anchored semaphorins in vertebrates. *Cell.* **99**, 71-80.

Taniguchi,M., Yuasa,S., Fujisawa,H., Naruse,I., Saga,S., Mishina,M., and Yagi,T. (1997). Disruption of semaphorin III/D gene causes severe abnormality in peripheral nerve projection. *Neuron.* **19**, 519-530.

Tannock,I.F., de,W.R., Berry,W.R., Horti,J., Pluzanska,A., Chi,K.N., Oudard,S., Theodore,C., James,N.D., Turesson,I. et al. (2004). Docetaxel plus prednisone or mitoxantrone plus prednisone for advanced prostate cancer. *N. Engl. J. Med.* **351**, 1502-1512.

Tannock,I.F., Osoba,D., Stockler,M.R., Ernst,D.S., Neville,A.J., Moore,M.J., Armitage,G.R., Wilson,J.J., Venner,P.M., Coppin,C.M. et al. (1996). Chemotherapy with mitoxantrone plus prednisone or prednisone alone for symptomatic hormone-resistant prostate cancer: a Canadian randomized trial with palliative end points. *J. Clin. Oncol.* **14**, 1756-1764.

Tong,Y. and Buck,M. (2005). ¹H, ¹⁵N and ¹³C Resonance assignments and secondary structure determination reveal that the minimal Rac1 GTPase binding domain of plexin-B1 has a ubiquitin fold. *J. Biomol. NMR.* **31**, 369-370.

Tong,Y., Chugha,P., Hota,P.K., Alviani,R.S., Li,M., Tempel,W., Shen,L., Park,H.W., and Buck,M. (2007). Binding of Rac1, Rnd1, and RhoD to a novel Rho GTPase interaction motif destabilizes dimerization of the plexin-B1 effector domain. *J. Biol. Chem.* **282**, 37215-37224.

Tong,Y., Hota,P.K., Hamaneh,M.B., and Buck,M. (2008). Insights into oncogenic mutations of plexin-B1 based on the solution structure of the Rho GTPase binding domain. *Structure.* **16**, 246-258.

Toyofuku,T., Yoshida,J., Sugimoto,T., Zhang,H., Kumanogoh,A., Hori,M., and Kikutani,H. (2005). FARP2 triggers signals for Sema3A-mediated axonal repulsion. *Nat. Neurosci.* **8**, 1712-1719.

Toyofuku,T., Zhang,H., Kumanogoh,A., Takegahara,N., Suto,F., Kamei,J., Aoki,K., Yabuki,M., Hori,M., Fujisawa,H. et al. (2004a). Dual roles of Semaphorin 6D in cardiac morphogenesis through region-specific association of its receptor, Plexin-A1, with off-track and vascular endothelial growth factor receptor type 2. *Genes Dev.* **18**, 435-447.

Toyofuku,T., Zhang,H., Kumanogoh,A., Takegahara,N., Yabuki,M., Harada,K., Hori,M., and Kikutani,H. (2004b). Guidance of myocardial patterning in cardiac development by Semaphorin 6D reverse signalling. *Nat. Cell Biol.* **6**, 1204-1211.

Trusolino,L. and Comoglio,P.M. (2002). Scatter-factor and semaphorin receptors: cell signalling for invasive growth. *Nat. Rev. Cancer.* **2**, 289-300.

Tse,C., Xiang,R.H., Bracht,T., and Naylor,S.L. (2002). Human Semaphorin 3B (SEMA3B) located at chromosome 3p21.3 suppresses tumor formation in an adenocarcinoma cell line. *Cancer Res.* **62**, 542-546.

Tsubakimoto,K., Matsumoto,K., Abe,H., Ishii,J., Amano,M., Kaibuchi,K., and Endo,T. (1999). Small GTPase RhoD suppresses cell migration and cytokinesis. *Oncogene.* **18**, 2431-2440.

Turner,L.J., Nicholls,S., and Hall,A. (2004). The activity of the plexin-A1 receptor is regulated by Rac. *J. Biol. Chem.* **279**, 33199-33205.

Vastrik,I., Eickholt,B.J., Walsh,F.S., Ridley,A., and Doherty,P. (1999). Semaphorin 3A-induced growth-cone collapse is mediated by Rac1 amino acids 17-32. *Curr. Biol.* **9**, 991-998.

Vermeij,J., Teugels,E., Bourgain,C., Xiangming,J., in, V., Ghislain,V., Neyns,B., and De,G.J. (2008). Genomic activation of the EGFR and HER2-neu genes in a significant proportion of invasive epithelial ovarian cancers. *BMC. Cancer.* **8:3**, 3.

Vikis,H.G., Li,W., and Guan,K.L. (2002). The plexin-B1/Rac interaction inhibits PAK activation and enhances Semaphorin 4D ligand binding. *Genes Dev.* **16**, 836-845.

Vikis,H.G., Li,W., He,Z., and Guan,K.L. (2000). The semaphorin receptor plexin-B1 specifically interacts with active Rac in a ligand-dependent manner. *Proc. Natl. Acad. Sci. U. S. A.* **97**, 12457-12462.

Weidner,K.M., Sachs,M., and Birchmeier,W. (1993). The Met receptor tyrosine kinase transduces motility, proliferation, and morphogenic signals of scatter factor/hepatocyte growth factor in epithelial cells. *J. Cell Biol.* **121**, 145-154.

Welch,H.G. and Albertsen,P.C. (2009). Prostate Cancer Diagnosis and Treatment After the Introduction of Prostate-Specific Antigen Screening: 1986-2005. *J. Natl. Cancer Inst.*

Westin,P., Stattin,P., Damber,J.E., and Bergh,A. (1995). Castration therapy rapidly induces apoptosis in a minority and decreases cell proliferation in a majority of human prostatic tumors. *Am. J. Pathol.* **146**, 1368-1375.

Wong,O.G., Nitkunan,T., Oinuma,I., Zhou,C., Blanc,V., Brown,R.S., Bott,S.R., Nariculam,J., Box,G., Munson,P. et al. (2007). Plexin-B1 mutations in prostate cancer. *Proc. Natl. Acad. Sci. U. S. A.* **104**, 19040-19045.

Xiang,R.H., Hensel,C.H., Garcia,D.K., Carlson,H.C., Kok,K., Daly,M.C., Kerbacher,K., van den,B.A., Veldhuis,P., Buys,C.H. et al. (1996). Isolation of the human semaphorin III/F gene (SEMA3F) at chromosome 3p21, a region deleted in lung cancer. *Genomics.* **32**, 39-48.

Yamada,T., Endo,R., Gotoh,M., and Hirohashi,S. (1997). Identification of semaphorin E as a non-MDR drug resistance gene of human cancers. *Proc. Natl. Acad. Sci. U. S. A.* **94**, 14713-14718.

Yao,S.L. and Lu-Yao,G. (2002). Understanding and appreciating overdiagnosis in the PSA era. *J. Natl. Cancer Inst.* **94**, 958-960.

Yarden,Y. and Sliwkowski,M.X. (2001). Untangling the ErbB signalling network. *Nat. Rev. Mol. Cell Biol.* **2**, 127-137.

Yu,H.H., Araj,H.H., Ralls,S.A., and Kolodkin,A.L. (1998). The transmembrane Semaphorin Sema I is required in Drosophila for embryonic motor and CNS axon guidance. *Neuron.* **20**, 207-220.

Zanata,S.M., Hovatta,I., Rohm,B., and Puschel,A.W. (2002). Antagonistic effects of Rnd1 and RhoD GTPases regulate receptor activity in Semaphorin 3A-induced cytoskeletal collapse. *J. Neurosci.* **22**, 471-477.

Zetter,B.R. (1990). The cellular basis of site-specific tumor metastasis. *N. Engl. J. Med.* **322**, 605-612.

Zhang,Z., Vuori,K., Wang,H., Reed,J.C., and Ruoslahti,E. (1996). Integrin activation by R-ras. *Cell.* **85**, 61-69.

Zhou,Y.Q., He,C., Chen,Y.Q., Wang,D., and Wang,M.H. (2003). Altered expression of the RON receptor tyrosine kinase in primary human colorectal adenocarcinomas:

generation of different splicing RON variants and their oncogenic potential. *Oncogene*. **22**, 186-197.